



Norwegian University of  
Science and Technology

# Soft wing impactor for testing of aviation masts

**Hans Erik Eidem**

**Kim Andre Krogsæter**

Subsea Technology

Submission date: June 2016

Supervisor: Terje Rølvåg, IPM

Co-supervisor: Torgeir Welo, IPM

Norwegian University of Science and Technology  
Department of Engineering Design and Materials



**MASTER THESIS SPRING 2016  
FOR  
STUD.TECHN. HANS ERIK EIDEM AND KIM ANDRE KROGSÆTER**

**SOFT WING IMPACTOR FOR TESTING OF AVIATION MASTS**

***Soft wing impactor for testing of aviation mast***

A NLR soft wing impactor was used for physical testing of Finnish, Swedish, Norwegian and Canadian aviation masts between 1976 and 2000. With the exception of one experiment at MIRA presented at the 2014 JAFSG meeting by Griffith, very few physical tests have been reported after 2000. Griffith did not use a soft wing impactor but the semicircular tube proposed in the ICAO standard. The results were dominated by noise due to resonance problems and the author therefore recommended a deformable soft impactor in future tests. The same type of problems have been observed and reported in virtual and physical tests by the supervisor.

However, The ICAO standard recommends rigid impactors, but there are reasons to believe there is a big difference to be hit by a rigid impactor compared to a soft wing impactor. They both weight 3 tons (the mass of a Beechcraft Model 80 Queen Air) and they shall hit the mast at a speed of 140 km/h according to the ICAO rules. The main difference is the initial peak force that occurs when an impactor with a 22 mm steel front plate versus a 0.8 mm aluminum sheet structure hits rigid components like hinges on an aviation mast.

Simulations performed by the supervisor prove that rigid impactors generate initial reaction forces far above the ICAO limits when they hit a typical aluminum mast. They are still being used due to low building and testing costs.

These are strong arguments for this master project, e.g. testing and qualification of a standard soft wing impactor. Unfortunately, there is no standard soft wing impactor and many variants have been used by different mast manufacturers. The documented crash results are therefore not directly comparable. The ICAO rules do neither provide guidelines for soft impactors nor restrict the use of data filtering which has a major impact on the peak forces.

The main objective with this project (and master) is therefore to document, benchmark and qualify a standard soft wing impactor based on the proposed NLR design.

**Tasks to be completed:**

1. Study and document the ICAO and FAA crash safety requirements for aviation masts.
2. Study the current soft wing impactor design, properties and test procedures proposed by NLR and the supervisors (ref. paper)
3. Build 2-4 prototypes of the soft impactor wing for physical testing
4. Perform quasi static crash tests of the impactors according specs from task 2
5. Compare the virtual and physical crash test results and calibrate the crash (material) models in Abaqus for optimal match
6. Write a paper with the supervisors

**Formal requirements:**

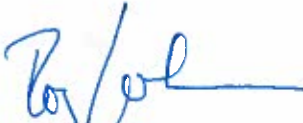
Three weeks after start of the thesis work, an A3 sheet illustrating the work is to be handed in. A template for this presentation is available on the IPM's web site under the menu "Masteroppgave" (<https://www.ntnu.edu/web/ipm/master-thesis>). This sheet should be updated one week before the master's thesis is submitted.

Risk assessment of experimental activities shall always be performed. Experimental work defined in the problem description shall be planned and risk assessed up-front and within 3 weeks after receiving the problem text. Any specific experimental activities which are not properly covered by the general risk assessment shall be particularly assessed before performing the experimental work. Risk assessments should be signed by the supervisor and copies shall be included in the appendix of the thesis.

The thesis should include the signed problem text, and be written as a research report with summary both in English and Norwegian, conclusion, literature references, table of contents, etc. During preparation of the text, the candidate should make efforts to create a well arranged and well written report. To ease the evaluation of the thesis, it is important to cross-reference text, tables and figures. For evaluation of the work a thorough discussion of results is appreciated.

The thesis shall be submitted electronically via DAIM, NTNU's system for Digital Archiving and Submission of Master's theses.

Torgeir Welo is co-supervisor.

  
Torgeir Welo  
Head of Division

  
Terje Rølvåg  
Professor/Supervisor

# Abstract

Due to the imminent danger of colliding into aviation aids located with close proximity to runways or taxiways, ICAO was in the early 80's specifically assigned to develop specifications for frangible lighting structures. As a result, the ICAO Frangible Aids Study Group (FASG) was established in 1981 to subsequently propose design specifications and crash test procedures regarding frangibility of aviation aids and supporting masts. Two specific types of impactors were used for testing and development of aviation lighting structures. These two types were rigid and soft impactors. However, during multiple tests conducted the last decades, the rigid impactor was soon discovered to generate initial peak forces far above the limit of 45kN stated by ICAO FASG. It was also impossible to analyse structural damage since National Aerospace Laboratory (NLR), Netherlands, stated that the pass/fail criteria considering frangibility of an ALS must be based on damage applied to the wing. Damage to the skin was accepted, but damage to supporting wing-structures like the front spar was unacceptable. The rigid impactor is still used based on arguments such as inexpensiveness of production and the simple and reusable construction. However, FASG soon stated that only soft-impactors allowed for damage identification and was therefore the correct choice during testing of aviation masts.

In this master project, the assigned students have been tasked to document, benchmark and qualify a *standard* Soft-Wing-Impactor (SWI) based on the proposed design by NLR. In total, four soft wing impactors are built and tested by conducting quasi-static compressions tests. The tests are conducted in accordance with the test procedure specified by NLR and supervisor Rølvåg. The results from testing are compared to criteria specified by ICAO. The main concern considering the validation of a SWI was that supporting aviation structures must not impose peak forces and energy to an aircraft wing higher than 45kN and 55kJ. Test results are also compared to a virtual test carried out by Rølvåg, and to physical compression tests carried out by Wiggenraad et.al. These are used as references in our discussions regarding the test results.

Tensile and shear tests of the aluminum 2024-T3 and rivets were also conducted to verify mechanical properties. The results and results from the physical compression tests are intended for further calibration of the virtual model in Abaqus.

The results proved that the SWI's were sensitive to large shear-stress in the transition between the skin and the tip of the nose-ribs. This happened to all SWI's since the test procedure specified to place the intruder in between the two centre nose-ribs.

Test 1 and 2 yielded low peak forces due to rivets with low shear and tensile strength. The force reached 43 and 37kN before the main-spar was detached from the supporting rib-structure. Based on these results, test 3 and 4 were substituted with stronger rivets which yielded sufficient shear and tensile strength based on tests carried out on the rivets. Test 3 and 4 resulted in a peak force of 47 and 55kN. According to the ICAO limit of 45kN, these were considered sufficient. Test 4 was the most reliable and sustainable impactor and can be used in future tests of aviation masts based on the margin of 10kN.



# Sammendrag

På bakgrunn av den overhengende faren for å kolliderer med installasjoner plassert langs rullebaner, ble ICAO i starten 80-tallet tildelt ansvaret for å utvikle spesifikasjoner angående utvikling av skjøre lysmaster. Som et resultat av dette ble ICAO Frangible Aids Study Group (FASG) etablert for å kunne kontinuerlig foreslå designspesifikasjoner og testprosedyrer relatert til skjørhet av lysmaster og tilhørende støttestruktur. To spesifikke typer verktøy er blitt brukt for testing og utvikling av lysmaststrukturer. Disse typene er solide testverktøy og deformerbare testverktøy ("vinger"). Solide vinger har vist seg gjennom flere tester å generere høye krefter under kollisjon med lysstrukturer. I de fleste tilfeller over 45kN som er grensen satt av ICAO. Det var også umulig å identifisere strukturelle skader påført den solide vingen. Dette gjorde bruk av en solid vinge upassende ettersom National Aerospace Laboratory (NLR) i Nederland spesifiserte at kravet for godkjenning var avhengig av skade påført vingen under kollisjon. Skade på vingeskallet var godkjent, men ikke skade av fremre bærestruktur i vingen. Den dag i dag er den solide vingen fortsatt i bruk på bakgrunn av argumenter som billig, enkel konstruksjon og gjenbrukbar. FASG var raskt ute med å påpeke at kun en deformerbar vinge gjorde inspeksjon av påførte skader mulig og var på bakgrunn av dette derfor det rette valget videre.

I dette prosjektet har de tiltenkte studentene fått ansvaret for å dokumentere, teste og verifisere en standard, deformerbar vingeseksjon basert på et design utviklet av NLR. Totalt er fire vinger blitt laget og testet ved å utføre en quasi-statisk kompresjonstest. Testene ble utført på bakgrunn av prosedurer fremlagt av NLR og veileder Rølvåg. Testene ble gjennomført med en inntrengningshastighet på 50mm/min over en lengde på 500mm. Resultatene ble sammenlignet mot regler spesifisert av ICAO. Støttestrukturer skal ikke kunne påføre en vinge høyere krefter og energi enn 45kN og 55kJ. Disse ble nøye tatt høyde for under testing og senere validering av den deformerbare vingen. Resultatene ble også sammenlignet med virtuelle tester utført av Rølvåg, samt fysiske kompresjonstester utført av Wiggenraad et.al. Disse resultatene ble brukt som referanse i noe av diskusjonen angående våres testresultater.

Resultatene viste at de deformerbare vingene var sensitive for store skjærkrefter som oppstod i overgangen mellom skallet og den innvendige nesestrukturen. Dette viste seg å være en gjenganger i alle de fire testene ettersom testmasten ble plassert mellom de to nesestrukturene.

Test 1 og 2 ga lave krefter ettersom naglene hadde lav skjær- og tøyingsmotstand. De høyeste kreftene ble målt til 43 og 37kN før main-sparen løsnet fra endene. Basert på disse resultatene ble de i test 3 og 4 byttet nagler til fordel for høyere skjær- og tøyingsmotstand. Dette på bakgrunn av tester utført på naglene. Test 3 og 4 resulterte i høyere krefter. Respektivt 47 og 55kN. Disse testene var av bedre kvalitet basert på kravet om 45kN. Til senere bruk ved fysiske krasjtester, er vinge nr. 4 den mest tillitsvekkende og motstandsdyktige ettersom den har en margin på 10kN å gå på.





# Preface

This master-thesis is written at the Department of Engineering Design and Materials at the Norwegian University of Science and Technology during the spring semester, 2016. It is the final part of our two-year master degree here at NTNU.

The work done during the spring semester has been motivating and rewarding, and has giving us the opportunity to work with a project we think is interesting. During the project we have gained a large amount of knowledge about the industry and requirements which are to be fulfilled in order to develop new and exiting soft-wing-impactors used for testing of aviation masts. The combination of practical and theoretical work is an interesting way of learning engineering methods by going through the steps of planning, designing, manufacturing and testing. If one gets the opportunity, a similar project is highly recommended for future students which like practical work and testing.

We would like to thank professor Terje Rølvåg and Torgeir Welo for the opportunity to participate and work with such an interesting and educational project. Terje has been one of the main contributors of this project from the very beginning. He has much experience on this field and has provided guidance and support during the development of the SWI's and their physical tests. He also provide a great foundation by handing over important documents, as well as being available for questions and discussion at any time. This has been important in order to conduct the intended objectives in a best possible way.

We would also like to thank Staff Engineer Halvard Støver for providing necessary computer hardware and guidance during testing of rivets. A big thank you goes to all the mechanical staff in the work-shop at the Department of Engineering design and materials which helped us during the building and testing process. We would also like to thank Karoline Drågen for guidance and English lessons during the development of this thesis.

Trondheim, June 10, 2016



Kim Andre Krogsæter



Hans Erik Eidem



# Contents

Summary . . . . .	i
Sammendrag . . . . .	ii
Preface . . . . .	iv
<b>Acronymes</b>	<b>xiii</b>
<b>1 Introduction</b>	<b>1</b>
1.1 Background . . . . .	1
1.2 Objectives . . . . .	3
1.3 Limitations . . . . .	4
1.4 Approach . . . . .	4
1.5 Structure of the thesis . . . . .	5
<b>2 Design and testing for frangibility</b>	<b>7</b>
2.1 Design . . . . .	8
2.2 Testing . . . . .	9
2.3 Test procedure . . . . .	11
2.3.1 Dynamic test . . . . .	11
2.3.2 Quasi-static test . . . . .	12
2.4 Acceptance/rejection criteria . . . . .	14
2.4.1 Dynamic test . . . . .	14
2.4.2 Quasi-static test . . . . .	14
<b>3 Impactors</b>	<b>15</b>
3.1 ICAO Rigid-Impactor . . . . .	15
3.2 NLR Soft-Wing-Impactor . . . . .	16
3.2.1 SWI failure modes . . . . .	17
3.3 "Dummy" intruder mast . . . . .	20
3.4 Rivets . . . . .	20
3.5 Material and manufacturing cost . . . . .	21
3.5.1 Material costs . . . . .	21
3.5.2 Consumption of material and material cost per SWI . . . . .	21
3.5.3 Man-hours . . . . .	22
3.5.4 Testing facility . . . . .	22
3.5.5 Cost from subcontractors . . . . .	23
3.5.6 Total costs . . . . .	23
<b>4 Methods</b>	<b>25</b>
4.1 SWI - manufacturing process . . . . .	25
4.1.1 Equipment . . . . .	25
4.1.2 Steel-base . . . . .	26
4.1.3 Main-rib . . . . .	27

4.1.4	Main-spar	27
4.1.5	Nose-rib	28
4.1.6	Form - design and manufacturing	29
4.1.7	Skin	30
4.1.8	"Dummy" intruder mast	31
4.2	SWI - overview	32
4.3	Quasi-static compression test	32
4.3.1	Equipment	32
4.3.2	Test procedure	33
4.3.3	Test setup	34
4.4	SWI - compression tests	35
4.4.1	Test 1 - SWI 1	35
4.4.2	Test 2 - SWI 2	36
4.4.3	Test 3 - SWI 3	37
4.4.4	Test 4 - SWI 4	38
4.5	Virtual compression test	39
4.6	Rivets - test of mechanical properties	40
4.6.1	Calibration of internal load cell	40
4.6.2	Test of maximum shear force	41
4.6.3	Test of maximum tensile force	42
4.7	Aluminium 2024-T3 - material tensile test	43
<b>5</b>	<b>Test results</b>	<b>45</b>
5.1	3 and 4mm rivets	45
5.1.1	Rivets 3mm - maximum shear force	46
5.1.2	Rivets 3mm - maximum tensile force	47
5.1.3	Rivets 4mm - maximum shear force	48
5.1.4	Rivets 4mm - maximum tensile force	49
5.2	Tensile test of Aluminium2024-T3	50
5.3	Soft-wing-impactor compression test	52
5.3.1	Virtual test	52
5.3.2	SWI 1	53
5.3.3	SWI 2	54
5.3.4	SWI 3	55
5.3.5	SWI 4	56
5.3.6	Comparison of SWI test results	57
<b>6</b>	<b>Discussion</b>	<b>59</b>
<b>7</b>	<b>Conclusion</b>	<b>63</b>
7.1	Further work	64
	<b>Bibliography</b>	<b>65</b>
<b>A</b>	<b>Dimensional drawings</b>	<b>67</b>
<b>B</b>	<b>Paper draft</b>	<b>79</b>

# List of Figures

1.1	The two common impactors used for ALS testing. . . . .	2
2.1	Lattix 4220 ALS [1]. . . . .	8
2.2	Force vs. energy during contact of crash-tests described in Table 2.1 [2, 3]. . . . .	10
2.3	Different methods of conducting full-scale dynamic impacts. . . . .	12
2.4	Intended locations for strain gauges. . . . .	13
2.5	Quasi-static test setup. . . . .	13
3.1	Rigid impactor. Photo taken by M.J. Nasad [4]. . . . .	15
3.2	Beechcraft Model 80 Queen Air wing section. [5] . . . . .	16
3.3	SWI assembly. . . . .	16
3.4	Virtual simulation carried out by Terje Rølvåg [2]. . . . .	18
3.5	Static compression test carried out by Wiggenraad et. al. [6]. . . . .	18
3.6	The intended intruder is a rigid replica of the Lattix 4220 mast. . . . .	20
3.7	A typical "blind"-rivet. . . . .	21
4.1	Steel-base. . . . .	26
4.2	Stiffener. . . . .	26
4.3	Manufacturing of main-ribs. . . . .	27
4.4	Manufacturing of the main-spar. . . . .	28
4.5	CAD model of nose-ribs. . . . .	28
4.6	Nose-rib assembly. . . . .	29
4.7	Form designed for shaping the nose-rib. . . . .	30
4.8	Skin mounting. . . . .	30
4.9	Complete assembly. . . . .	31
4.10	Intruder intended for the compression tests. . . . .	31
4.11	Test setup in a hydraulic rig. . . . .	34
4.12	Compression test 1. . . . .	35
4.13	Compression test 2. . . . .	36
4.14	Compression test 3. . . . .	37
4.15	Compression test 4. . . . .	38
4.16	Virtual compression test. . . . .	39
4.17	Calibration. . . . .	40
4.18	Sheartest . . . . .	41
4.19	Tensile test. . . . .	42
4.20	Test specimen before tensile testing. . . . .	43
4.21	Test specimen after tensile testing. . . . .	43
4.22	Test specimen after tensile testing. . . . .	44
5.1	Shear Strength 3mm. . . . .	46
5.2	Tensile Strength 3mm. . . . .	47

---

5.3	Shear Strength 4mm. . . . .	48
5.4	Tensile Strength 4mm. . . . .	49
5.5	The resulting force vs. displacement from the tensile test. 1: Yield and 2: UTS. . . . .	51
5.6	Stress vs. strain. . . . .	51
5.7	Virtual compression test. . . . .	52
5.8	Compression test 1. . . . .	53
5.9	Compression test 2. . . . .	54
5.10	Compression test 3. . . . .	55
5.11	Compression test 4. . . . .	56
5.12	Comparison of all tests. . . . .	57
6.1	Deformation of main-spar and shear of rivets. . . . .	61
A.1	SWI assembly . . . . .	68
A.2	Steel-base . . . . .	69
A.3	Steel-base parts . . . . .	70
A.4	Main-rib . . . . .	71
A.5	Main-spar . . . . .	72
A.6	Nose-rib . . . . .	73
A.7	Skin . . . . .	74
A.8	Mast intruder . . . . .	75
A.9	Mast intruder cut . . . . .	76
A.10	Form lower part . . . . .	77
A.11	Form upper part . . . . .	78

# List of Tables

2.1	Frangibility tests intended for elaboration of frangibility requirements. Reproduced from [7]. . . . .	10
3.1	Associated parts of the SWI illustrated in Figure 3.3. . . . .	17
3.2	Materials applied to different parts of the SWI. . . . .	17
3.3	Materials applied to different parts of the SWI . . . . .	21
3.4	Material consumption and cost per SWI . . . . .	22
3.5	Hours spent on building a single SWI . . . . .	22
3.6	Total costs in Euro per impactor . . . . .	23
4.1	Rivet material data of SWI 1 and 2. . . . .	32
4.2	Impactor 1. . . . .	35
4.3	Impactor 2. . . . .	36
4.4	Impactor 3. . . . .	37
4.5	Impactor 4. . . . .	38
5.1	Force resistance of rivets. . . . .	45
5.2	Test aluminium. . . . .	50
5.3	Soft wing deformation modes virtual test. . . . .	52
5.4	Soft wing deformation modes test 1. . . . .	53
5.5	Soft wing deformation modes test 2. . . . .	54
5.6	Soft wing deformation modes test 3. . . . .	55
5.7	Soft wing deformation modes test 4. . . . .	56





# Acronymes

**SWI** - Soft-Wing-Impactor

**NLR** - National Aerospace Centre

**ALS** - Aviation Lighting Systems

**FAA** - Federation Aviation Administration

**ICAO** - International Civil Aviation Organization

**VAP** - Visual Aid Panel

**FASG** - Frangible Aids Study Group

**ADM** - Aerodrome Design Manual

**CAD** - Computer Aided Design

**CNC** - Computer Numerical Control



# Chapter 1

## Introduction

In this master project, the assigned students have in cooperation with supervisor professor Terje Rølvåg, and co-supervisor professor Torgeir Welo, been tasked to document, benchmark and qualify a standard Soft-Wing-Impactor (SWI) based on the proposed design by National Aerospace Laboratory (NLR), Netherlands. The SWI will be intentionally used for frangibility tests of aviation masts located nearby airport runways.

### 1.1 Background

Each year thousands of flights are committed from both small and large airports worldwide. To provide sufficient safety and avoid misleading aircrafts, various types of signal equipment are located within close proximity of runways and taxiways. According to Federation Aviation Administration (FAA) and International Civil Aviation Organization (ICAO), all international airports worldwide have detailed technical standards developed to ensure safety, and common coding systems implemented to provide global consistency [8, 9, 10]. Such systems are necessary for providing guidance during landing and take-off in almost any weather condition, to prevent delays, and also to maintain sufficient flow of air and ground traffic. Occasionally, sudden emergencies or incidents occur and emergency landings or aborted take-offs are necessary. Severe collisions with unforeseen objects are rarely controllable, and multiple structures along the runway or taxiways contributes into creating potential risks to both aircraft and passengers. Numerous times such impacts have been recorded. Some more severe than others [11].

For several decades professional organizations worldwide, collectively named ICAO Visual Aids Panel (VAP), have been working on various safety issues regarding aviation lighting structures (ALS) located at airports. In the early 80's, ICAO VAP were specifically assigned to develop specifications for frangible lighting structures. As a result, the ICAO Frangible Aids Study Group (FASG) was established in 1981 to subsequently propose design specifications like requirements, criteria, guidelines and test procedures [7]. Preventing loss of structural integrity of aircrafts during impact and further harm to passengers, was one of the main arguments regarding *frangibility* of an ALS. FASG specified that frangibility of fixed objects located at any area where aircrafts move or approach/leave, must be defined as;

*"the ability of a structure to break, distort or yield at a certain impact load while absorbing minimal amount of energy and leave minimal damage to the aircraft"*  
[12, 13].

Based on their research and work, the Aerodrome Design Manual (ADM)[14] Part 6; Frangibility, was made.

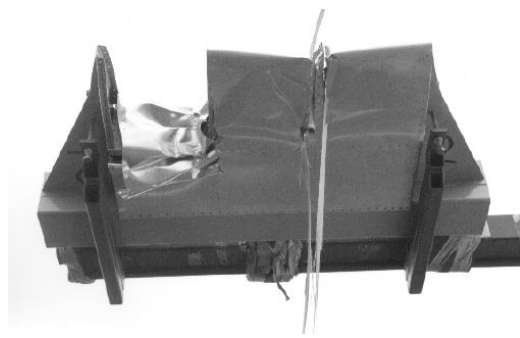
To benchmark and qualify various types of masts and identify damages and dynamics during impacts as a whole, FASG found it necessary to use a reference impactor. Several impactors were designed and tested by various members of ICAO throughout the years, but NLR later came up with an improved version of a SWI made out of aluminium sheets connected to a steel-base in 1988 [7]. This was an 1:1 cut-out of a wing-section from the Beechcraft Model 80 Queen Air. They used this aircraft as a reference since it was appropriate according to elaborated standards [2, 7]. Scandinavian ALS mast manufacturers with help from ICAO members, used it as a standard during various tests from 1991-1997. Canadian ALS mast manufacturers used a slightly different design of a SWI, and also a rigid impactor between 1998-2000. These tests will be further described in [section 2.2](#)

During the development of frangible requirements, two kinds of impactors have been used for full-scale dynamic testing. Rigid and soft impactors respectively as can be seen in [Figure 1.1](#). ICAO still recommend use of rigid impactors contrary to a SWI in their ADM based on arguments established from testing of Canadian ALS's carried out by Zimcik et. al [15]. They stated that rigid impactors provided conservative and repeatable results, and additionally being rigid in a manner which made it reusable for physical testing. The initial peak force and amount of energy absorbed were within reasonable limits, and the production cost of a single impactor was low. This was pointed out as a conclusion from results of a test campaign which tested aluminum lattice structures.

However, rigid impactors have proven to provide some ambiguous results. Especially during testing of an ALS consisting of a single large fiberglass/polymer tube without integrated couplings. When using a rigid impactor it often tends to slice through the tube while a SWI did not [16, 15, 2]. From an engineering point of view these results might not always be conservative. Later studies also revealed problems regarding noise and high peak forces during impact both virtual and physical, especially during tests of aluminium lattice structures [2, 17]. The rigid impactor did not yield higher kinetic energy values than soft-impactors, and it was not possible to perform further inspections of structural damages. Tower response and failure modes have also proven to be quite different between the two [7, 17].



(a) Rigid impactor. Photo taken by Nejad En-san [18].



(b) Soft-wing-impactor. Photo taken by Hanka et.al[4].

Figure 1.1: The two common impactors used for ALS testing.

Although ICAO recommend use of a rigid impactor based on many arguments such as inexpensiveness, repeatable, constant contact time regardless of shape and material, short contact duration, etc, the pass/fail criteria considering frangibility of an ALS is based on damage applied to the wing[12]. Damage to the skin is accepted, but damage to supporting structures like the front spar is not. Thus, only soft-impactors allow for damage identification and is therefore the correct choice when testing an ALS. However, there are currently no properly developed standard regarding such impactors. In recent decades, mast manufacturers have been using various designs, but only a few were comparable with respect to the test results, which

was mostly due to design inequalities.

## 1.2 Objectives

Considering the arguments presented above the main target of this project is hence to document, benchmark, and qualify a *standard* soft-wing-impactor based on the proposed NLR design. Supervisor professor Terje Rølvåg, has been working on prior aspects such as benchmarking and qualifying a virtual NLR SWI-model designed in NX and crash-simulated in Abaqus. To verify and optimize the virtual model and its mechanical properties, the assigned students have been assigned to build 2-4 SWI prototypes consisting of similar material and measurement as in the NLR design guidelines. By conducting a quasi-static compression test in laboratory, representative deflection-force characteristics of a crash-test will be covered, as well as fracture strain and material hardening of the SWI. In addition, material and associated parts such as rivets do also need to be verified by conducting tensile and shear tests. Results from SWI compression tests and tensile/shear tests of rivets extracts the necessary amount of information needed for further calibration of the virtual model and to achieve an optimal match between the virtual and physical model. The benefit of an optimized visual crash-simulation is less need for physical tests, as well as being cost-saving due to the reduced amount of physical tests needed.

Based on work to be done, the following objectives will be addressed throughout the thesis:

- Study and document ICAO and FAA crash safety requirements for aviation masts.
- Study the current SWI design, properties and test procedure proposed by NLR and the supervisors.
- Build 2-4 prototypes of the SWI for physical testing.
- Perform quasi-static compression tests of the impactors according to specs from task 2.
- Compare the virtual and physical crash test results and calibrate the material model in Abaqus for optimal match.
- Write a paper in association with the supervisors.

This project is highly practical due to a large amount of work-hours devoted for production of prototypes and conduction of physical tests in order to verify and qualify the SWI.

## 1.3 Limitations

In Part 6, Chapter 5.2.13 of the Aerodrome Design Manual (ADM) [12], FASG recommend use of several load cells which must be incorporated between the impactor and the interface on the vehicle. When a quasi-static compression test is carried out, our supervisor recommend use of two separate load cells between the SWI steel-base and the hydraulic rig base. However, the intended test rig for this project will be using a single load cell. This will be mounted by using an interface between the cylinder rod and the "dummy" mast (intruder) which can be seen later in this thesis. Upon further discussion with Rølvåg, the solution was concluded to be convenient.

To avoid misunderstandings in the thesis since the word "mast" is often used, the dummy mast intended for the compression tests will be deliberately called an "intruder".

One part of this thesis which was not considered, was to calibrate the material model in Abaqus for optimal match between the physical and virtual model. The optimization of the virtual model in Abaqus is a time-consuming task and some software issues made it impossible to perform this calibration. Upon further discussion with supervisor Rølvåg, it was concluded to not be consider in this part. This will however be proposed as a possible new master thesis.

Regarding the paper which should be written in cooperation with the supervisor, the assigned students were tasked to propose a draft of this. This is carried out such that the supervisor(s) can proceed with the paper and finally complete it. This has been added to [Appendix B](#).

## 1.4 Approach

In order to qualify and benchmark a proper SWI design, a thorough background study will be carried out. This includes studying how to perform qualitative crash-tests, research of existing SWI designs and structural characteristics, and also crash safety requirements for an ALS. Previous work and tests have been studied intentionally to get an overview of re-going problems and improvement potentials, as well as requirements, guidelines, test procedures etc. This will be further discussed in [chapter 2](#) and [chapter 3](#).

Regarding building of prototypes, a detailed and carefully prepared building process will be worked out. Time and costs are important aspects, and will vary due to the complexity of the structure, in this case the SWI. The intended material, Aluminium 2024-T3, is primarily developed for the aircraft- and aerospace-industry. Since the flight industry demands strict regulations, the chosen material is expensive due to its mechanical properties. For this reason, the goal was to obtain the least amount of material waste caused by faults during production, and also low amount of work-hours as a result of thorough preparation and practical knowledge and skills.

Initially, the plan was to do all the work ourselves, but due to lack of proper tools designed for bending corners considering the main-ribs, manufacturing expert Skala Fabrikk AS were contacted. Due to the radius at the "leading edge", the nose-ribs were also prone to difficulties. The decision was to make a form which made it possible to press and form the nose-rib as desired. A constructed 3D model of the form was made in NX and sent to a local manufacturer on campus.

The steel-base was designed and built as a rigid part with reinforcement since the base must be unaffected to applied forces. This made the base reusable considering re-building the SWI assembly. After finishing testing the first SWI's, one could quickly tear down and re-build a second time.

Quasi-static compression tests were performed in a crash-test lab. As mentioned, two and two SWI's were separately tested. The reason for this was mostly because of potential problems to occur regarding aluminium parts or other parts which had to be re-designed in a second attempt. In this case the rivet properties resulted in further testing with respect to shear and tension. After multiple tests new rivets were ordered. A material tensile test designed to verify mechanical properties of the aluminium 2024-T3 was also carried out.

The assigned students have also documented the building process by filming a step by step video. The video may also be used as a manual. This can be found at: [https://www.youtube.com/watch?v=3LZJgBe9\\_Xw](https://www.youtube.com/watch?v=3LZJgBe9_Xw)

## 1.5 Structure of the thesis

The rest of the thesis is structured as following:

- Chapter 2: This chapter describes various design and test requirements regarding aviation masts stated by ICAO. These requirements will be of interest regarding testing of the SWI. Also a brief background study on development of such requirements is carried out. Furthermore test procedures of dynamic and quasi-static tests, and acceptance/rejection criteria for an aviation mast is listed.
- Chapter 3: This chapter is emphasized on the NLR SWI, but also the rigid impactor is briefly described. A failure mode study of two previously static compression tests are carried out. These will be referred to in the discussion when an analyse of our test results are carried out. Here the most interesting failure modes for our tests are listed. Since this have been a highly practical project, it has been decided to carry out a material and manufacturing cost analysis in this chapter as an extension of the SWI part.
- Chapter 4: In this chapter the methods used during the manufacturing and testing process are described. Both with respect to the SWI's, but also regarding testing of rivets and the aluminium 2024-T3.
- Chapter 5: Results of rivet, aluminium and compression tests.
- Chapter 6: Detailed discussions of test results.
- Chapter 7: Conclusion and further work.





## Chapter 2

# Design and testing for frangibility

Designing and testing of aviation lighting structures (ALS) are from an engineering point of view both demanding and prone to various amounts of challenges. Structure design and choice of material depend on knowledge, laws and regulations, and multiple tests. This implies both virtual and physical testing. Mast manufacturers works for the aim to fulfill multiple requirements and decide if the structure is within reasonable limits or to be rejected in order to be further developed and tested. The foundation which development and testing of impactors are based upon, are various requirements described in ICAO's Aerodrome Design Manual (ADM) Part 6; Frangibility [14]. As stated in the objectives, the main focus in this thesis is to further benchmark and qualify a proper SWI. This by doing a quasi-static compression test, and not a dynamic test. However, the scope of this work also relates to future verification of new and existing ALS's where the SWI is an important tool intentionally designed for testing purposes. There are a lot of similarities between an ALS and a SWI regarding requirements for design and testing, thus, for this reason and as an outline of this thesis, it is chosen to study and document these rules and methods for designing and testing of frangible aviation masts. Also provided information from NLR and the supervisor about the intended quasi-static compression test and the SWI will be covered.

## 2.1 Design

According to standards, an ALS must be strong enough to carry the required amount of equipment on top, as well as being resistant against jet blasts and environmental influences. But on the other hand it is required to fail during sudden impacts with small, commute aircrafts [14]. As mentioned in the introducing chapter, equipment located with close proximity along runways and taxiways must be constructed as a frangible structure due to the imminent danger of colliding into it from any approaching direction. An accidental impact between an aircraft and an ALS can potentially affect the aircraft in three different ways:

- Loss of momentum
- Change of direction
- Suffer from structural damage



Figure 2.1: Lattix 4220 ALS [1].

ICAO's ADM [14] describes the amount of momentum lost during an impact as a mathematical governed problem solved by using the integral of force over time. This implies the necessity of minimizing and keeping the impact load and duration to a minimum. The affection of friction between mast and impactor during impact enables mast deformation which allows it to entangle the wing. With respect to frangibility criteria this cannot be tolerated. A common solution implies the use of structural and cable segmentation which can be separable to ensure selected break-away points to be disconnected. In case of a one-piece design, frangibility must be ensured by a complete failure of the structure. This involves failure of random members of the structure, and not failure caused by segmentation. By taking these solutions into consideration, impact force and duration will be minimized and can prevent loss of momentum or sudden change of direction.

Regarding consumption of energy, ICAO's ADM [14] explains the structural damage to the aircraft as directly related to the amount of energy absorbed during an impact. With respect to frangibility the amount of energy required can be limited. The energy can be divided into energy for activation of break-away or failure mechanisms, elastic or plastic deformation of obstacles, and acceleration of obstacles up to aircraft velocity. Aircraft velocity, which in this case is not a design variable, and mass to be accelerated, are the main parameters for measuring the amount of kinetic energy required to accelerate the obstacle. The purpose of break-away mechanism is to absorb impact forces through the structural member and by this fail due to overload. A stiff and light structure provides the necessary amount of force transported to break-away points and low amount of energy absorption. Plastic or elastic deformation of the structure depends on the choice of material. High yield-strain alloys imply higher values. The use of light-weight alloys and a frangible structure is preferable for the reason that it decrease the amount of mass to be accelerated. Additionally, the contact area between obstacle and wing affects the amount of energy absorbed. A large contact area prevents obstacles cutting deeply into the wing as a result of force distribution.

Considering the choice of material, frangibility is achieved by using lightweight materials which yield or distort easily [14], either metallic or non-metallic. From a test point of view non-metallic materials are exceptional with respect to frangibility, but considering their elastic modulus and material isotropy, analysing of results are prone to uncertainties due to the material

behaviour. Chosen materials for an ALS must be able to withstand all kinds of environmental influences. The ALS needs to be light, brittle and consist of segment or a one-piece structure in order to deflect or fail during a sudden impact to allow safe passage of aircrafts during flight or ground maneuvering.

Allowing the aircraft safe passage, an ALS is required to fail in three different failure modes:

- Fracture
- Windowing
- Bending

One of the main requirements regarding an ALS is that the supporting structure cannot impose peak loads and energy to the aircraft that is higher than:

- 45kN
- 55kJ

Considering the quasi-static compression tests intentionally carried out by the assigned students, these values will be the requirements to be fulfill.

## 2.2 Testing

Based on various requirements as mentioned in [section 2.1](#), an ALS can be considered valid when these are fulfilled. As stated in ICAO's ADM [14], a dynamic full-scale test is preferable regarding aviation masts taller than 1.2m. These masts are commonly located where they are in danger of being hit by an aircraft during flight. When using a SWI, dynamic tests reveals inertia and damping reaction forces, as well as peak forces created during the initial stage of a crash [2]. For masts commonly located where aircrafts maneuver on ground, static tests are recommended for testing of low weight structures lower than 1.2m. In this case inertia and damping forces will not be disclosed. This is however not necessary since the aircraft is already located on the ground.

Dynamic tests were executed for the first time in 1979 for FAA at the Naval Air Engineering Centre, New Jersey [7, 14]. At the time, dynamic tests were performed by carrying the impactor which was a rigid pipe-section or a small aircraft-wing on a rail-car down an airstrip. The approximate height of the impactor interface was 5m and during the impact the speed was approximately 130km/h. The test was carried out on a fibre glass tube with break-away couplings. Results showed promising failure modes regarding the wing-section, and the affection of cables mounted inside the ALS was described as a frangibility problem which had to be implemented in the frangibility requirements. FASG stated at their first meeting that the mass of a colliding aircraft had to be sufficiently low with respect to small, commute aircrafts. In 1990, FASG decided that the impactor mass must be 3000kg carried at an test speed of 140km/h which represent aircrafts during flight, and 50km/h during ground maneuvering. The speed, weight and cable requirements are still valid in ICAO's ADM today.

ICAO still recommend use of a rigid impactor for virtual and dynamic testing of an ALS as mentioned in [section 1.1](#). Since the mid 80's multiple tests with rigid impactors have been conducted to verify structural integrity of masts produced by various mast manufacturers. Although some tests were executed earlier, tests carried out from 1984 and beyond were specified to be valid, dynamic tests according to test speed and weight requirements. At a fifth meeting, FASG made an overview of various test executed between 1984-1998 [7]. These can be seen

in Table 2.1 and Figure 2.2. These tests were however carried out by using both rigid- and soft-impactors. Also, not all tests were carried out at 140km/h, some were also done at lower speeds.

Table 2.1: Frangibility tests intended for elaboration of frangibility requirements. Reproduced from [7].

Year	Ref.	Nation	Design concept	Impactor(s)	Nr. of tests
1984	5	Sweden	Alu. tripod, 3legs	Non-std. wing-impactor	5
1989	6	Finland	Fibre glass lattice, 4legs	Rigid	3
1990	7	Netherlands	Fibre glass tube structure, 4 legs	Rigid and pre-std. SWI	1 and 2
1991	9	Finland	Fibre glass lattice, 4 legs	SWI	6
1997	10	Norway	Fibre glass lattice, 3 legs	SWI	4
1997	11	Canada	Fibre glass lattice, 3 legs	Rigid and non-std. wing	12 and 14
1998	12	Canada	Alu. lattice, 3 legs	SWI	5

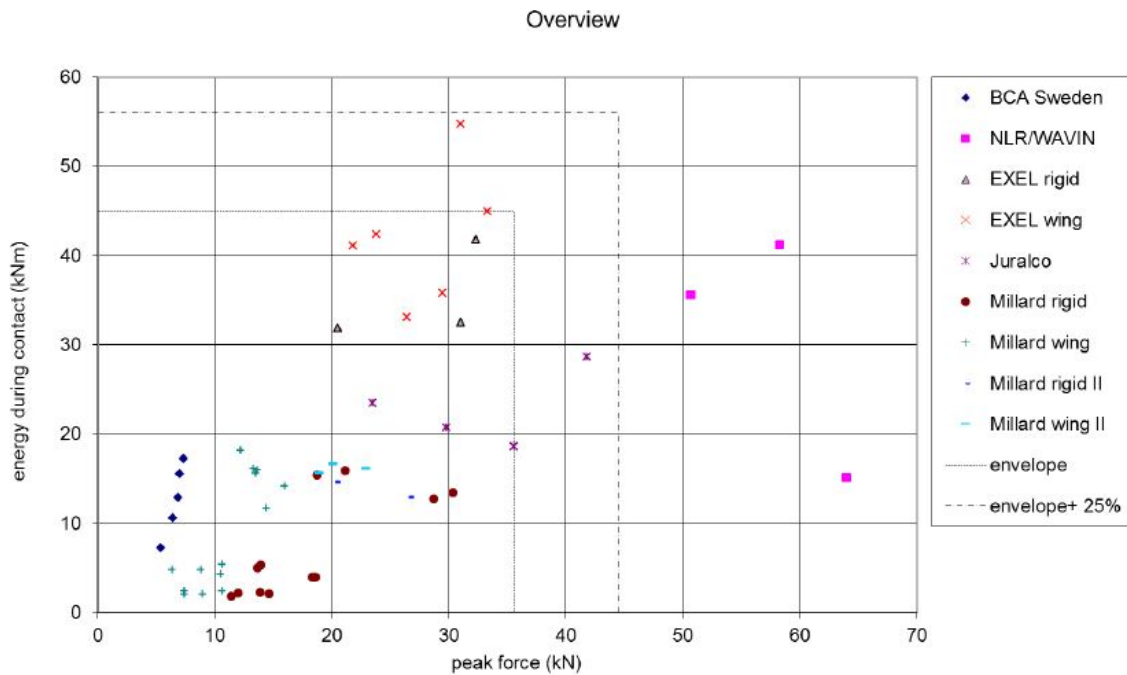


Figure 2.2: Force vs. energy during contact of crash-tests described in Table 2.1 [2, 3].

The phantom line in Figure 2.2 indicates the limited peak force and energy of 45kN and 55kJ respectively. Test results carried out between 1984-1998 revealed that rigid impactors were prone to high peak forces and short contact duration. Terje Rølvåg [2] and Dan Duke [17] also observed problems regarding structural noise by using rigid impactors due to resonance problems in their virtual and physical tests. Since there is virtually no structural damping, it dissipates vibrational energy which escalates and radiates as sound. A SWI however has the ability to flex and deform, and for this reason does not create the amount of vibrational energy based on its ability to dissipate mechanical energy.

During tests carried out on soft impactors listed in Table 2.1, varying skin thickness was tested. Based on test results the SWI designed by NLR was concluded to use skin thickness of 0.8mm since mast manufacturers like EXEL and others were using it [6]. The SWI designed by NLR is the intended impactor for quasi-static compression test in this project.

As mentioned in [section 1.2](#), rigid impactors do not support damage identification of the wing. Skin damage is acceptable, but not damage applied to the front spar based on structural integrity and protection of fuel tanks. M.H. van Houten [19] disclosed some interesting observations during comparison of a rigid and a soft impactor. The rigid impactor was made with a 25mm thick steel nose, and the soft impactor of a 0.8mm aluminium sheet. During impact testing the initial peak forces were in some cases not the highest when hitting rigid components such as hinges on the mast. As the impactor went further into the ALS, increasing peak forces were observed. The reason was due to structural resistance created by the rigid hinges which did not deform properly during the impact.

NLR, Duke and the supervisor stated the necessity of using a deformable SWI based on various arguments against the use of a rigid impactor. To enable inspection of structural damage and restrict the amount of structural noise and peak forces created during a dynamic test, a SWI is therefore preferable [2, 17, 3, 7].

## 2.3 Test procedure

### 2.3.1 Dynamic test

A dynamic test must be executed in such manner that the impact conditions between a wing and an aviation structure are closely related to reality and carried out on a worst-case basis. According to the ADM [14], the test must be carried out by mounting a 3000kg replica of a wing-section on a rail-car carried down an airstrip at 140km/h, as mentioned in [section 2.2](#). The mast height must be at least 4m, or the hit mark 1m below the top of the impacted structure. [Figure 2.3](#) illustrates examples of how dynamic tests are carried out.

Recreation of realistic conditions imply mounting a load on top of the ALS to mimic the identical load of lighting equipment. Cables and associated equipment inside the mast must be mounted before testing.

The ADM, paragraph 5.2.14 [14], states that an impactor must be rigidly mounted on the interface back of the vehicle to ensure zero deflection during impact. Forces created during impact must be recorded by using the necessary amount of load cells attached between the interface and the impactor. This in order to cover any moments generated in the impactor due to impacts off its centre line or reaction forces and moments of the tower on its mounting fixture. When the vehicle is moving at 140km/h, the wing slices through the mast at 38,9mm/ms. By using a sampling rate of 50kHz, 50 measurements each millisecond will be covered. This would be appropriate considering the ability of covering all peak forces during the distance of 38,9mm. The ADM however specifies a sampling rate of at least 10kHz between 2-5ms of the impact.

The test must be recorded by using a high speed camera to monitor the exact deformation and recorded data from the load cells during an impact sequence.



(a) Dynamic impact between impactor and mast [3].



(b) Submerged ALS to reduce amount of interface needed [3].

Figure 2.3: Different methods of conducting full-scale dynamic impacts.

### 2.3.2 Quasi-static test

The ADM does not support any proper standard considering testing of aviation masts when using a SWI. However, NLR and supervisor Rølvåg have proposed a test procedure regarding a quasi-static compression test of the intended SWI [2, 6]. This has been done to cover deformation modes, reaction forces and the consumption of energy related to intrusion of the intruder. The ADM mostly describes regulations targeting aviation masts since a rigid-impactor not have to be tested due to its rigidity. In this case, testing is hence to cover the impact an mast intrusion has on the structural integrity of the SWI, and also cover fracture strain and material hardening.

The quasi-static compression test must be carried out by using a hydraulic rig. An intruder will be pressed through the aluminium parts. It is critical that the SWI is properly mounted to prevent uncertainties in the test results if any movements or tipping has occurred during testing. Rølvåg and NLR emphasized the necessity of using a pair of load cells mounted between the rig foundation and the rigid steel-base of the SWI. The total sum recorded from these cells will be the amount of reaction force created during the compression sequence. However, as mentioned in [section 1.3](#), the conclusion was to use a single load cell since it is already located above the intruder. Upon further discussion with Rølvåg, the solution was concluded to be convenient.

The intruder must be mounted perpendicular and in the centre of the SWI. This creates an intrusion between the centre nose-ribs. It is also desirable to measure the amount of strain created throughout the compression sequence. The conclusion was to glue three strain gauges on three different locations which were assumed to be prone to high tensional forces. One at each supporting structure at the steel-base, and one underneath the main-spar. The locations can be seen at [Figure 2.4](#). The validity of strain results are uncertain, but is included due to vested interests. [Figure 2.5a](#) and [Figure 2.5](#) illustrate the set up for a quasi-static test.

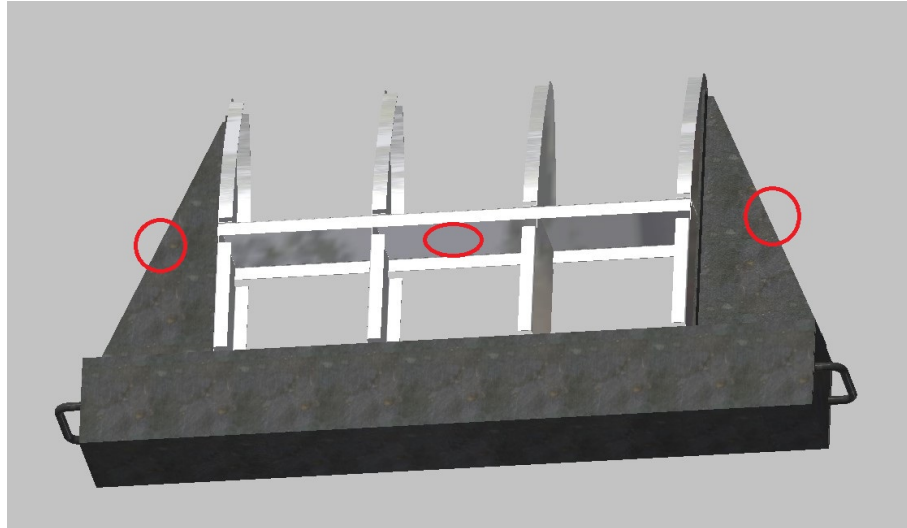
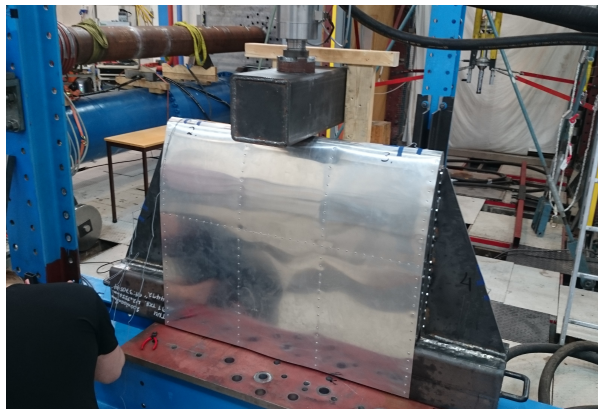


Figure 2.4: Intended locations for strain gauges.

The intended test parameters are:

- 50mm/min (compression speed)
- 500mm (intrusion)
- 45kN (max. peak force)
- 55kJ (max. energy absorption)

The speed is set based on recommendation from previous tests carried out by NLR and Rølvåg. The intrusion length is set based on damage supplied to the main-spar. Any further intrusion is not acceptable since the wing damage is far out of the accepted range considering structural integrity and deformation of the main-spar.



(a) Test setup and calibration in a hydraulic rig.



(b) The rigid intruder mounted on a self-made interface between the load cell and the mast.

Figure 2.5: Quasi-static test setup.

## 2.4 Acceptance/rejection criteria

### 2.4.1 Dynamic test

An aviation lighting structure does not satisfy frangibility requirements if the imposed force is higher than 45kN and the energy infused to the aircraft is higher than 55kJ over the contact period caused by the impact. As mentioned in [section 2.1](#), the ALS must give passage to an aircraft by distort in three different failure modes; bending, windowing and fracture. This eliminates potential interference with the flight trajectory, and enables visual inspection of failure modes which determines acceptance or rejection. Other criteria which are essential are [\[14\]](#);

- Fragmentation into several components which do not cause any secondary hazard to the aircraft (parts which potentially can penetrate the cabin e.g.).
- Structure above the impact point cannot "grasp" the wing. Break-away points further down at the structure must fail.
- Damage caused by ground maneuvering is allowed to be more severe since the aircraft is already located on the ground.

### 2.4.2 Quasi-static test

The quasi-static compression tests in this project imply structural testing of a SWI. In [section 2.1](#) it is specified that the SWI must survive the limited peak force of 45kN and the absorbed amount of energy of 55kJ, especially when entering the main-spar. This is essential compared to real aircraft wings. If the SWI breaks before the peak force of 45kN is reached, it needs to be strengthened. If the SWI is being used in a dynamic test, the SWI cannot fail at 40kN and the mast still be intact. Thus it has to be strengthened such that 45 kN is achieved since a wing has to endure a force of 45kN. When a structural resistance of 45kN is achieved the frangibility problem will concern the mast. By studying failure modes and test results from the compression test, any weaknesses will be disclosed and based on this must be substituted in order to further optimize the SWI structure.



## Chapter 3

# Impactors

As mentioned in [chapter 1](#), two specific types of impactors have been used for testing and development of ALS's and frangible requirements in ICAO's ADM. These two types are rigid and soft impactors. As the SWI is of main interest, it will therefore be emphasis in the following chapter. The following chapter will also contain a further detail description of design and challenges of using a SWI. Lastly, a description of the intruder and rivets used in testing will also be presented.

### 3.1 ICAO Rigid-Impactor

The ADM [\[14\]](#) specifies that the recommended rigid impactor must be made out of a semi-circular steel tube with an outer diameter of 250mm and wall thickness of at least 25mm. By using a steel tube the rigid impactor will act as a rigid body which is not affected by elastic deformations during an impact. When testing, the overall width must be approximately 1000mm or five times greater than the outer cross-section of the intended mast. The surface must be smooth to lower the amount of friction during impact.



Figure 3.1: Rigid impactor. Photo taken by M.J. Nasad [\[4\]](#).

A firm and rigid attachment is required for the supporting structure where the impactor is attached to the vehicle. This to avoid deflection during impact. ICAO does however not specify any proper design regarding the interface between the impactor and vehicle. A typical setup of a rigid impactor ready for testing is illustrated in [Figure 3.1](#).

## 3.2 NLR Soft-Wing-Impactor

The latest SWI designed by NLR were based on the commute aircraft Beechcraft Model 80 Queen Air. The SWI was designed as an 1:1 cut-out to replicate the intended wing module. This can be seen in [Figure 3.2](#). The aerodynamic shape was however simplified. The reason for choosing this aircraft was due to its mass and take-off speed, which is 3000kg and 140km/h [7].

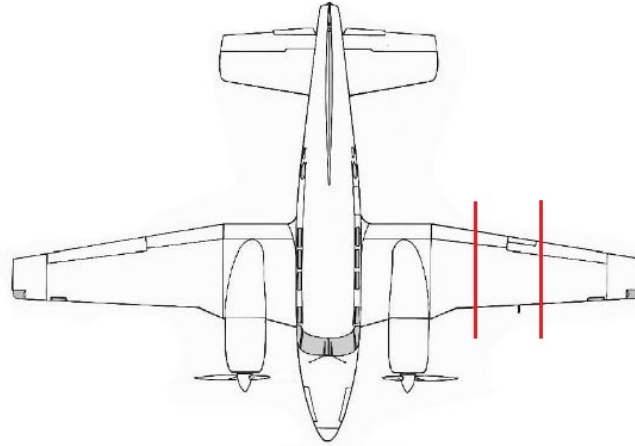


Figure 3.2: Beechcraft Model 80 Queen Air wing section. [5]

The SWI is assembled together with a total number of 12 parts. The 12th part is a large amount of rivets used for connecting the structure. In [Figure 3.3](#) one can identify the respective parts. In [Table 3.1](#) the part, thickness and amount for each parts is listed. In [Table 3.2](#) material and material properties for each part is given. Rivets and bolts are listed in the table, but not visualized in the figure.

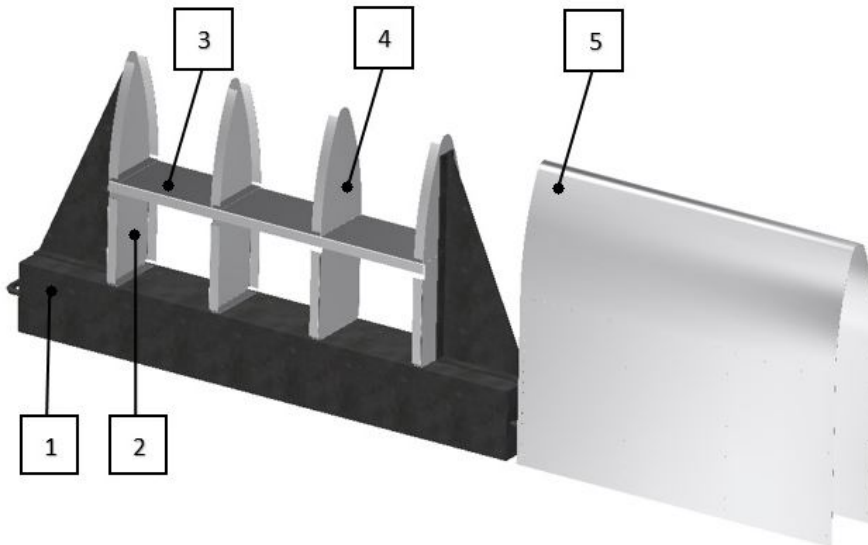


Figure 3.3: SWI assembly.

Table 3.1: Associated parts of the SWI illustrated in [Figure 3.3](#).

Number	Part	Thickness (mm)	Amount
1	Steel-base	200x200x8	1
2	Main-rib	1.6	4
3	Main-spar	2	1
4	Nose-rib	1.6	4
5	Skin	0.8	1
6	Rivets	Ø3 and Ø4	≈ 500
7	Bolts	M6	72

Table 3.2: Materials applied to different parts of the SWI.

Part	Steel-base	Rib structure	Bolts
Material	Steel S355JR	Al 2024-T3	Steel 8.8
Density (kg/m <sup>3</sup> )	7850	2780	7850
E-modulus (GPa)	210	73,1	110
Poisson ratio	0.3	0.33	0.3
Yield (MPa)	355	345	640
UTS (MPa)	570	483	800

A dimensional drawing for each part of the SWI has been conducted. These can be seen in [Appendix A](#). The overall length of the SWI is 1000mm and the overall height is 640mm, which only includes the aluminium section. The widest point on the SWI is across the main-rib section which has a width of 200mm. The distance between each of the four main-ribs and nose-ribs are equal, and the main-spar runs across the entire wing section. The skin must be cut at 1760x1000mm to cover the entire SWI-assembly. The SWI is backed by a steel column with a square cross-section of 200x200x8mm. As stated in a compression test carried out by Wiggenraad et. al[6], steel side-supports are made as an addition to the steel column. This to prevent unrealistic failure mode of the outer support-ribs from collapsing inward during the compression sequence. As seen in [Figure 3.3](#), these are welded on each side. The individual components are joined together by using rivets, and the outer support ribs are connected to the steel side-supports with bolts. The manufacturing process will be further described in [chapter 4](#).

### 3.2.1 SWI failure modes

To achieve desired stiffness and strength to quantify a proper SWI, one must rely on static compression and dynamic crash tests. A brief study has been carried out on some common failure modes from previous compression tests. The same applies to some key characteristics of failure modes which can be expected to occur during compression tests carried out by the assigned students. Since the SWI is still being developed there is no particularly amount of information regarding previous static compression tests. As previously mentioned, the magnitude of tests have been dynamic tests.

To this date, only two static compression tests have been carried out. These by Terje Rølvåg[2] and Wiggenraad et. al.[6]. As mentioned in the introduction, Rølvåg carried out a virtual simulation where he performed a quasi-static compression test of an identical SWI of the proposed NLR design. The model was designed in NX and exported to Abaqus as a NASTRAN bulk file for further crash-simulation. Rølvåg conducted the test with an intrusion speed of 50mm/min. But with a longer stroke than 500mm as specified in [subsection 2.3.2](#). The

stroke was set to 620mm due to the expected deformation distance of an NLR SWI which has a overall height of 640mm. To eliminate elastic deformations of the intended intruder, this was defined as a rigid body. A bi-linear material (hardening) model and 15% fracture strain yielded the most realistic deformation modes and force-level compared to earlier physical tests carried out by Wiggenraad et.al. This can be seen by compare Figure 3.4 and Figure 3.5. However, the fracture strain and strain hardening must be further verified by extracted results from the compression tests carried out by the assigned students. Wiggenraad et. al. performed a static compression test with a non-standard soft-impactor delivered by Transport Canada. Rølvåg and Wiggenraad were however using the same skin thickness of 0.8mm.

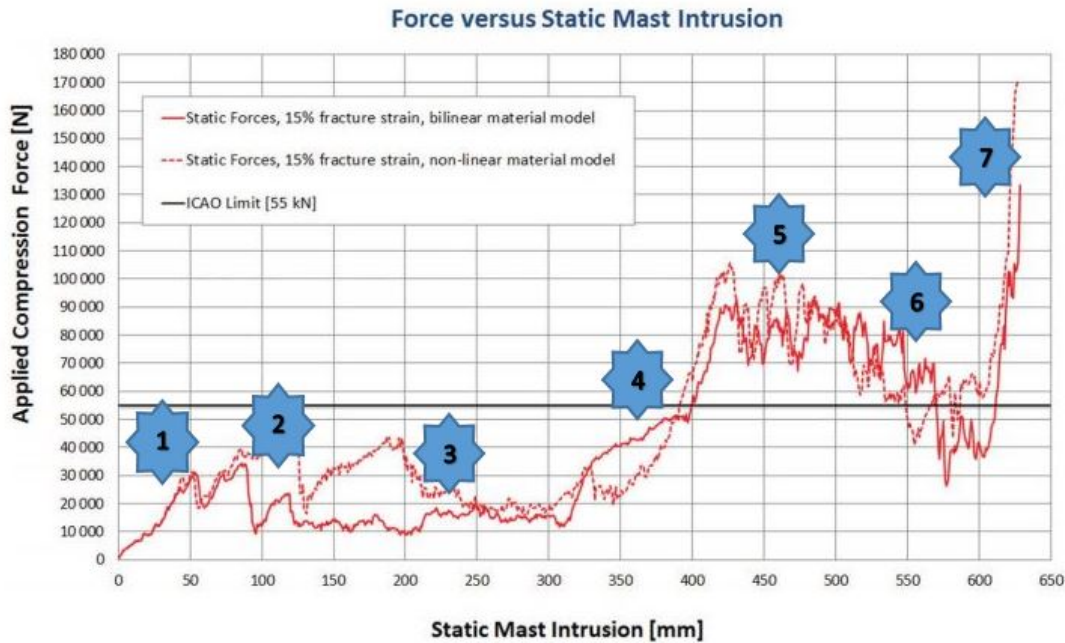


Figure 3.4: Virtual simulation carried out by Terje Rølvåg [2].

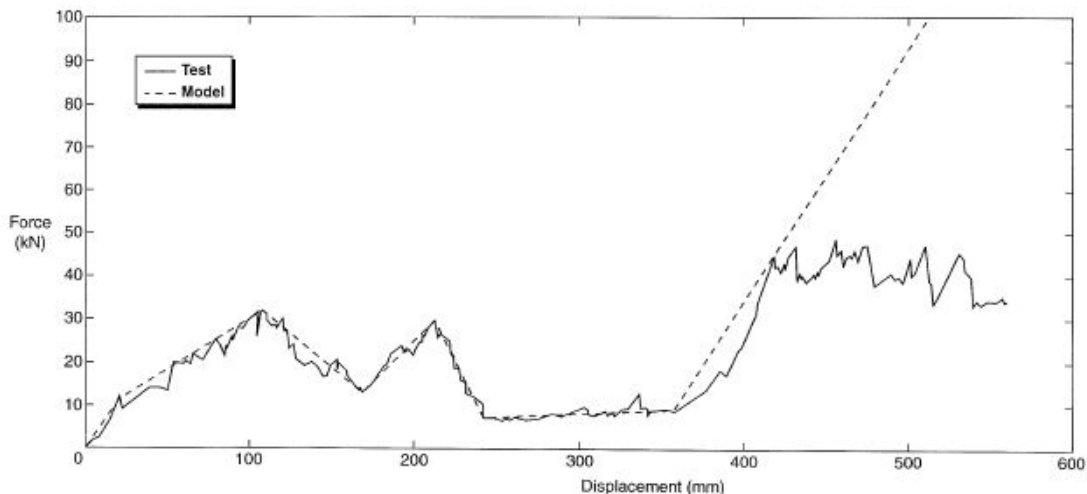


Figure 3.5: Static compression test carried out by Wiggenraad et. al. [6].

One of the differences discovered in the respective models designed by Rølvåg (NLR) and Wiggenraad et.al, was that the NLR main-spar was mounted approximately 340mm from the leading edge. In the soft-impactor designed by Wiggenraad et.al. the main-spar was located 450mm from the leading edge. This implied a smaller nose-rib regarding the NLR SWI as

opposed to Wiggenraads. The next difference discovered was in the test setup. Rølvåg used a rigid intruder based on the Lattix 4220 mast, and Wiggenraad used a represented EXEL mast with a different cross-section. Rølvåg placed the intruder between the centre nose-ribs, meanwhile Wiggenraad placed it on top of the nose-rib. One can see from the test results that the initial intrusion of the SWI in phase 1 is stiffer, but tearing of the aluminium occurs at an earlier stage when examining the displacement. The tearing may occur due to a sharper nose edge regarding the NLR impactor. Furthermore, the phases of the test sequence are quite similar. But due to the variation of distance between leading edge and the main-spar, the SWI initialises an earlier material stack-up against the main-spar.

Hopefully, the intended compression tests will disclose a similar force pattern presented in [Figure 3.4](#) to prevent an too extensive calibration of the virtual model. In most cases it is the physical tests which covers the correct deformation modes and will provide guidelines for a virtual test simulation. The results provided by Rølvåg and Wiggenraad will be used as a reference for comparison of results from tests carried out by the assigned students.

As depicted in [Figure 3.4](#), the force pattern is marked with numbers where characteristic deformation modes potentially will occur. This was reproduced from Rølvåg [2]. For the physical tests carried out in this project, the mast intrusion length will be 500mm. The length of 500mm is sufficient based on damage applied to the main-spar. Since the main-spar can not be severely damaged during an impact, the conclusion of 500mm was appropriate. Phase 7 is therefore reasonable to not be considered. The following phases are:

1. Linear elastic deformation of skin and main-spars.
2. Skin failure (tear open), plastic shear deformation mode.
3. Skin in plastic shear deformation mode, constant force.
4. Skin in plastic shear, stacking up against main spar.
5. Plastic deformation of main spar and buckling of supporting ribs. Side supports start to deform.
6. Rib buckling failure. Main-spar detach from ribs and skin - FAILURE

These will be of great interest regarding analysing of test results in this thesis.

### 3.3 "Dummy" intruder mast

The intruder intended for the SWI compression test is a replica of a Lattix 4220 aviation mast. The reason for using this type of mast is due to the typical aviation mast cross section which must provide realistic reaction forces versus soft-wing intrusion characteristics. A Lattix 4220 mast has a cross-section of 200mm x 200mm, and is built of aluminium. These are delivered in modules with break-away points. The rigid "dummy" mast is constructed of S355JR steel. Dimensions can be seen in [Appendix A](#).

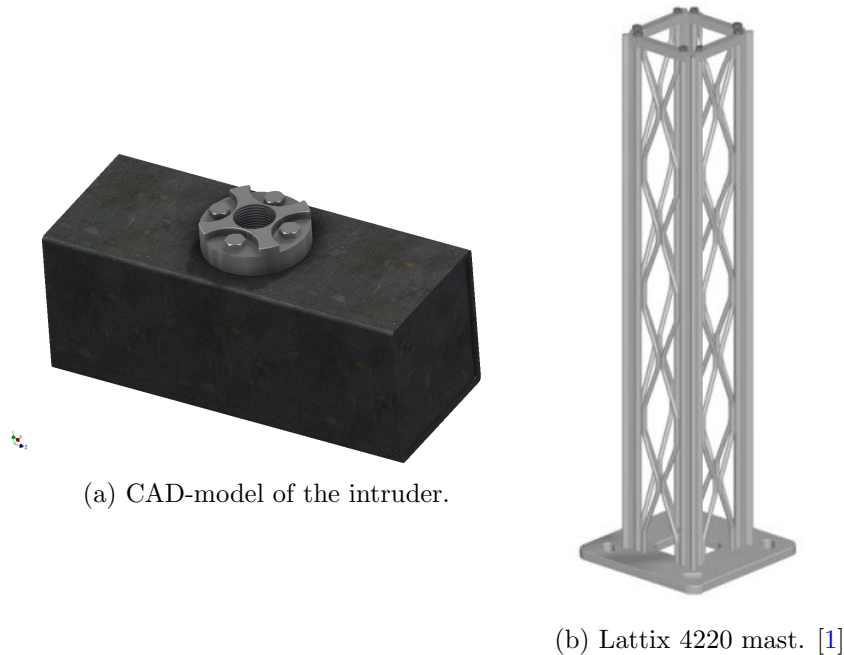


Figure 3.6: The intended intruder is a rigid replica of the Lattix 4220 mast.

### 3.4 Rivets

A rivet is a permanent mechanical fastener. Rivets are delivered in different materials, shapes and strength ranges. "Blind"-rivets are non-threaded "bolts" which are placed in predrilled holes and expanded to combine two or more elements together. Rivets consist of a flanged or forged head and a body which in many cases are hollow. However, some are delivered as massive which must be hammered at one end. The surface head of a rivet is delivered in different varieties such as flat head, small head, big head or countersunk.

To join two or more materials together, a rivet is placed in a hole slightly larger in diameter than the rivet itself. A force from the mounting tool is applied on the rivet by pulling a steel rod located inside until it disconnects with the aluminium rivet body (see [Figure 3.7](#)). By doing this, the rivet expands and the end deforms. This provides the necessary amount of tension to hold separate materials together.

Rivets are also produced in different materials including steel, copper, plastic or other metal alloys. The choice of rivets depends on the materials being joined together, the possible weight constraints, and the potential for corrosion. Aluminium/steel rivets are commonly used on aluminium sheet metal structures and consist of a aluminium body and a steel pin. [20]

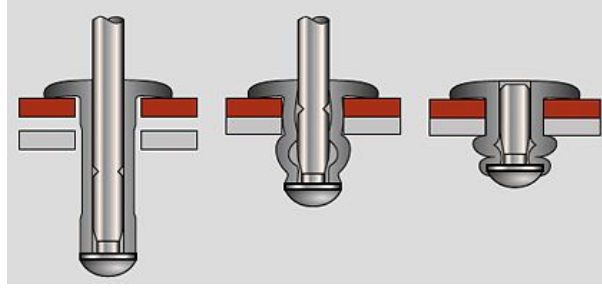


Figure 3.7: A typical "blind"-rivet.

### 3.5 Material and manufacturing cost

Manufacturing of a SWI is a time-consuming and expensive task. For this reason, it is decided to unveil the approximate amount of funds needed for the entire production process. This implies material costs as well as man-hours devoted for the entire process. The cost analysis covers both manufacturing costs of a single SWI, and all four SWIs combined. The labour costs of manufacturing the impactors are not taken included, but the devoted man-hours are listed.

#### 3.5.1 Material costs

As mentioned in [Table 3.2](#), the prior materials used for manufacturing the SWI were aluminium and steel. Aluminium sheets were purchased from Sandelwing Aviation Supply and delivered in standard dimensions which are listed in [Table 3.3](#). The structural steel intended for manufacturing of two steel-bases were purchased from a local supplier named E.A Smith AS, Trondheim.

Table 3.3: Materials applied to different parts of the SWI

Item	Material	Std. size mm (LxWxT)	Uses	Price per item(Euro)
1	Al2024T3-Sheet metal	1200x600x2	Main Spar	87,9
2	Al2024T3-Sheet metal	1200x600x1,6	Main Rib and Nose Rib	64
3	Al2024T3-Sheet metal	2400x1200x0,8	Skin	146,3
4	S355JR-Flat bar	6000x60x6	Flanges	16
5	S355JR-Beam	200x200x8 l=6000	Beam	340
6	S355JR-Plate	1200x600x5	Flanges	100

#### 3.5.2 Consumption of material and material cost per SWI

The aluminium 2024-T3 was purchased in advance of this project. To avoid shortage of the material, the ordered amount was decided to imply more than necessary. Considering international shipment time, the ordered amount of aluminum was more than needed. The cost analysis listed in [Table 3.4](#) is based on the consumption of material with respect to a single SWI.

Table 3.4: Material consumption and cost per SWI

Item	Material	Quantity	Price (Euro)
1	Al2024T3-Sheet metal	0,5	44
2	Al2024T3-Sheet metal	2	128
3	Al2024T3-Sheet metal	1	146,3
4	S355JR-Flat bar	0,25	4
5	S355JR-Beam	0,25	85
6	S355JR-Plate	0,5	50
7*	Rivets	500	30
Total material cost per SWI			487,3

\*Average cost of rivets per SWI.

### 3.5.3 Man-hours

A thorough process plan containing an estimate of man-hours was written. The plan consists of exclusively construction on the SWI's. Hours spent on planning and creating the dimensional drawings are not included in the plan. As expected, the time consumed in manufacturing the first and second SWI was greater than for the following builds. Table 3.5 shows the average amount of hours spent on manufacturing a single SWI. As the assigned students had no experience with manufacturing of the SWI's, it was expected a larger amount of devoted man-hours than usual.

Table 3.5: Hours spent on building a single SWI

Item	Hours spent
Cutting and welding steel base	30
Cutting and bending aluminium	30
Drilling holes steel base	8
Drilling holes aluminium	10
Mounting Rib-structur	6
Mounting skin	10
Total amount of hours spent	94

### 3.5.4 Testing facility

The test facility which had a suitable rig designed for compression tests was located at the Institute of Construction Technology. Due to highly expensive equipment, the institute required a local operator from the department to operate the rig, and to execute and monitor the compression tests. They charged an hourly fee of 110 Euro to cover the labour expenses and the use of facilities. In average, each test had a duration of approximately 1,5 hours and the total cost of each test was 165 Euro. A total amount of four tests were carried out, and eventually cost 660 Euro in total. The disposed hours at the test facility also included the time used for setup and calibration of the equipment intended for testing.



### 3.5.5 Cost from subcontractors

Due to lack of proper tools designed for bending sheet metals, Skala Fabrikk AS produced the main-ribs. Manufacturing of main-ribs included laser cutting and Computer Numerical Control (CNC) bending of the sheet metal. In total the manufacturing process of main-ribs considering one impactor cost 125 Euro. A total number of 18 main-ribs were produced at a total cost of 562.5 Euro. The two extra main-ribs were used as a back-up in case of any unexpected faults during manufacturing of the SWI's.

### 3.5.6 Total costs

The total cost of producing one SWI is presented in [Table 3.6](#). The costs include the material costs, the cost of work done by the subcontractor, and finally the cost for renting the test facility. As can be seen in [Table 3.6](#), the total costs of materials and manufacturing of a single impactor is listed. However, this calculation does not contain an overview of the total costs regarding facility rent and rent of tools. When taking the whole process into consideration, the costs increase significantly.

These SWI's were made by students with craft certificate which contribute to decreasing the costs, but yet maintaining sufficient quality of the product. If the work is too time consuming, a different solution can allow commercial producers to manufacture the entire SWI. This will however be more expensive due to hourly wages and the amount of hours devoted for production. If possible the recommendation is to carry out the work themselves as far as possible.

Table 3.6: Total costs in Euro per impactor

Item	Costs/impactor
Material costs	487,3
Subcontractor costs	125
Test facilities	165
Total cost(Euro)/impactor	777,3



# Chapter 4

## Methods

The following chapter contains a detailed description of the workflow of the manufacturing process of soft-wing-impactors and the intruder. In addition, the quasi-static compression test, tensile and shear tests of 3 and 4mm rivets, and tensile test of Aluminium 2024-T3 are described. Calibration of test equipment is also included in this chapter.

To obtain a perfect design match between the intended SWI and the SWI specified by NLR and the supervisor, CAD models, papers and reports have been carefully studied. The goal has been to achieve the necessary amount of knowledge and background information regarding dimensions and geometry. Test requirements and criteria have also been examined. In order to carry out a flawless manufacturing and test process without any major problems or faults this process has been important. The work was conducted by students with craft certificates. Prior knowledge and acquired skills within the previously named areas has made the process quite accessible. Based on the proposed design by NLR and the supervisor, and a number of parameters and requirements described in [chapter 2](#) and [chapter 3](#), the final SWI has been thoroughly manufactured and tested. This also includes rivets and the aluminium.

### 4.1 SWI - manufacturing process

#### 4.1.1 Equipment

The SWI's were manufactured in the work-shop at the Department of Engineering Design and Materials at NTNU. A large amount of the required equipment needed during the manufacturing process was available for use in the work-shop. Primary equipments like sheet metal cutter, drill press, arc welding machine, grinder and sheet metal bender were used to achieve the desirable geometries of various parts. Several other equipments were used, but is not taken into consideration based on the large amount of equipment used during this project.

Parts such as the main-rib had a complex geometry which was not possible to manufacture in the student work-shop. The solution was to contact a local expert on sheet metal manufacturing. In this case the subcontractor was Skala Fabrikker AS in Trondheim.

To be able to bend the nose-rib flanges as desirable, a form had to be designed and manufactured. The design and the dimensional drawings were carried out in NX and sent to the Department of Production and Quality at NTNU. They had equipment specifically designed for cutting plates up to approximately 200mm. In this case electric spark erosion cutting was applied to accomplish accurate measurements. The form proved to be one of the most important tools during the manufacturing process of the SWIs.

### 4.1.2 Steel-base

The steel-base was built according to the design from NLR and the supervisor [2]. The steel-base was designed to withstand forces applied to the SWI during the compression test. This way the same steel-base can be used for several tests without any major plastic or elastic deformations. In total two equal steel-bases were built. The intended function of the steel-base was to support the SWI from unrealistic failure modes such as collapsing inward during testing.



Figure 4.1: Steel-base.

1. Steel beam, 200x200x8mm.
2. Outer steel-supports with welded flat bar flanges.

Figure 4.1 shows the two steel-bases that were made. The aluminium section of the SWI was backed by a steel column with a square cross-section of 200x200x8mm and an overall length of 1550mm. The steel column was modelled as a rigid body in Abaqus by Rølvåg. It was therefore necessary to weld stiffeners inside the beam to prevent elastic deflections during the compression test. Stiffeners were made of square steel tubes with a cross-section of 60x60x6mm. The stiffeners were welded inside the beam and end lids were welded to each side of the beam which can be seen on Figure 4.2).

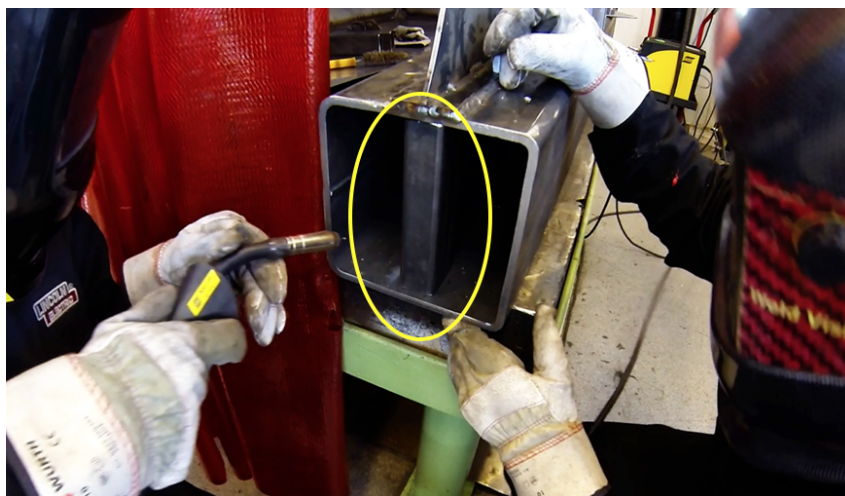


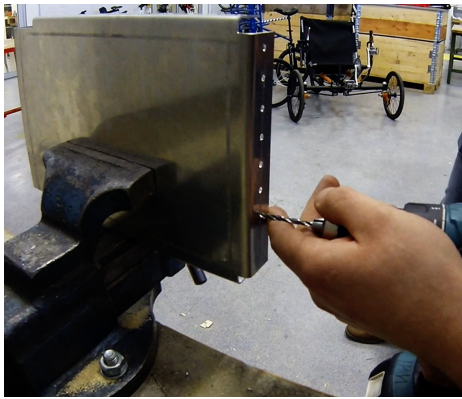
Figure 4.2: Stiffener.

To be able to mount the outer aluminium support-ribs to the steel-base and additionally apply extra support, it was necessary to weld a pair of outer steel-supports to the steel-base (nr.2 in [Figure 4.1](#). The outer steel-supports had welded flat bar flanges with holes intentionally to be used as a bolt connection between the outer support-ribs and the steel-base. The hole pattern on the flanges were first drilled, then welded to the outer steel-supports.

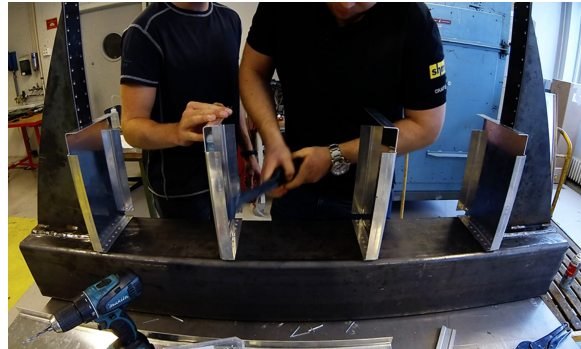
### 4.1.3 Main-rib

The main-ribs were made of 1,6mm thick aluminium 2024-T3 sheet-metal. The sheet-metal was cut by a laser tool and bent in an automatic bending machine. The main-ribs were however manufactured by Skala Fabrikker AS as mentioned earlier. The final outcome from their manufacturing process was a product with high quality and precision. All main-ribs were identical which made the assembly work easier and more efficient.

The hole pattern of the bottom section of the main-rib was marked identical to the steel-base and the main-spar. The hole pattern of the main-spar was used as a measurement for drilling holes at the steel-base since the distance and amount of holes were identical. [Figure 4.3a](#) shows the hole pattern on the main-rib. Furthermore, the main-ribs were mounted to the steel base by using 4mm rivets. In total, each soft wing impactor consisted of four main-ribs. [Figure 4.3b](#) shows the assembly process of the main-ribs.



(a) Drilling of main-rib.



(b) Mounting of main-ribs.

Figure 4.3: Manufacturing of main-ribs.

### 4.1.4 Main-spar

The main-spar was made of a 2mm thick aluminium 2024-T3 sheet-metal. The main-spar was cut and bent according to measurements specified in the dimensional drawings. The overall length of the main-spar was equal to the width of SWI, 1000mm respectively. The width of the main-spar was equal to the width of the main-rib and nose-rib, 200mm respectively. This was the least complex part to manufacture. The plate had only two 90 degree bent flanges lengthwise shown in [Figure 4.4a](#), and the height of the flanges were 30mm. The flange-surface was used when attaching the skin to the internal rib-structure. The main-spar was drilled according to the exact identical hole pattern as the main-rib and the nose-rib. It was necessary to be accurate with the hole pattern since the main-spar was mounted between the main-rib and the nose-rib. This transition was crucial with respect to shear forces applied to the rivets. Since the compression stroke was set to 500mm, the main-spar would suffer from large deformation forces. Based on the requirement of 45kN which is the max permissible force applied to the wing, the rivets must not break before this limit is reached. This required that the hole transition between

the nose-rib, main-spar and main-rib was perfectly aligned and equally sized. Only by this an equal force distribution could be achieved.

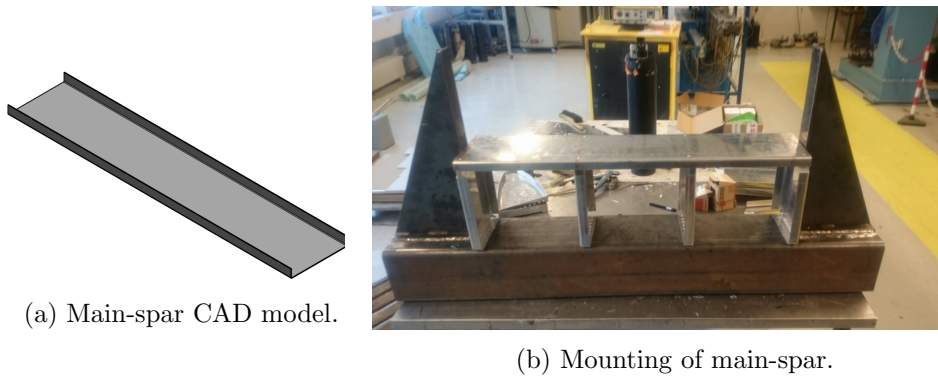


Figure 4.4: Manufacturing of the main-spar.

Figure 4.4b shows the main-spar mounted on top of the main-ribs. The main spar was drilled in this position to ensure identical hole pattern between the main-spar and the main-rib.

#### 4.1.5 Nose-rib

The nose-ribs were made of 1,6mm thick aluminium 2024-T3 sheet metal. These supporting ribs were the most complex parts to manufacture. The nose-ribs have flanges that must be bent in order to make a radius. To be able to make this part, a form had to be designed and manufactured. This is further described in subsection 4.1.6. The idea behind the form was to be able to form the sheet metal in an appropriate way. The plate had to be cut out from a flat-pattern drawing. The flat-pattern model was designed by using the sheet-metal function in NX. Figure 4.5a shows the design of the flat-pattern model which was used to make the flat-pattern cutting drawing.

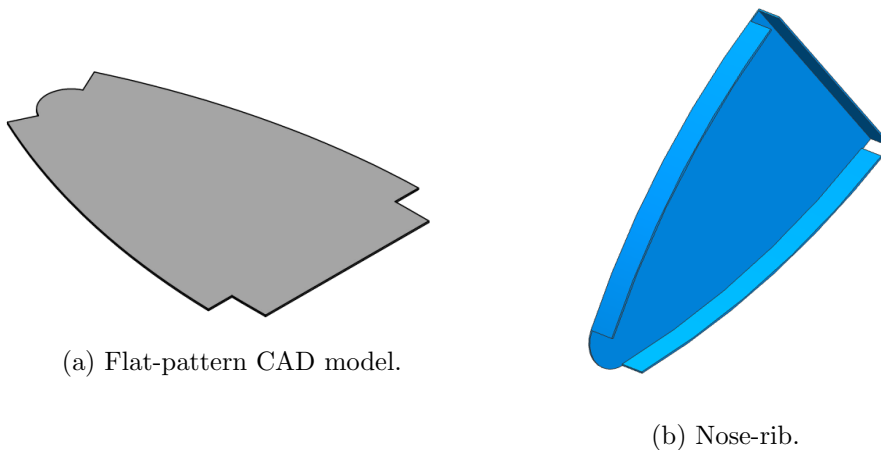
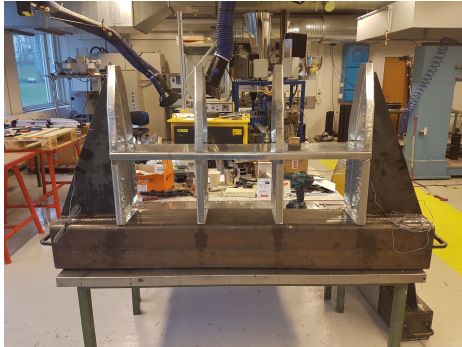


Figure 4.5: CAD model of nose-ribs.

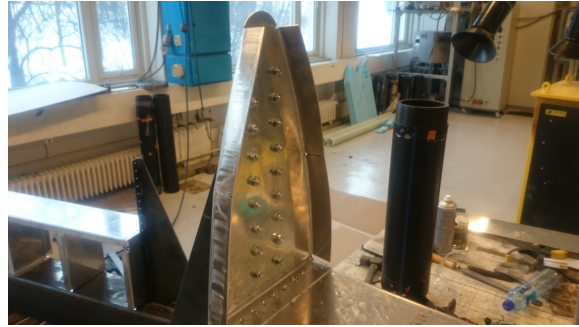
The plate was pressed through the form by using a hydraulic press. Grease was applied to the plate and form to avoid high shear forces on the aluminium during the stance operation. Figure 4.5b illustrates the final shape designed by making a NX-CAD drawing of the nose-rib. A solution often used when forming aluminium sheet-metals is to pre-heat the metal and instantly cool it down by using cold water. In one case this was carried out, but proved to be impossible for

this type of aluminium as it started to crack up. The conclusion was to proceed by cold-shaping the material.

Holes through the straight flange which must be mounted against the main-spar were drilled in order to replicate the same hole pattern as the main-spar and main-rib. This simplified the assembly of the nose-ribs. Rivets were used to attached the main-rib, main-spar and nose-rib together.



(a) Mounting of nose-ribs.



(b) Bolt connection.

Figure 4.6: Nose-rib assembly.

The nose-ribs were mounted to the main-spar and main-rib shown in [Figure 4.6a](#). The supporting rib structure was connected to the steel-base by using M6 bolts shown in [Figure 4.6b](#).

#### 4.1.6 Form - design and manufacturing

The shape of the nose-rib was set in advance, because of the complex shape it was challenging to find a good solution to produce the part. There were two realistic options on how to produce the nose-rib. One of the options was to manually form the sheet metal by using a hammer. The other option was to shape the sheet metal by using a form together with a hydraulic press. The conclusion was to make a form since hammering on the aluminium could potentially damage the material properties and create initial cracks or other deformations.

A form which consisted of a outer part and an inner part was manufactured based on design executed in NX. Both the outer and the inner part were cut out from the same 30 mm thick aluminium plate. The plate was cut by using an electric spark erosion cutter. The form was designed with tolerances to ensure clearance between outer and inner parts during pressing. Total clearance between the inner and outer form was 7,2mm. During pressing of the sheet metal, the clearance was  $(7,2\text{mm}-1,6\text{mm}-1,6\text{mm})$  4mm. This ensured a gap of 2mm on each side during pressing. The gap was important in order to reduce shear force acting on the sheet metal surface during the process of shaping the rib.

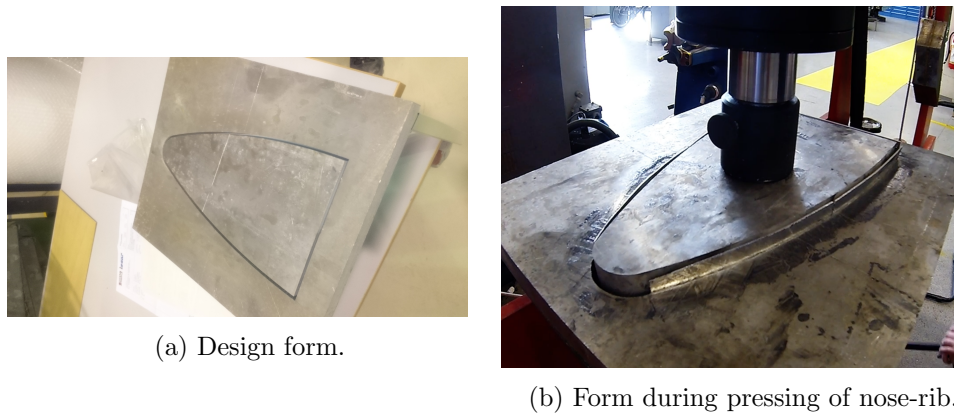


Figure 4.7: Form designed for shaping the nose-rib.

Figure 4.7 illustrates the method of shaping the sheet-metal to its final shape. The form combined with the applied hydraulic compression force was a good solution that work well. Producing the nose-ribs in this manner was time saving compared to manufacture it by use of hand tools.

#### 4.1.7 Skin

The skin was made of a 0,8mm thick aluminium 2024-T3 sheet metal. The skin was cut to a width of 1000mm and a length of 1740mm. Since the skin was made out of a thin aluminum plate, it was ductile which made it easy to form. To simplify the assembly of the skin, the form of the leading edge was made in advance by making a tool specifically design to form a radius of 30mm. This was executed by pressing a steel tube down at the middle of the plate. The steel tube had equal radius as the leading edge of the SWI. By doing this the skin fit easily over the nose-rib during the assembly. Figure 4.8 shows the final result after mounting the skin.

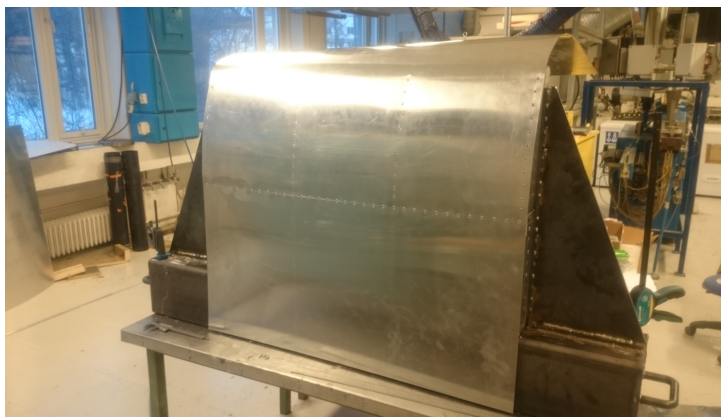


Figure 4.8: Skin mounting.

The skin was attached to the rib-structure by using rivets with a center-center distance of 30mm. The center-center distance of the rivets was identical to the one used in the virtual model. In total approximately 300 rivets were used to attach the skin. The holes were drilled with a 0,1mm larger diameter than the rivets, which was the minimum recommended from the supplier, a 3.1mm drill respectively. The rivets were placed in the hole and a pneumatic rivet pistol was used to drive the rivets. To ensure proper connection between the skin and the rib-structure, the rivets were attached simultaneously as the holes were drilled.





Figure 4.9: Complete assembly.

#### 4.1.8 "Dummy" intruder mast

Figure 4.10a illustrates the manufactured intruder. It was manufactured based on identical measurements with respect to the intruder used in the virtual compression test. In Abaqus the intruder was modelled as a rigid body. Since the intended intrusion mast was modelled as a rigid body to prevent elastic deformation during the compression sequence, the physical mast had to be manufactured identical to the one in Abaqus. To achieve a rigid body for the physical model, stiffeners were welded inside the beam and lids were welded to each side of the beam. See Appendix A for more detailed drawings.

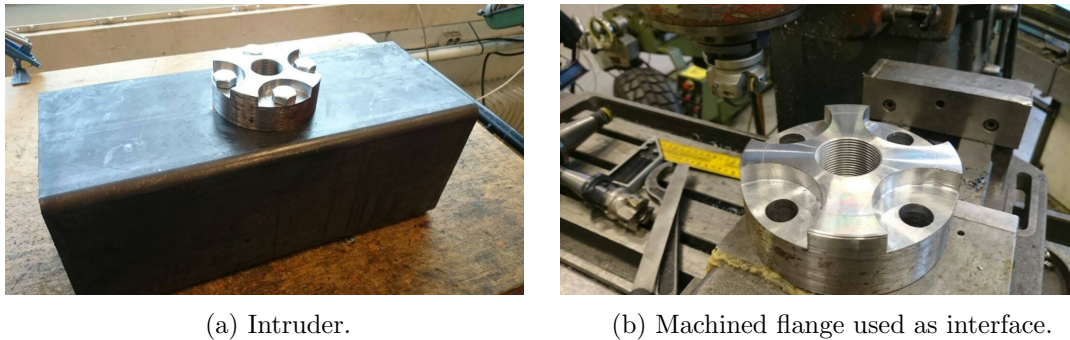


Figure 4.10: Intruder intended for the compression tests.

Since the intended compression rig was using a large, threaded bolt below the load cell, an interface between the intrusion mast and the load cell had to be made. The threaded hole in the flange (Figure 4.10b) was machined to fit the threaded bolt connection at the load cell of the test rig. Due to the large threaded dimension (M59x2), it was necessary to machine the threads in the lathe.

## 4.2 SWI - overview

In total four SWI's were built throughout this project. Identical manufacturing methods were used at each SWI. Impactor number 1 and 2 were identical. Impactor number 3 and 4 have identical designs and materials as 1 and 2, but the rivet quality is improved. The skin rivet diameter is slightly increased on Impactor 4. In this case sealed aluminium rivets were used on impactor 4. Increasing the diameter of the skin rivets to 3,2mm was necessary since 3,2mm was the only standard available from supplier for this type of rivet.

Table 4.1: Rivet material data of SWI 1 and 2.

Part	Impactor 1	Impactor 2	Impactor 3	Impactor 4
Rib rivet diameter (mm)	4	4	4	4
Maximum shear strength* (N)	850	850	1330	1640
Maximum tensile strength* (N)	1200	1200	1910	2220
Skin rivet diameter (mm)	3	3	3	3,2
Maximum shear strength* (N)	800	800	800	1110
Maximum tensile strength* (N)	1000	1000	1000	1400

\*Material data from supplier.

## 4.3 Quasi-static compression test

The Quasi-static compression test was performed in the Construction Laboratory at NTNU. In cooperation with professionals from the laboratory, four tests were carried out.

### 4.3.1 Equipment

The main equipment used for testing was a hydraulic compression test rig. The test rig was equipped with a load cell which measured the applied force. The test rig also measured time and piston stroke during testing. All measured data was processed by the Catman-AP V3.3-2 software. To be able to measure strain in the component it was necessary to mount strain gauges. The strain gauges were glued to the SWI and connected to the computer. The software processed the electrical signal, and the output values from Catman measured strain in micrometer. As the strain gauges were mounted to vested interests, no detailed description will follow.

### 4.3.2 Test procedure

A test procedure was made to ensure that the tests were performed similar each time and similar to the virtual simulation in Abaqus. The reason was to ensure realistic results so that all tests were performed identical without any deviations. A test procedure was also necessary for the operators. Based on the procedure they were able to adjust the settings on the test rig equally for each test. Some of this procedure are already mentioned in advance in [subsection 2.3.2](#), but will be reproduced in this section to provide an overview of the test sequence.

- Mount the intrusion mast to the threaded bolt located at the load cell.
- Install a guide to make sure the intrusion mast will keep its position during the test.
- Place the SWI in center of the intrusion mast.
- Adjust compression settings in Catman (+-2% margin of failure):
  - 50mm/min
  - 500mm stroke
  - Logging: 10Hz
- Attach strain gauges:
  - Verify the electrical connections
  - Calibrate by adjusting the values equal to zero.
  - Gaugefactor: 2,12
  - Bridgefactor: 1
- Live monitoring to verify force vs. intrusion.
- Start test.
- Record the compression sequence with a camera.
- When finished, receive the final output data.

### 4.3.3 Test setup

The hydraulic test rig had to be adjusted especially for the testing of the SWI. The height of the rig was adjusted to an equivalent height as the impactor. A clearance of 5mm was added to the height of the test rig, this to ensure clearance between the SWI and the intrusion mast. Figure 4.11 shows the rigging of the SWI. It was important to ensure that the SWI was placed in the center in relation to the mast. To ensure this, measurements were taken and controlled before testing.



(a) Rigging.



(b) Centering the SWI.

Figure 4.11: Test setup in a hydraulic rig.

During testing of the first SWI, a fault was detected. The mast rotated and had a small misalignment relative to the baseline. The results were however not particularly affected, but a guideline made of wood was applied to avoid misalignment for the next tests.

To ensure the necessary amount of measurements during the testing, the Catman software settings was set to 10Hz. This means that the software will measure and store data 10 times each second. Due to the intrusion speed of 50mm/min this was concluded to be appropriate.

## 4.4 SWI - compression tests

The testing was spread over a period of two days. This was necessary due to the reuse of the steel bases. Testing of SWI 1 and 2 took place on the first day, on the second test 3 and 4. After testing of the two first SWI's it was determined to change the rivet quality for the two next builds. The forces obtained in the two first tests were not sufficient, and it was clear that the rivets used on these did not withstand the applied shear forces created when the intrusion mast entered the main-spar.

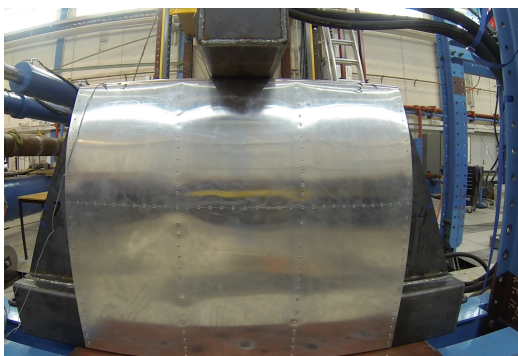
### 4.4.1 Test 1 - SWI 1

Test 1 was carried out according to the test procedure and proceeded without any major problems. After a stroke length of 100mm the mast impactor started to slowly rotate, but the test continued despite this. As the test had already begun, the conclusion was to finish the test before the error can be rectified. For the following tests the guideline made of 2X4" wood was mounted. The guideline prevented the mast impactor from rotating during the compression sequence. [Figure 4.12](#) shows the SWI before and after the quasi-static compression test. The figure reveals the misalignment of the mast after the test (lower position). Logging of force, displacement and time was done simultaneously as the test unfolded.

Table 4.2: Impactor 1.

Part	Impactor1
Rib rivet diameter (mm)	4
Maximum shear strength* (N)	850
Maximum tensile strength* (N)	1200
Skin rivet diameter (mm)	3
Maximum shear strength* (N)	800
Maximum tensile strength* (N)	1000

\*Suppliers material data



(a) Before testing.



(b) After testing.

Figure 4.12: Compression test 1.

#### 4.4.2 Test 2 - SWI 2

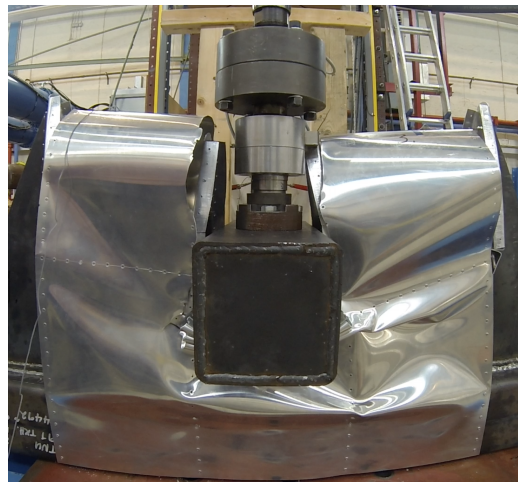
Test 2 was carried out according to the same test procedure. Unlike test 1, the test rig was equipped with a guiding on the intrusion mast. Figure 4.13 shows that the mast impactor is centered and has not rotated during the test.

Table 4.3: Impactor 2.

Part	Impactor2
Rib rivet diameter (mm)	4
Maximum shear strength* (N)	850
Maximum tensile strength* (N)	1200
Skin rivet diameter (mm)	3
Maximum shear strength* (N)	800
Maximum tensile strength* (N)	1000



(a) Before testing.



(b) After testing.

Figure 4.13: Compression test 2.

### 4.4.3 Test 3 - SWI 3

Compression test 3 was the first test carried out after the rivet quality was upgraded. The 3mm rivets remained equal to previous tests since the 3mm rivets were already the strongest rivets delivered from the supplier. In this test the 4mm rivets used for mounting the rib structure had 56% higher shear strength compared to test 1 and 2. The purpose of the new rivet quality was to approach a higher maximum compression force during testing. The previous tests (1 and 2) disclosed that the rivets on the main spar were the weak link during testing. The rivets were cut off as a result of high shear forces.

Table 4.4: Impactor 3.

Part	Impactor3
Rib rivet diameter (mm)	4
Maximum shear strength* (N)	1330
Maximum tensile strength* (N)	1910
Skin rivet diameter (mm)	3
Maximum shear strength* (N)	800
Maximum tensile strength* (N)	1000



(a) Before testing.

(b) After testing.

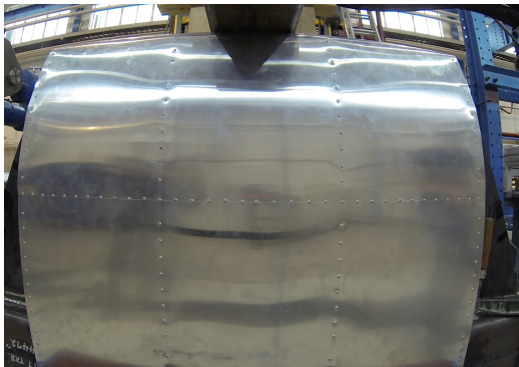
Figure 4.14: Compression test 3.

## 4.4.4 Test 4 - SWI 4

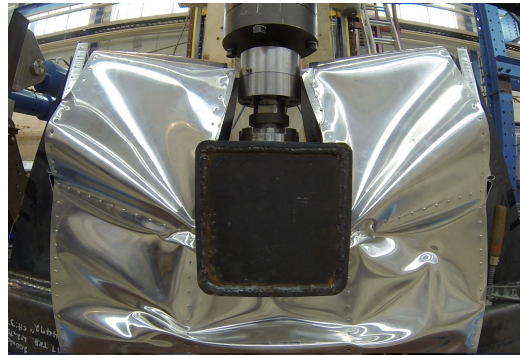
Compression test 4 was the final test conducted of the SWI's. Impactor 4 was the only impactor built with sealed rivets. The reason for using sealed rivets was due to similar mechanical properties as massive rivets. Due to lack of knowledge regarding aircraft rivets, the technical flight department at Notodden was contacted. In most cases they used massive rivets which were hammered. Due to the design of the SWIs it was difficult to reach inside when the skin was mounted, the choice was to substitute with rivets of similar mechanical properties. The sealed rivets used on impactor 4 were by far the strongest rivets used. Since the supplier not was able to deliver rivets which were 3mm in diameter, the next standard of 3,2mm were used for the skin. Rivets for the rib-structure have the same dimensions as the previous tests. In test 4 the 4mm rivets had 93% higher shear strength compared to test 1 and 2. Compared to test 3 the 4mm rivets had 23% higher shear strength. The 3,2mm rivets used for mounting the skin had 39% higher shear strength compared to test 1, 2 and 3.

Table 4.5: Impactor 4.

Part	Impactor4
Rib rivet diameter (mm)	4
Maximum shear strength* (N)	1640
Maximum tensile strength* (N)	2220
Skin rivet diameter (mm)	3,2
Maximum shear strength* (N)	1110
Maximum tensile strength* (N)	1400



(a) Before testing.



(b) After testing.

Figure 4.15: Compression test 4.



## 4.5 Virtual compression test

The virtual compression test of the SWI was carried out by the supervisor. The software used for this simulation was Abaqus. This test was conducted with relatively similar test procedure as the physical tests. This implied a speed of 50mm/min, but with a longer stroke of 620mm. Logging of both force and displacement have been done during the test. In the virtual test there were no limitations according to the stroke length of the intruder. This test was therefore conducted with maximum stroke length. To be able to compare the virtual and physical results, a limitation of the stroke length was set. The physical tests had a maximum stroke length of 450mm. It was therefore naturally to limit the virtual test to an equal stroke length as the physical test. The start position of the test is shown in Figure 4.16a. Here the stroke length is 0mm. Figure 4.16b shows the SWI 9 minutes into the virtual test. After 9 minutes the stroke length is 450mm. This test was however not the optimized model, and results were therefore not directly comparable since results from the physical tests are meant to be used during calibration.

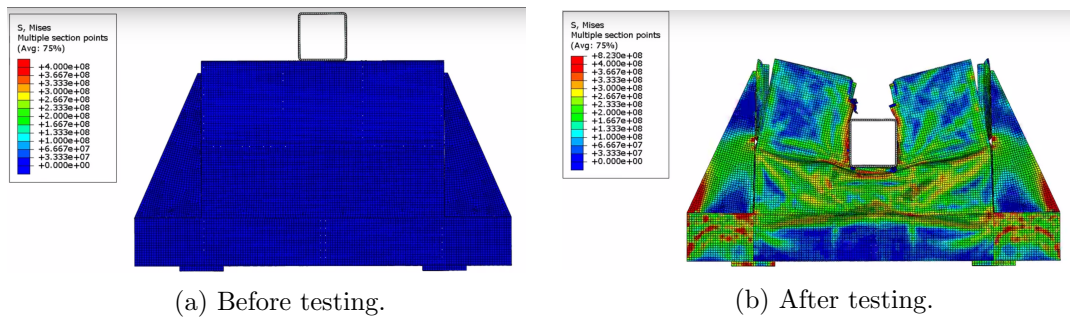


Figure 4.16: Virtual compression test.

## 4.6 Rivets - test of mechanical properties

In order to verify its mechanical properties, material testing of the rivets was necessary. The purpose of the tests was to disclose the maximum shear and tensile strength that the rivets were able to withstand. To be able to optimize the virtual model so the results from the virtual crash test in Abaqus can be compared with physical compression tests in lab, the mechanical properties of the rivets must be known. It was assumed that a certain safety factor was added to the rivets by the suppliers. Since the safety factor was unknown, it was necessary to perform shear and tensile testing of the rivets to be able to verify the results. The rivets used in SWI 1 and 2 were tested. The results of these tests were enough to calibrate the material model in Abaqus. Rivets used on SWI 3 and 4 are therefore not tested, but is sufficient with respect to safety factor and mechanical properties provided by the subcontractor.

### 4.6.1 Calibration of internal load cell

A calibration of the internal load cell in the tensile test rig was necessary to verify the load cells measurements. An already calibrated external load cell was attached in the tensile test rig. The external load cell (load cell used for calibration of test equipment) had live monitoring on a computer by using the Catman software. The internal load cell in the test rig had also live monitoring in the test rig. The internal load cell showed exactly the same values as the internal load cell and no further calibration was necessary. See [Figure 4.17](#) for test rig setup.

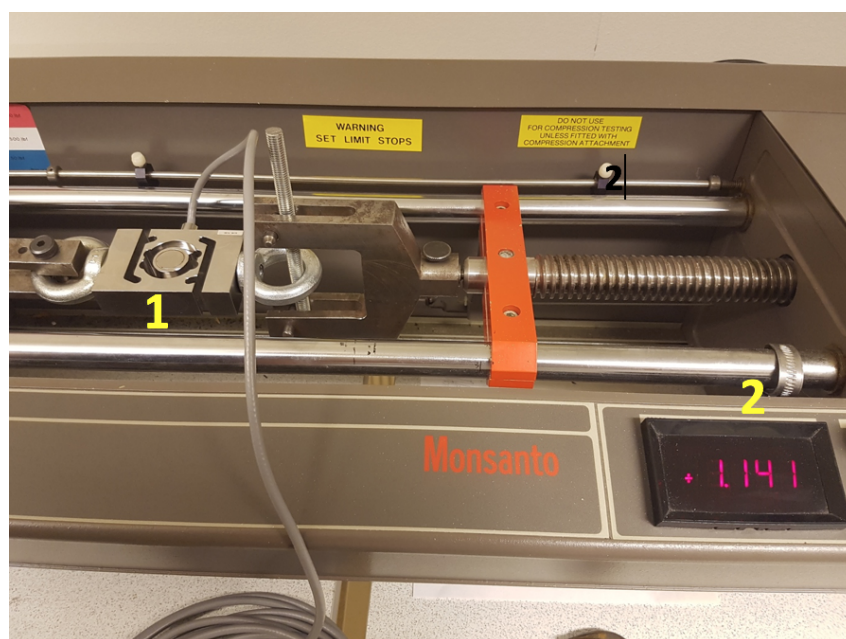


Figure 4.17: Calibration.

1. External load cell.
2. Internal load cell tensile test rig.

#### 4.6.2 Test of maximum shear force

To be able to test the maximum shear force of a single rivet, two plates were bonded together by a single rivet. The plates were made of steel and had higher material quality than the rivet itself. The plates were bonded together with a certain overlapping and by this both ends could be mounted in the tensile test rig. [Figure 4.18](#) shows the test set up. In total six rivets of each size were tested to find an average maximum shear force. Six rivets with a nominal diameter of 3mm and six rivets with a nominal diameter of 4mm.

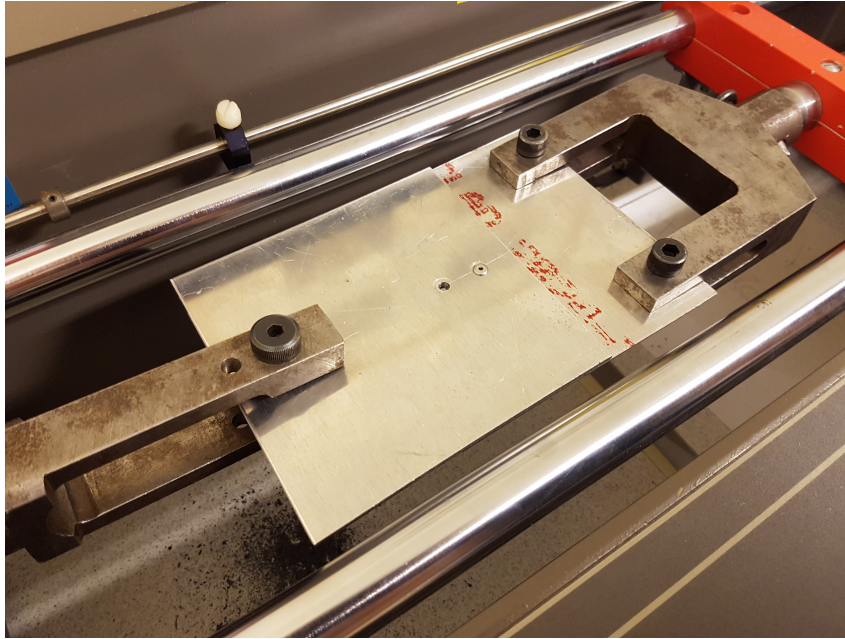


Figure 4.18: Sheartest

### 4.6.3 Test of maximum tensile force

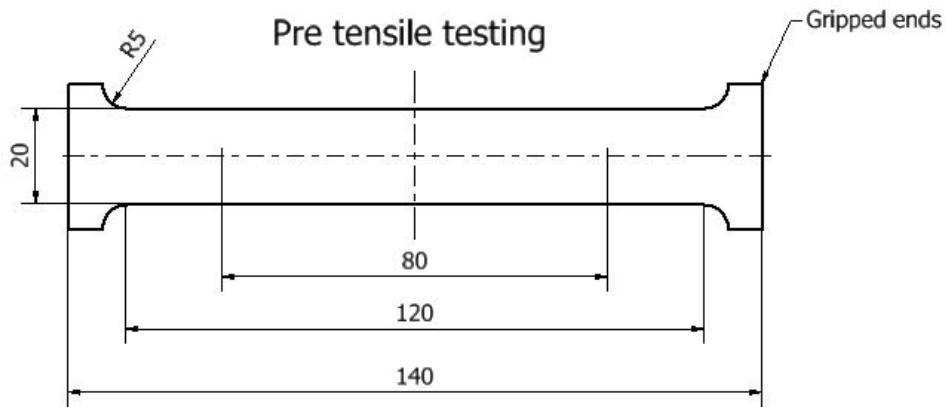
To be able to test the maximum tensile force of a single rivet, two plates were bonded together by a single rivet. Unlike the shear force test the plates now had to lay in the horizontal plane. Therefore some modifications to the plates and the test rig had to be implemented. M12 nuts were welded on each plate and M12 threaded rods were used to stretch the plates in the test rig. The threaded rods had to be machined to fit inside the tool of the test rig. [Figure 4.19](#) shows the machined threaded rods which were attached to the tensile test rig. The plates were combined by a single rivet placed in the centre of the nuts.



Figure 4.19: Tensile test.

## 4.7 Aluminium 2024-T3 - material tensile test

To verify the material properties of the purchased Aluminium 2024-T3, a material test was necessary. The purpose of the test was to ensure correspondence between the material data used in the virtual analysis and in the physical test. Material properties of the Aluminium 2024-T3 were available from MatWeb, but a material test was necessary to assure the quality of the material. Material data from MatWeb were used to compare the test results. The aluminium was tested according to standard ISO 6892-1: "Metallic materials - Tensile testing - Part 1: Method of test at ambient temperature" [21]. A test specimen was made out of a 2mm thick aluminium plate and tested in a hydraulic tensile test rig. The dimensions of the specimen is described in ISO 6892-1. Figure 4.20 shows the geometry of the test specimen before testing.



Note: (All measures in mm)  
 Original gauge length=80  
 Parallel length=120  
 Total length of test piece=140  
 Original width of the parallel length of the flat test piece=20  
 Thickness of test piece=2mm  
 ISO 6892-1:2009, Annex B

Figure 4.20: Test specimen before tensile testing.

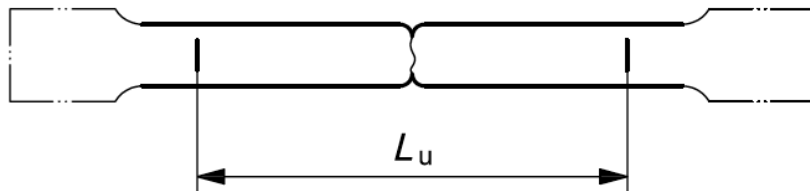


Figure 4.21: Test specimen after tensile testing.

Figure 4.21 illustrates the test piece after testing. After the tensile test, new measurements of the width and thickness were taken. The new cross-sectional area was used to calculate true stress. The force and displacement during the test were logged on a computer by using the Catman software. The data was used to verify the mechanical properties which intentionally will be used to calibrate the material model in Abaqus.

Figure 4.22 shows the aluminium test specimen after the tensile testing. The local constriction was easy to spot around the fracture area. As mentioned above, this constriction created a new cross-sectional area.

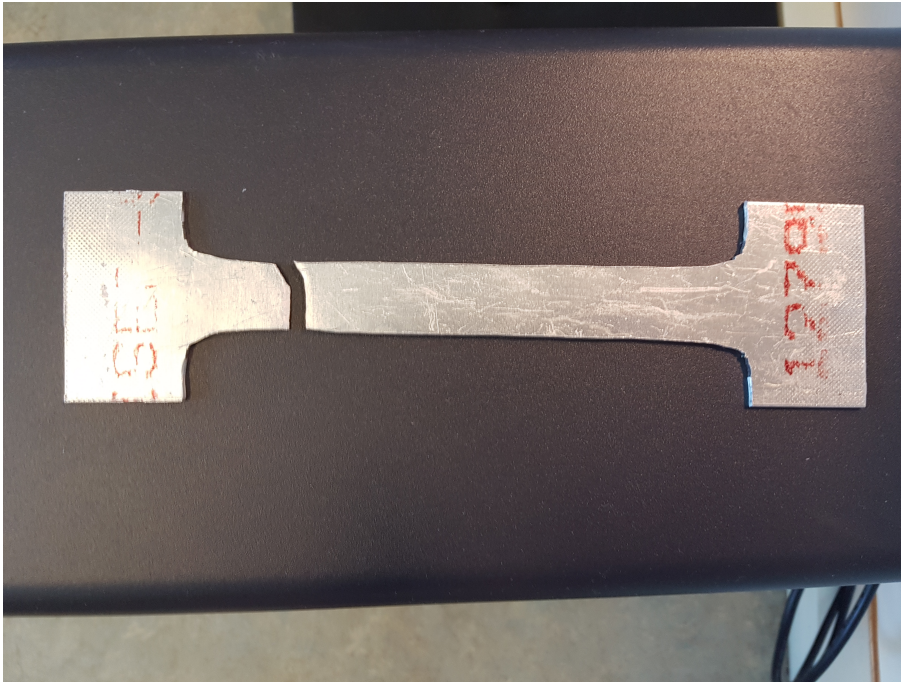


Figure 4.22: Test specimen after tensile testing.

# Chapter 5

## Test results

In this chapter various results from tests carried out during the project will be covered. This implies results from each of the four compression tests carried out on various soft-wing-impactors, and tests carried out to verify mechanical properties of rivets and the Aluminium 2024-T3. The results are listed chronological and begins with rivets, secondly the Aluminium 2024-T3 and finally various SWI compression tests. Mode 1-6 in the quasi-static compression tests are further described in [subsection 3.2.1](#).

Rivets were tested by conducting multiple test iterations with respect to shear and tensile resistance. 3mm and 4mm rivets respectively. The results are listed in order to cover all tests carried out on 3mm first and secondly 4mm.

As an outline, it is chosen to briefly comment some of the characteristics that were detected in the test results listed in the following sections. A more detailed description and discussion about various test results will be further presented in [chapter 6](#). Results regarding strain gauges are not listed in the results since these were logged based on vested interests.

### 5.1 3 and 4mm rivets

As mentioned above these tests were carried out with respect to shear and tensile strength of 3 and 4mm rivets. As expected, each and one of the rivets tested during this project had greater maximum shear and tensile strength than specified by the supplier. The reason was due to a supplied safety factor. [Table 5.1](#) shows the average force created from the most reliable tests. These are further listed as graphs which illustrate the material characteristic throughout various tests.

Table 5.1: Force resistance of rivets.

Rivet 4mm	Max strength from supplier	Max strength tested
Max shear strength (N)	850	1220
Max tensile strength (N)	1200	2060
Rivet 3mm	Max strength from supplier	Max strength tested
Max shear strength (N)	800	900
Max tensile strength (N)	1000	1200

### 5.1.1 Rivets 3mm - maximum shear force

The maximum shear strength tested on a 3mm rivet were 900N. This is 12,5% greater than material data available from the supplier. [Figure 5.1](#) visualize force vs. displacement for this test.

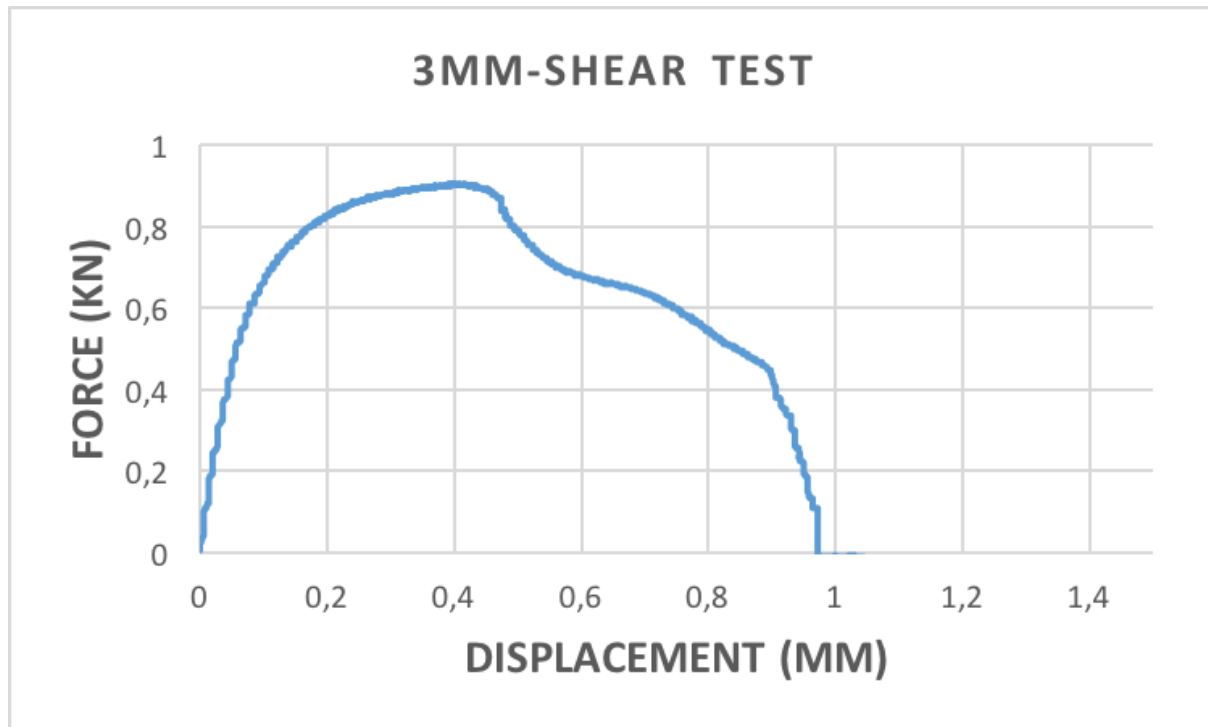


Figure 5.1: Shear Strength 3mm.



### 5.1.2 Rivets 3mm - maximum tensile force

The maximum tensile strength tested on a 3mm rivet was 1200N. This is 20% greater than material data available from the supplier. [Figure 5.2](#) visualize force vs. displacement for this test.

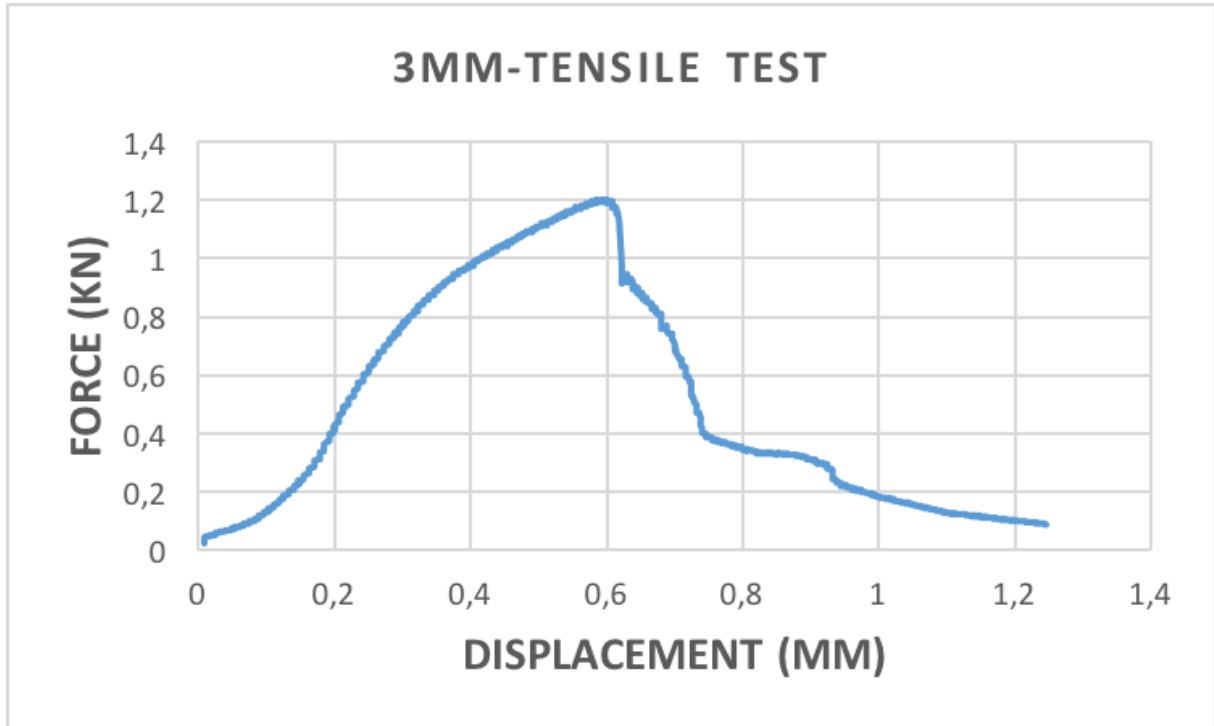


Figure 5.2: Tensile Strength 3mm.

### 5.1.3 Rivets 4mm - maximum shear force

The maximum shear strength tested on a 4mm rivet was 1220N. This is 43,5% greater than material data available from the supplier. [Figure 5.3](#) visualize force vs. displacement for this test.

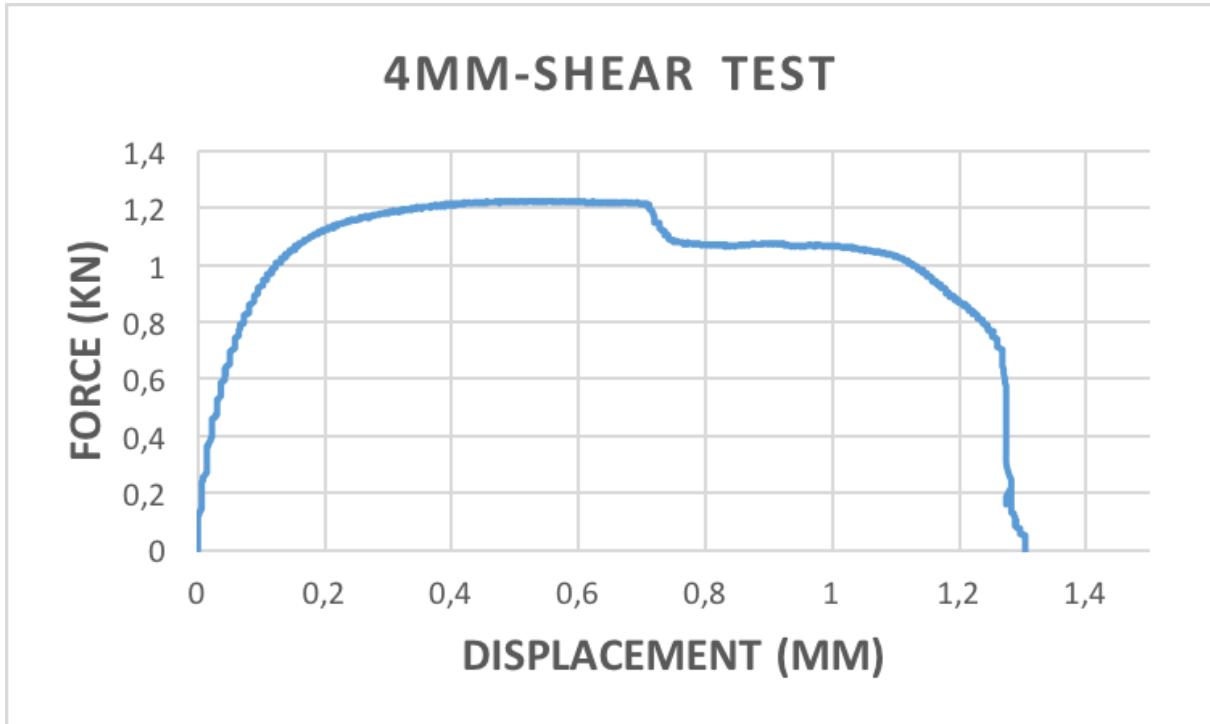


Figure 5.3: Shear Strength 4mm.

#### 5.1.4 Rivets 4mm - maximum tensile force

The maximum tensile strength tested on a 4mm rivet was 2060N. This is 76% greater than material data available from the supplier. [Figure 5.4](#) visualize force vs. displacement for this test.

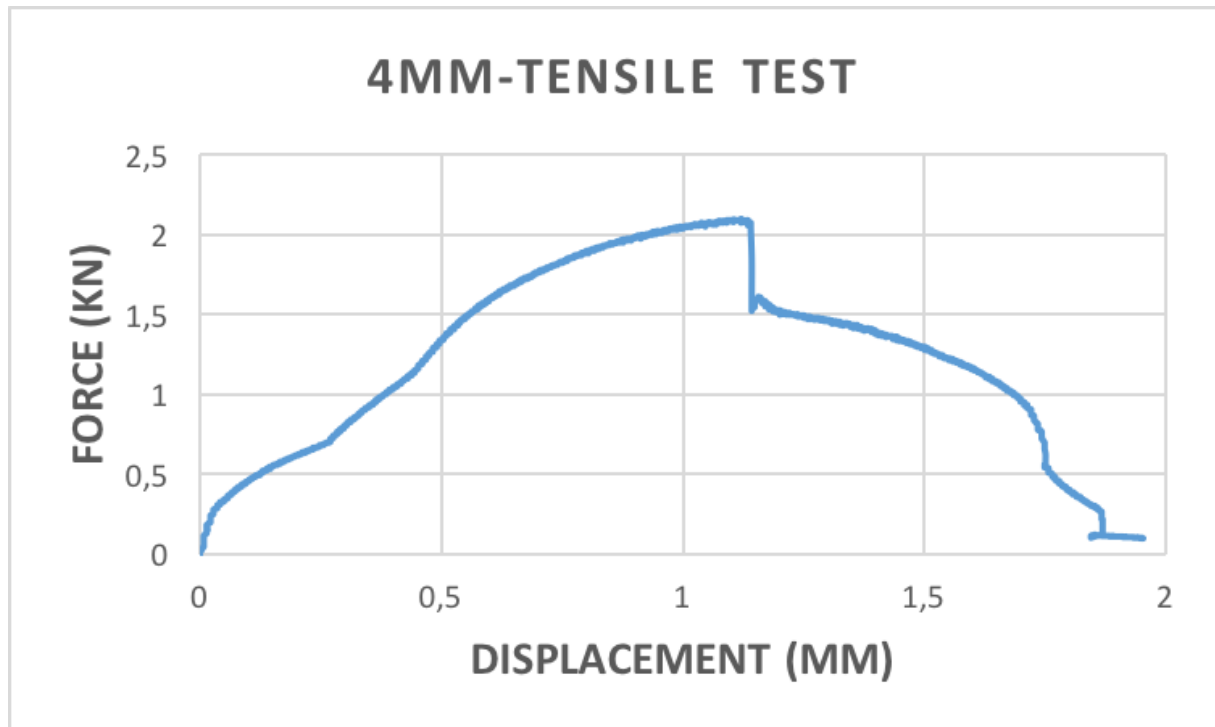


Figure 5.4: Tensile Strength 4mm.

## 5.2 Tensile test of Aluminium2024-T3

Results from the material tensile test of the Aluminium 2024-T3 sheet are presented in [Table 5.2](#). These results are compared to the mechanical properties specified in Matweb [[22](#)]. The original cross-section of the test specimen was used to calculate both yield strength and ultimate tensile strength (UTS). Yield and UTS calculations are shown in [Equation 5.1](#) and [Equation 5.2](#). Maximum elongation was also calculated which can be seen in [Equation 5.3](#). The initial length of the test specimen was set to 80mm and the total displacement before fracture was 14mm (15mm-1mm). See [Figure 5.5](#). Dimensions regarding the pre-tested specimen are available in [Figure 4.20](#). Before testing the original length of the intended test piece was 80mm. After testing the measured value of the new gauge length  $L_u=94\text{mm}$ . The width was 18,5mm and the thickness was measured to be 1,85mm. The new cross-sectional area calculated after the tensile test was  $34,225\text{mm}^2$ . This cross-sectional area was used to calculate true stress in the test specimen. [Figure 5.6](#) shows the result of true stress vs. strain of the aluminium 2024-T3.

$$\sigma_{yield} = \frac{F_{yield}}{A_{original}} = \frac{14000N}{40\text{mm}^2} = 350\text{MPa} \quad (5.1)$$

$$UTS = \frac{F_{max}}{A_{original}} = \frac{19000N}{40\text{mm}^2} = 475\text{MPa} \quad (5.2)$$

$$Elongation = \frac{Final\ length - Initial\ length}{Initial\ length} \times 100\% = \frac{94\text{mm} - 80\text{mm}}{80\text{mm}} \times 100\% = 17,5\% \quad (5.3)$$

The mechanical properties provided by Matweb were virtually equal to those revealed from the tensile test. Since there is a correlation between the tests, it is appropriate to use the material data from Matweb.

Table 5.2: Test aluminium.

Mechanical properties	Matweb	Test result
Tensile yield strength (MPa)	345	350
Ultimate tensile strength (MPa)	483	475
Elongation at break-point (%)	18	17,5

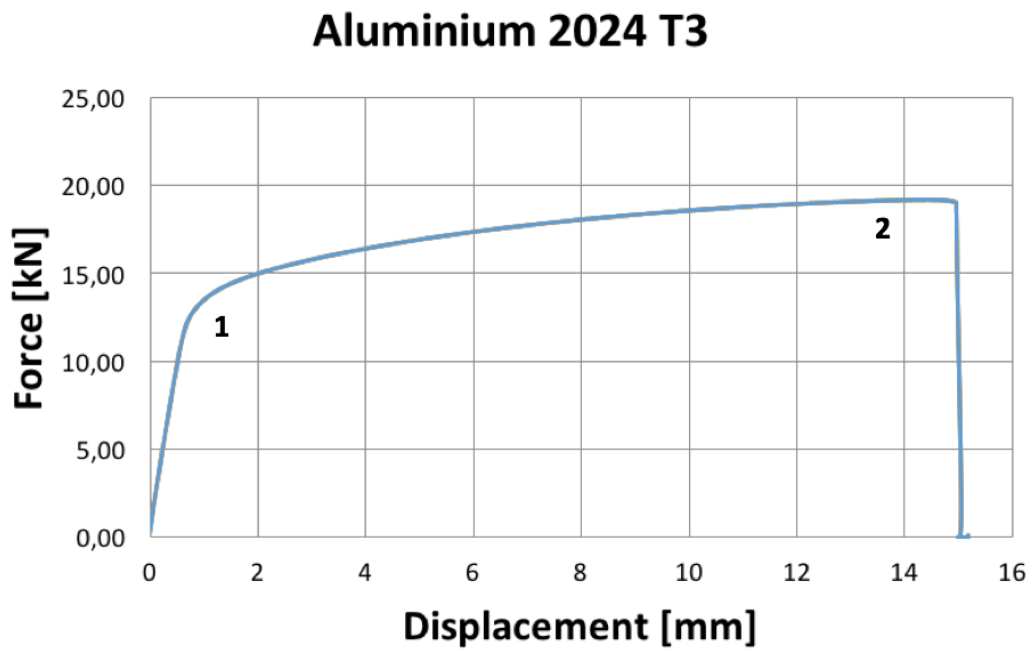


Figure 5.5: The resulting force vs. displacement from the tensile test. 1: Yield and 2: UTS.

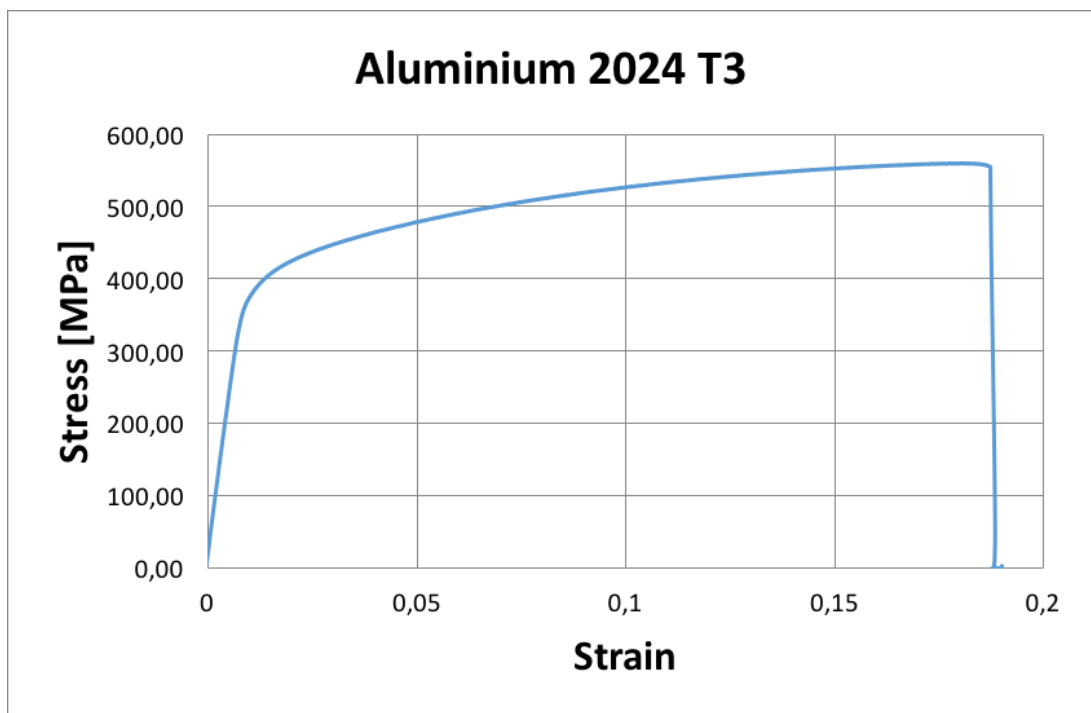


Figure 5.6: Stress vs. strain.

## 5.3 Soft-wing-impactor compression test

### 5.3.1 Virtual test

Results from the virtual compression test carried out in Abaqus by the supervisor are shown in [Figure 5.7](#). This is however not an optimized model, but it has been taken into consideration as a reference. After a displacement of 100mm the initial compression peak force reached approximately 34kN. A rather constant force was logged from 120mm to 375mm. From 375mm to 450mm the aluminium was stacked towards the main spar and the forces increased drastically. After a displacement of 450mm the force had reached 50kN.

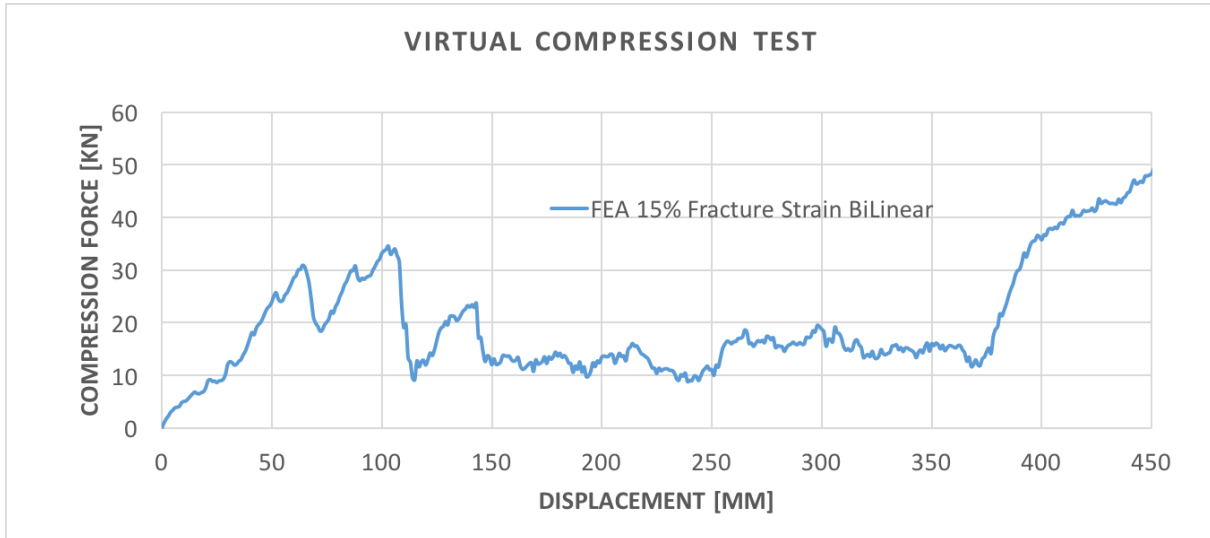


Figure 5.7: Virtual compression test.

Table 5.3: Soft wing deformation modes virtual test.

Mode no.	Deformation Mode description	Mast Intrusion [mm]	Force Range [kN]
1	Linear elastic deformation of skin.	0-100	0-34
2	Skin failure (tear open), plastic shear deformation mode.	100-115	34-11
3	Skin in plastic shear deformation mode, aprx.constant force.	115-375	11-11
4	Skin in plastic shear, stacking up against main spar.	375-450	11-50

## 5.3.2 SWI 1

The initial peak force of 13kN was reached after a displacement of 50mm. The compression force was approximately constant from 50 to 300mm. Maximum force of 43kN was reached after a displacement of 430mm. Figure 5.8 shows the test sequence of test 1.

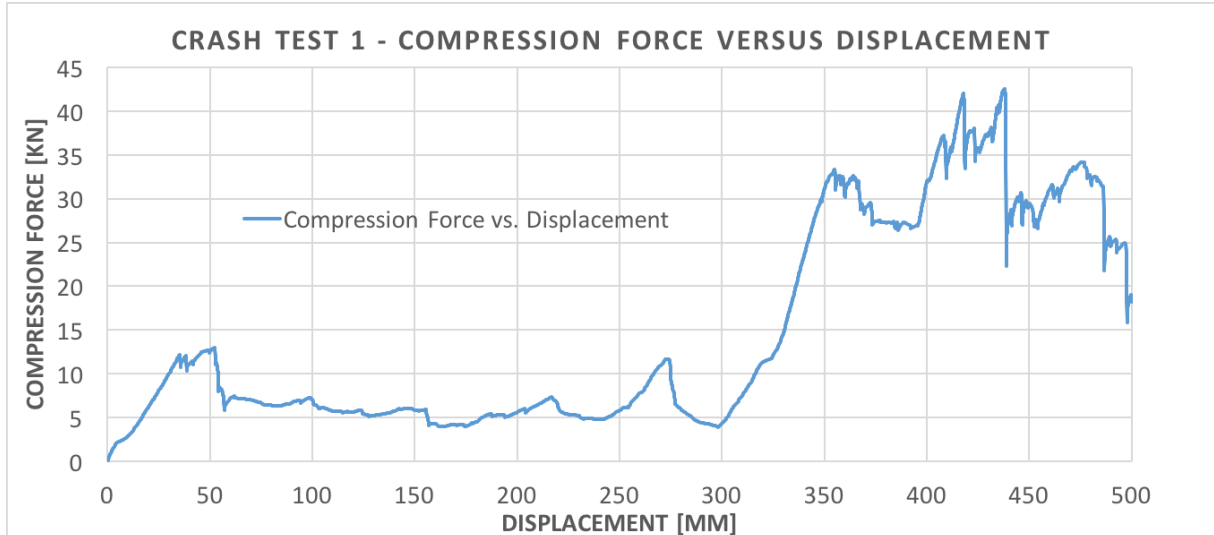


Figure 5.8: Compression test 1.

Table 5.4: Soft wing deformation modes test 1.

Mode no.	Deformation Mode description	Mast Intrusion [mm]	Force Range [kN]
1	Linear elastic deformation of skin.	0-50	0-13
2	Skin failure (tear open), plastic shear deformation mode.	50-55	13-6
3	Skin in plastic shear deformation mode, aprx.constant force.	55-300	6-6
4	Skin in plastic shear, stacking up against main spar.	300-410	6-43
5	Plastic deformation of main spar and buckling of supporting ribs.	410-430	43-43
6	Rib buckling failure, main spar detach from ribs and skin.	430-500	43-15

5.3.3 SWI 2

The initial peak force of 12kN was reached after a displacement of 50mm. The compression force was approximately constant from 50 to 300mm. Maximum force of 38kN was reached after a displacement of 435mm. Figure 5.9 shows the test sequence of test 2.

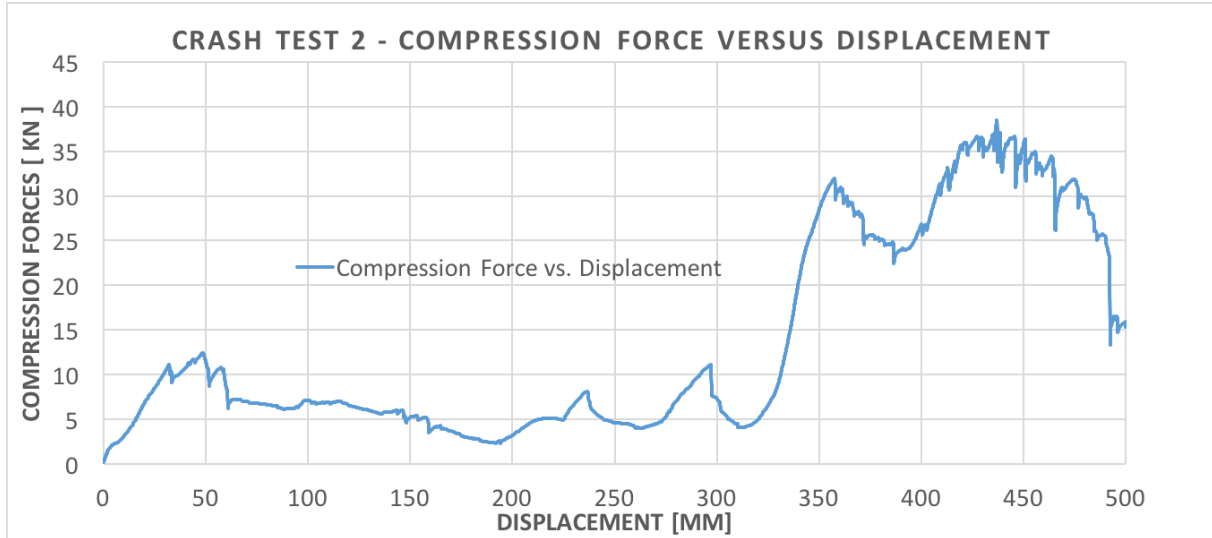


Figure 5.9: Compression test 2.

Table 5.5: Soft wing deformation modes test 2.

Mode no.	Deformation Mode description	Mast Intrusion [mm]	Force Range [kN]
1	Linear elastic deformation of skin.	0-50	0-12
2	Skin failure (tear open), plastic shear deformation mode.	50-60	12-6
3	Skin in plastic shear deformation mode, aprx.constant force.	60-310	6-6
4	Skin in plastic shear, stacking up against main spar.	310-410	6-37
5	Plastic deformation of main spar and buckling of supporting ribs.	410-450	37-37
6	Rib buckling failure, main spar detach from ribs and skin.	450-500	37-15



### 5.3.4 SWI 3

The initial peak force of 12kN was reached after a displacement of 50mm. The compression force was approximately constant from 50 to 300mm. Maximum force of 47kN was reached after a displacement of 440mm. Figure 5.10 shows the test sequence of test 3.

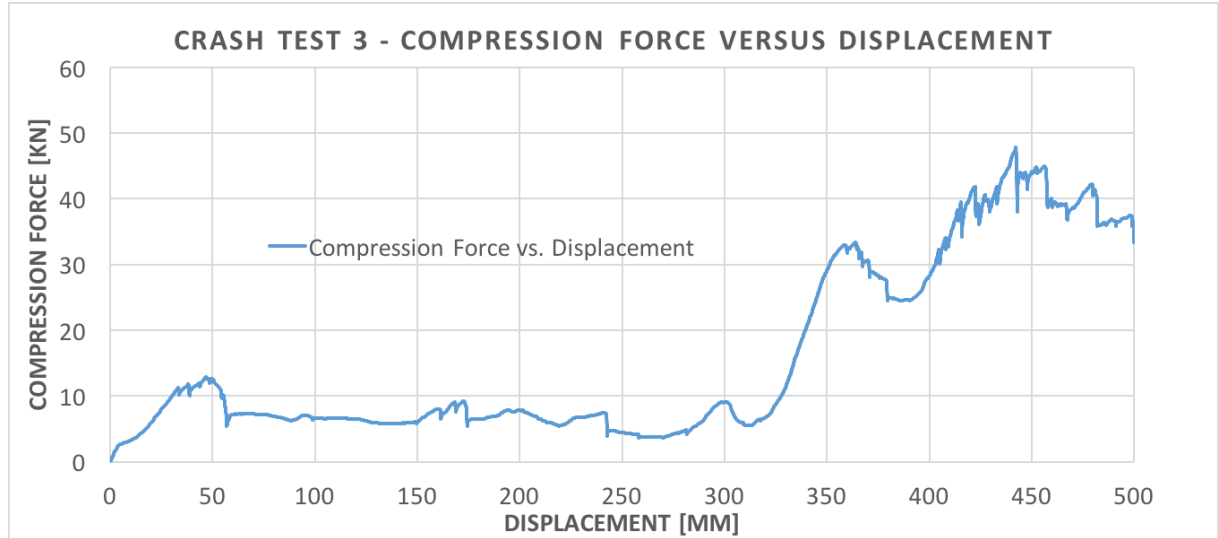


Figure 5.10: Compression test 3.

Table 5.6: Soft wing deformation modes test 3.

Mode no.	Deformation Mode description	Mast Intrusion [mm]	Force Range [kN]
1	Linear elastic deformation of skin.	0-50	0-12
2	Skin failure (tear open), plastic shear deformation mode.	50-60	12-7
3	Skin in plastic shear deformation mode, aprx.constant force.	60-310	7-7
4	Skin in plastic shear, stacking up against main spar.	310-440	7-47
5	Plastic deformation of main spar and buckling of supporting ribs.	440-460	47-47
6	Rib buckling failure, main spar detach from ribs and skin.	460-500	47-35

## 5.3.5 SWI 4

The initial peak force of 12kN was reached after a displacement of 50mm. The compression force was approximately constant from 50 to 300mm. Maximum force of 58kN was reached after a displacement of 470mm. Figure 5.11 shows the test sequence of test 4.

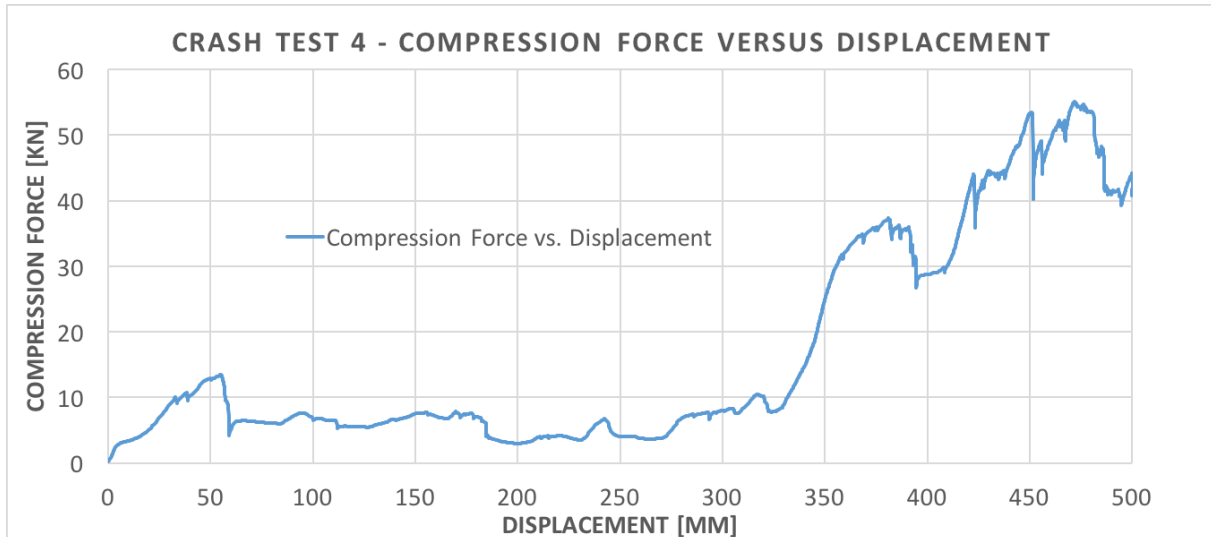


Figure 5.11: Compression test 4.

Table 5.7: Soft wing deformation modes test 4.

Mode no.	Deformation Mode description	Mast Intrusion [mm]	Force Range [kN]
1	Linear elastic deformation of skin.	0-55	0-12
2	Skin failure (tear open), plastic shear deformation mode.	55-60	12-7
3	Skin in plastic shear deformation mode, aprx.constant force.	60-330	7-7
4	Skin in plastic shear, stacking up against main spar.	330-450	7-55
5	Plastic deformation of main spar and buckling of supporting ribs.	450-475	55-55
6	Rib buckling failure, main spar detach from ribs and skin.	475-500	55-40

### 5.3.6 Comparison of SWI test results

All four crash tests and the virtual test are presented in [Figure 5.12](#). The graph shows the comparisons of all the tests combined. The comparison shows that there was consistency between the physical tests.

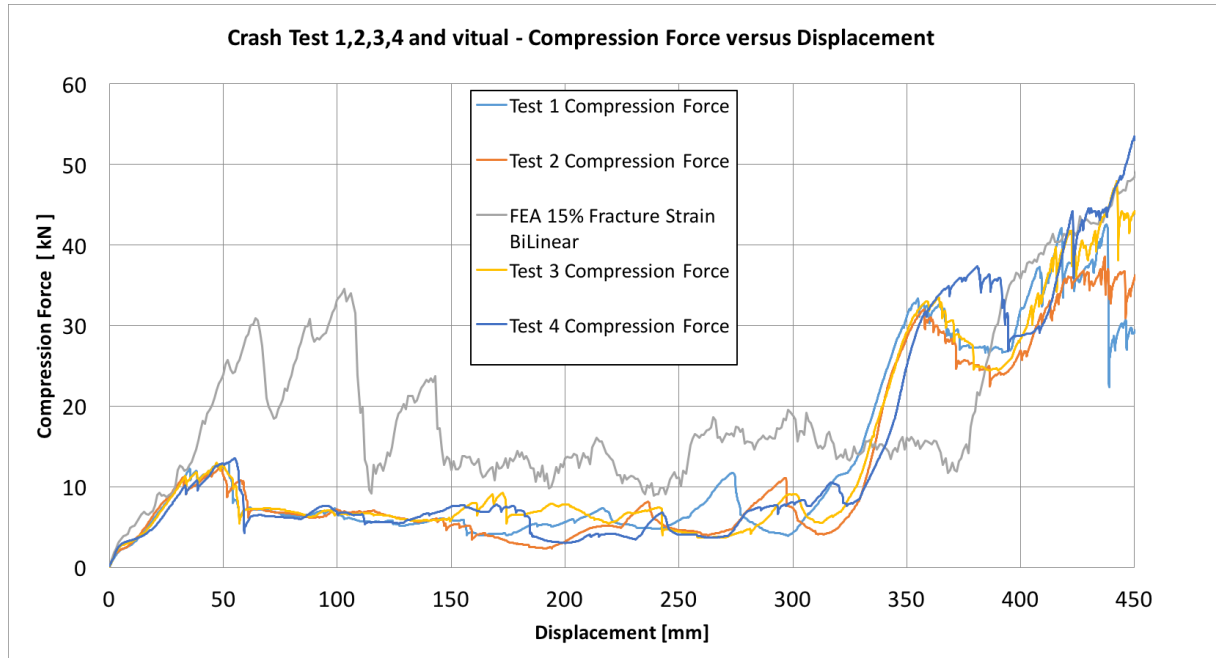


Figure 5.12: Comparison of all tests.



## Chapter 6

# Discussion

As expected, the force pattern discovered in our test results followed relatively similar patterns as discovered in the test results from the virtual and physical tests carried out by Rølvåg and Wiggenraad et.al. The main differences were the initial peak forces. In the test carried out by Wiggenraad et.al, the main-spar was mounted at a distance of 450mm from the leading edge. The peak force was therefore expected to occur later than in our tests. This corresponded well with our test results. The initial peak force in Wiggenraads test yielded almost three times the peak force compared to our tests. An obvious reason can be that since Wiggenraad et.al. placed the intruder above the nose-rib, larger forces were expected. The design of the outer steel-supports were also slightly different from our steel-base. How this influenced the test results compared to our tests is however yet unknown, but it is believed that the influence is not of major concern. The virtual SWI model designed by Rølvåg was identical to our physical SWI model. Here the main-spar was mounted 340mm from the leading edge. The physical test results however revealed initial peak forces almost 1/3 of the force created in the virtual simulation. The peak force was also maintained at a much longer intrusion distance in the virtual test. Since this is not the optimized Abaqus version, the fracture strain and material hardening are somehow preventing the skin from tearing at an earlier stage which also had an extensive impact on the force distribution. This could be a possible reason for the high initial peak forces which are also maintained longer than in our tests. This can possibly be fixed by tuning the material model in Abaqus based on results disclosed in our tests.

When examining the force pattern created during our tests, as mentioned above, the six key characteristics are captured based on failure modes from the virtual test described in [subsection 3.2.1](#). This pattern can be seen from the test results in [subsection 5.3.6](#) where a comparison of all four compression tests are combined. Since the geometry, distance between rivets, material and plate thickness were identical in all four SWI's manufactured in this project, it was expected to achieve approximately similar results. For all four compression tests the initial peak force was reached after a displacement of approximately 50-60mm. At this point the skin began to fail due to high shear forces created in the transition between the skin and the centre nose-ribs. This occurred to all SWI's since the test procedure specified to place the intruder in between the two centre nose-ribs. The skin was torn open and the compression force dropped significantly at an intrusion of 50-70mm. Since the tip of the nose-rib was designed as a sharp edge, the small contact area across the nose created high local shear-stresses. The intruder has a width of 200mm and the distance between the nose-ribs was 350mm. This implies a distance of 75mm on each side. Due to the short distance, the local stress created at the contact area between the nose-rib and the intruder increased rapidly with each millimeter of intrusion. From the tensile test results of the Aluminium 2024-T3, we disclosed a fracture strain of approximately 17.5%. A material elongation of 17.5% before fracture is however not achieved as something

is affecting the skin before this limit is reached. Based on the stress concentration across the nose-rib tip, high shear forces are causing the problem in this phase. Unlike the physical testing, the virtual model was not able to recreate the same stress concentration. This could be one of the main reasons of a peak force three times the peak force discovered in our tests. A solution may be to look at different designs of the nose-rib tip so the force acting on the tip is distributed over a larger area. Tuning the material model may also be a solution to improve this. This will contribute to lowering the stress concentration across each of the nose-ribs.

Furthermore, the compression force was approximately constant from 60 to 310mm. Here the skin suffered from a plastic shear deformation mode. When the stroke was close to 310mm, the skin was stacked towards the main-spar by the intruder and the compression force increased significantly over a short distance of intrusion. Maximum compression force was reached after a displacement of 430mm.

In test 1 and 2, all associated parts such as rivets, bolts, material, skin and rib-structure were similar. In test 3, the rivets were substituted with stronger rivets, and in test 4 both stronger and slightly larger rivets were used. The rivets on the skin in test 3 were similar (3mm) to the rivets used in test 1 and 2. The difference was the 4mm rivets used on the main-spar which yielded higher shear and tensile strength than in test 1 and 2. In test 4 the conclusion was to use 3.2mm skin rivets to increase the overall strength. Also significantly stronger 4mm rivets were substituted from test 3 to test 4. The reason for using 3.2mm skin rivets was due to the rivet dimensions supplied from the subcontractor. To achieve desired strength of such rivets the dimensions had to be slightly larger. Both NLR and the supervisor used 3mm skin rivets in their tests, but our conclusion was to proceed by using 3.2mm rivets and similar spacing between each rivet. The influence of such rivets only increases the overall strength and stiffness, and nothing more.

In the aftermath of the two first tests we discovered some problems regarding selection of rivets. The chosen rivets intended for the physical tests were hollow, and after executing test 1 and 2, results revealed that a majority of the rivets were prone to high shear forces. This occurred especially when the intruder entered the main-spar. Rivets mounted through the main-spar and on to the outer supporting ribs were cut off. This can be seen in [Figure 6.1b](#). Graphs showed significant differences between the virtual and the physical test in test 1 and 2, and the solution was to substitute with stronger rivets as mentioned above. Test 1 and 2 yielded only a peak force of 43 and 37kN which is not within the accepted region with respect to the force limit of 45kN specified by ICAO. Since the SWI is intended for use during tests of aviation masts, the SWI need to sustain larger forces than 45kN. If not, the SWI will be a major concern when analysing results regarding acceptance of aviation masts. In an ideal world, such as in a virtual test, every hole distributes similar amount of force when they are aligned and stretched in one direction. In the physical model, the holes will not be perfectly aligned nor have similar size as manually drilling is an inaccurate process. Unequal distribution of force will cause some rivets to snap before others do. A better solution can be to use CNC-drilling or laser/water-jet cutting. This can however be unnecessarily expensive.

Another reason for rivet failure can be that, since the outer supporting rib-structure is connected with bolts to the outer steel-supports, the ribs will be slightly pulled inwards. This creates high stress concentrations to the outer rivets mounted at both ends of the main-spar. This can also be seen in one of the tests from the physical model where two rivets still were attached in the centre of the main-rib at one side. However, in all tests the main-spar was detached from one side during the compression sequence, and nearly all rivets on the opposite side had been cut off. Due to our limited knowledge about rivets specifically designed for the flight industry, we contacted the technical flight department at Notodden. Normally, they use massive rivets that are hammered, but due to regions inside the SWI which are difficult to

reach, we decided to use hollow rivets with similar mechanical properties as massive rivets. If one should have made a perfectly correct wing module, massive rivets should have been used. One option can be to use massive rivets only on the rib-structure inside the SWI, but since the hollow rivets used have similar mechanical properties as the massive rivets, the conclusion was to proceed with using hollow rivets.

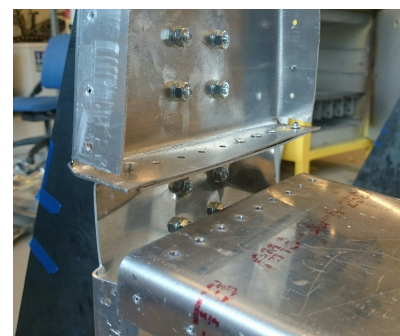
The compression tests disclosed that the skin-rivets had less influence on the test results than rivets used on the structure inside the SWI. This could be seen during tests since the skin tear failure initiated before failure of the rivets. The skin was torn open at an early stage (approximately after 50-60mm), and the maximum applied force at this stage was 1/3 of the force in the virtual test. Test results show that the skin rivets did not have any major impact throughout the compression sequence. In test 4 the skin rivets mounted on the outer supporting ribs towards the leading edge was able to sustain slightly larger forces than in the other tests. This can be seen in the graph where all SWI's were combined. However, this resulted in less than 2-3kN of extra force before also these rivets failed. A validation of various rivets was carried out by executing physical rivet tests in the laboratory. The final results confirmed our choice of new rivets. Rivets used in test 4 were not tested, but based on the applied safety factor and mechanical properties provided from the subcontractor, these yielded the most reliable test results regarding desired shear and force resistance compared to massive rivets. They yielded a peak force of 55kN which is enough to fulfill ICAO's criteria of 45kN.

One of the main criteria listed in [subsection 2.3.2](#) is that the structural damage to an aircraft is directly related to the amount of energy accumulated during an impact. The quasi-static compression test showed that the accumulated deformation energy is far below the ICAO limit of 55kJ. During our tests we disclosed a maximum energy accumulation of 8kJ. This even when the force created in the tests (55kN) was exceeding the force limit of 45kN. Based on the low amount of energy accumulated during our tests it was therefore decided not to consider these energy results in [chapter 5](#).

The steel-bases were constructed to withstand supplied compression forces during testing so that elastic and plastic deformations could be neglected. This meant they could be reused for multiple tests. The steel-bases were easy to manufacture and have low material costs. If desired, the steel-bases could be used in a dynamic impact-test. It is however recommended to strengthen the steel side-supports so any moments generated in the impactor due to impacts off its centre line is not affecting the steel-base by plastic deformation or critical deflections which interfere with the results.



(a) Deformed main-spar after compression test.



(b) Detach of main-spar due to high shear forces on rivets.

Figure 6.1: Deformation of main-spar and shear of rivets.





# Chapter 7

## Conclusion

The quasi-static compression test results were sensitive to local shear-forces in the transition between the skin and the tip of the nose-ribs. This happened to all four SWI's since the test procedure specified to place the intruder in between the two centre nose-ribs. The reason for high local stress concentrations between the skin and the nose-ribs can be due to the small contact area. Due to these stress concentrations, the tensile tested material elongation of 17.5% is invalid in this phase. This is also the main reason for the mismatch between the virtual and the physical tests in this phase.

Test 1 and 2 yielded low peak force resistance due to rivets with a low shear and tensile strength. The tests resulted in a peak force of 43 and 37kN before the main-spar was detached from the supporting rib-structure. Based on results from test 1 and 2, and results from rivet testing, test 3 and 4 were substituted with stronger rivets which yielded sufficient are sufficient with accordance to shear and tensile strength. Test 3 and 4 resulted in a peak force of 47 and 55kN. Test 3 and 4 is sufficient according to the ICAO limit of 45kN. In future testing of ALS, SWI 4 in test four will be the most reliable impactor for use. Test results of all four SWI's indicate that the skin rivets have less influence on the overall structure strength, and the main-spar rivets is therefore of main interest regarding the overall strength of the SWI.

The quasi-static compression test results show that the accumulated deformation energy is far below the ICAO limit of 55kJ. During our tests we disclosed a maximum energy accumulation of 8kJ. This low amount of accumulated energy was achieved even when the force created in the tests (55kN) exceeded the force limit. The energy limit stated by ICAO could however be more applicable for testing of heavier aviation masts with integrated cables since these potentially accumulate higher energy values.

Since the optimization of the model (material) in Abaqus has not been considered upon further discussion with supervisor Rølvåg. Our tests are crucial when optimizing the virtual model and its material properties. Based on our test results from compression tests and tests carried out on rivets and the aluminium, a closer match between test results from the virtual and our physical tests can be achieved.

The benefits of the work carried out in this thesis will in a long term view contribute to a decrease of critical accidents at airports worldwide, and also an increase of air-traffic safety in general. Standardisation of test procedures regarding ALS's, and comparison of failure modes and results amongst various mast manufactures, are more convenient and feasible due to a qualified, standard SWI.

## 7.1 Further work

Based on our analysis of test results, some work has to be carried out in order to perfectly optimize the physical and virtual model. This concerns:

- The shape and design of the nose-ribs had influence on the initial peak forces. It is therefor recommended to consider a new design of these. Since the tip of the nose-ribs was designed as a sharp edge, the skin was easily torn up due to high local stress concentration. A new design of the leading edge radius of the nose-ribs may prevent the skin from tearing up at an early stage. If early skin failure is prevented, the initial peak forces may be more similar to the virtual test. It is however sufficient to tune the virtual model based on results from a physical test, and not vice verca.
- A quasi-static compression test does not imply all dynamic forces created in a dynamic test, and inertia and damping forces is therefor not considered. To cover the affection of such forces, a dynamic impact test must be conducted on the SWI's.
- To further optimize the model (material) in Abaqus based on test results from our tests, supervisor Rølvåg will include this in a new master-thesis.

# Bibliography

- [1] Lattix - Lightweight aluminum masts and gantries. [http://www.lattix.net/no/index.php/products/aviation/approach\\_lights/](http://www.lattix.net/no/index.php/products/aviation/approach_lights/).
- [2] Terje Rølvåg, Torgeir Welo, J.F.M Wiggenraad, and Rien Van Houten. FE simulation of soft wing impactor for aviation mast frangibility testing – sensitivity to model assumptions. Technical Report International Journal of Crashworthiness, DOI: 10.1080/13588265.2016.1168609, May 2016.
- [3] Jaap FM Wiggenraad and David G Zimcik. Frangibility of approach lighting structures at airports. 2001.
- [4] Juhani Hanka and Markku Vahteri. Test report of impact test of EXEL light mast. Technical report, October 1991.
- [5] Beechcraft model 80 queen air. [http://richard.ferriere.free.fr/3vues/queenair\\_3v.jpg](http://richard.ferriere.free.fr/3vues/queenair_3v.jpg).
- [6] R.H.W.M. Frijns and J.F.M Wiggenraad. Static compression tests and computer models of wing impactors used for impacts on frangible airport approach lighting towers. Technical report, Netherlands Department of Civil Aviation, Netherlands, November 1999.
- [7] J.F.M Wiggenraad, M.H. van Houten, and C. Rooks. Development of requirements, criteria and design guidelines for frangibility of structures at airports. Report, ICAO, 2003.
- [8] FAA Engineering Office of Airport Safety & Standards. 150/5340-18f - Standards for Airport Sign Systems, August 2010.
- [9] FAA Engineering Office of Airport Safety & Standards. 150/5340-11 - Standards for Airport Markings, September 2013.
- [10] ICAO Frangible Aids Study Group. Aerodrome design manual, first edition. *Chapter 2: Siting considerations*, 2006.
- [11] Pan Am Flight 845. [https://en.wikipedia.org/w/index.php?title=Pan\\_Am\\_Flight\\_845&oldid=717693724](https://en.wikipedia.org/w/index.php?title=Pan_Am_Flight_845&oldid=717693724), April 2016. Page Version ID: 717693724.
- [12] ICAO Frangible Aids Study Group. Aerodrome design manual, first edition. *Chapter 1.2: What is frangibility?*, 2006.
- [13] D. G. Zimcik, A. Selmane, and M. H. Farha. A Study on the Frangibility of Airport Approach Lighting Towers. *ResearchGate*, 45(1), January 1998.
- [14] ICAO Frangible Aids Study Group. Aerodrome design manual, first edition. *Part 6: Frangibility*, 2006.
- [15] D.G. Zimcik, M. Nejad Ensan, Syh Tsang Jenq, and Mao Chao Chao. Finite Element Analysis Simulation of Airport Approach Lighting Towers. Technical report, Institute of Aeronautics and Astronautics, National Cheng Kung University, May 2006.

- 
- [16] R Dinan, Dan Duke, and C. Rooks. Airfield frangibility criteria: Questions and concerns with current standards. October 2014.
- [17] Dan Duke. Impactor studies. Section 1 & 5 - IESALC. Technical report, JAFSG meeting II, Orlando, 2014.
- [18] M. Nejad Ensan. Frangibility analysis of approach lighting composite tower. Technical report, July 2009.
- [19] M.H. van Houten, H Gottschalk, C. Rooks, R Miller, and P Tolken. International Crashworthiness Conference ICRASH2010. Technical report, Leesburg, VA, 2010.
- [20] Rivets - T.Bentsen AS. <http://www.tbentsen.no/pop/festemateriell/popnagler>, January 2012.
- [21] ISO 6892-1:2009 - Metallic materials – Tensile testing – Part 1: Method of test at room temperature.
- [22] ASM Material Data Sheet. <http://asm.matweb.com/search/SpecificMaterial.asp?bassnum=MA2024T3>, april 2016.

## Appendix A

# Dimensional drawings

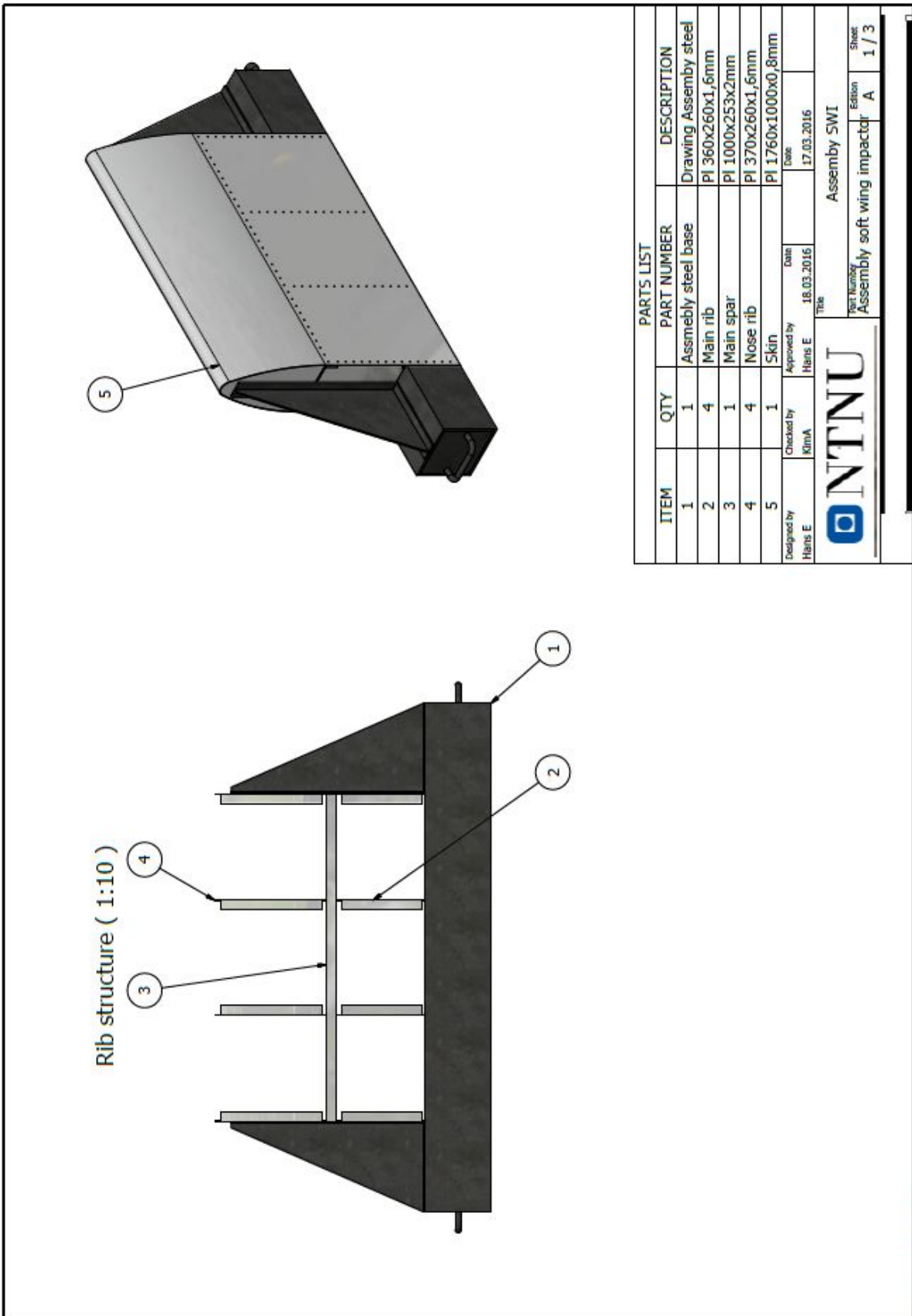


Figure A.1: SWI assembly

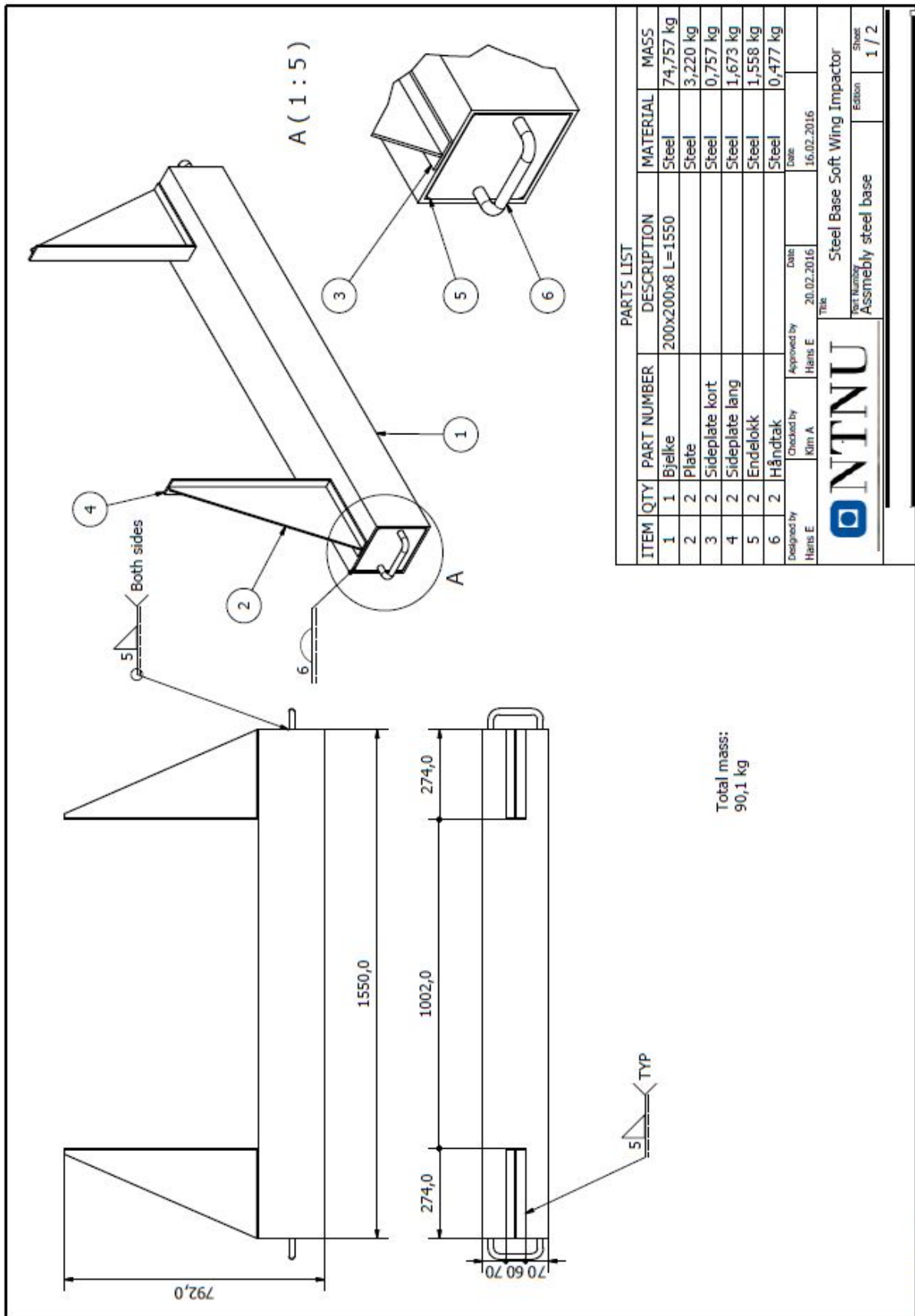


Figure A.2: Steel-base

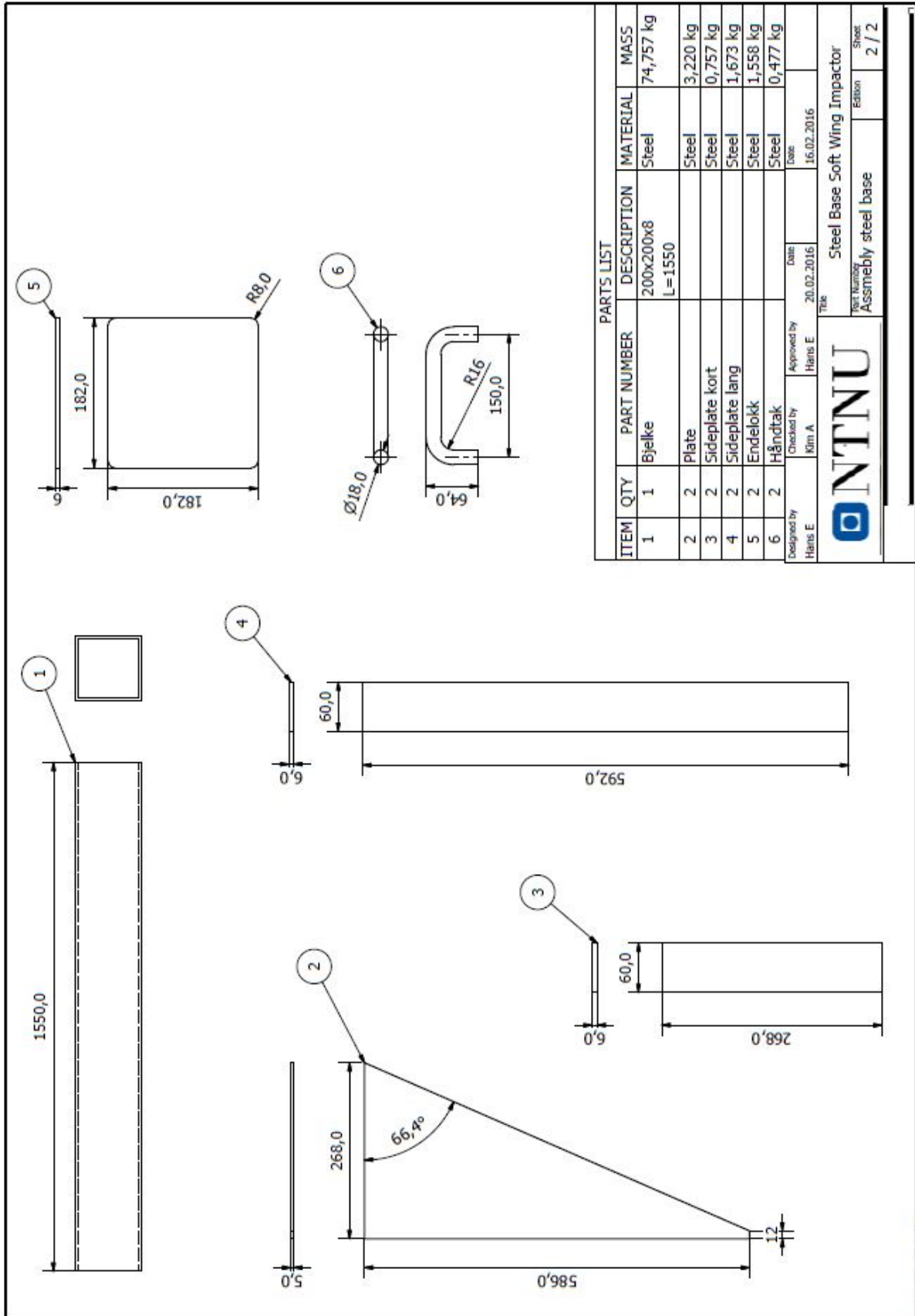


Figure A.3: Steel-base parts



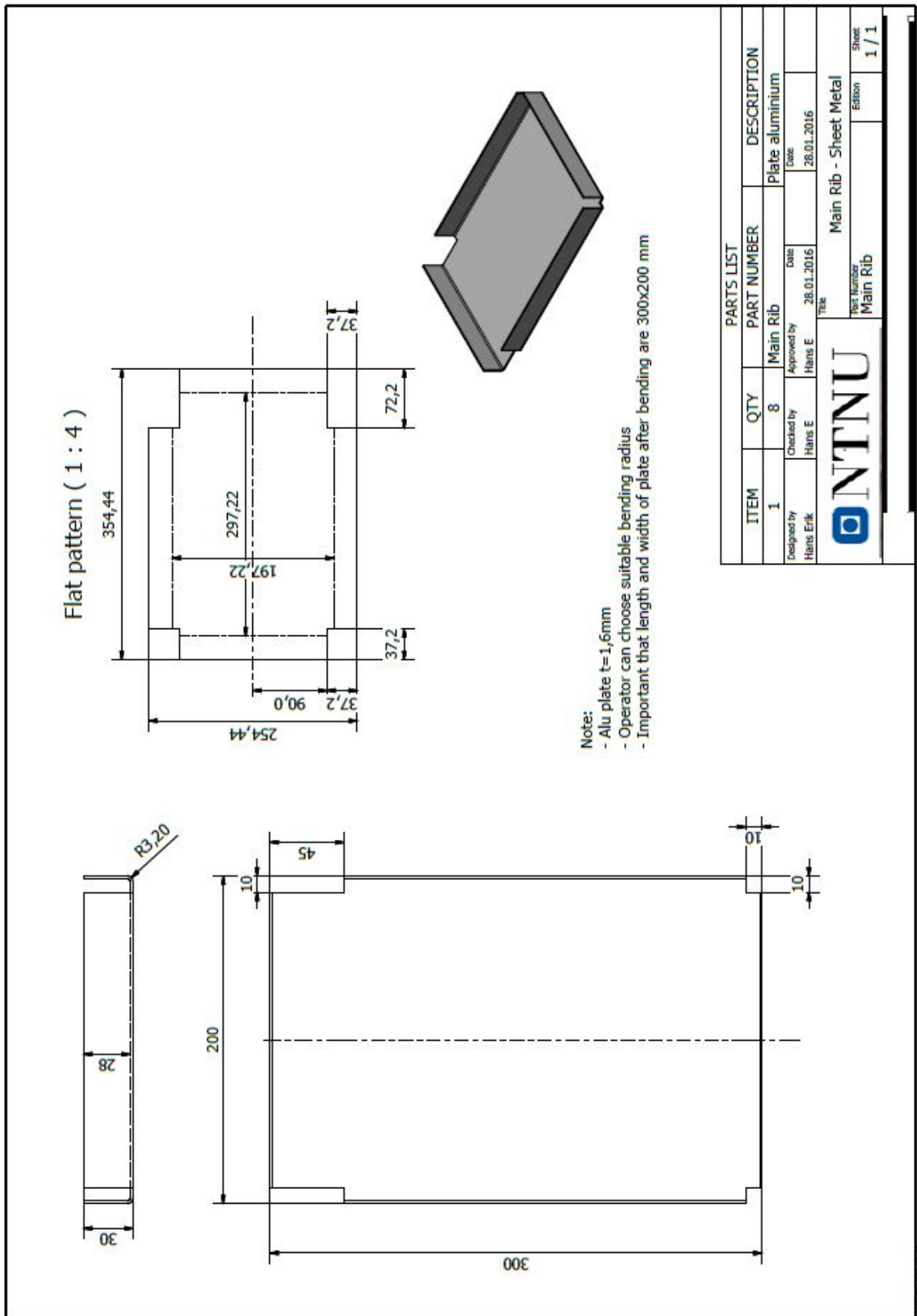


Figure A.4: Main-rib

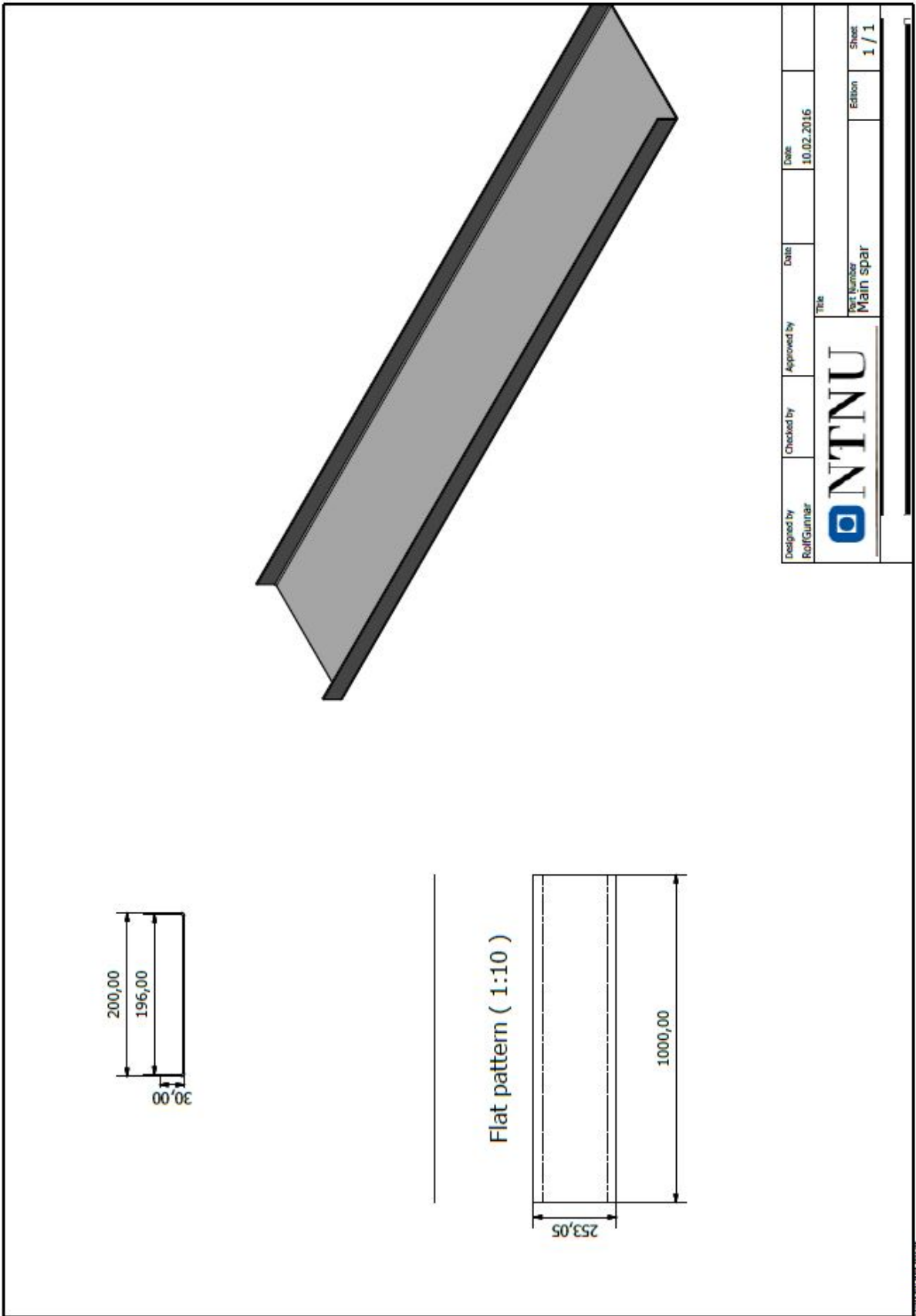


Figure A.5: Main-spar

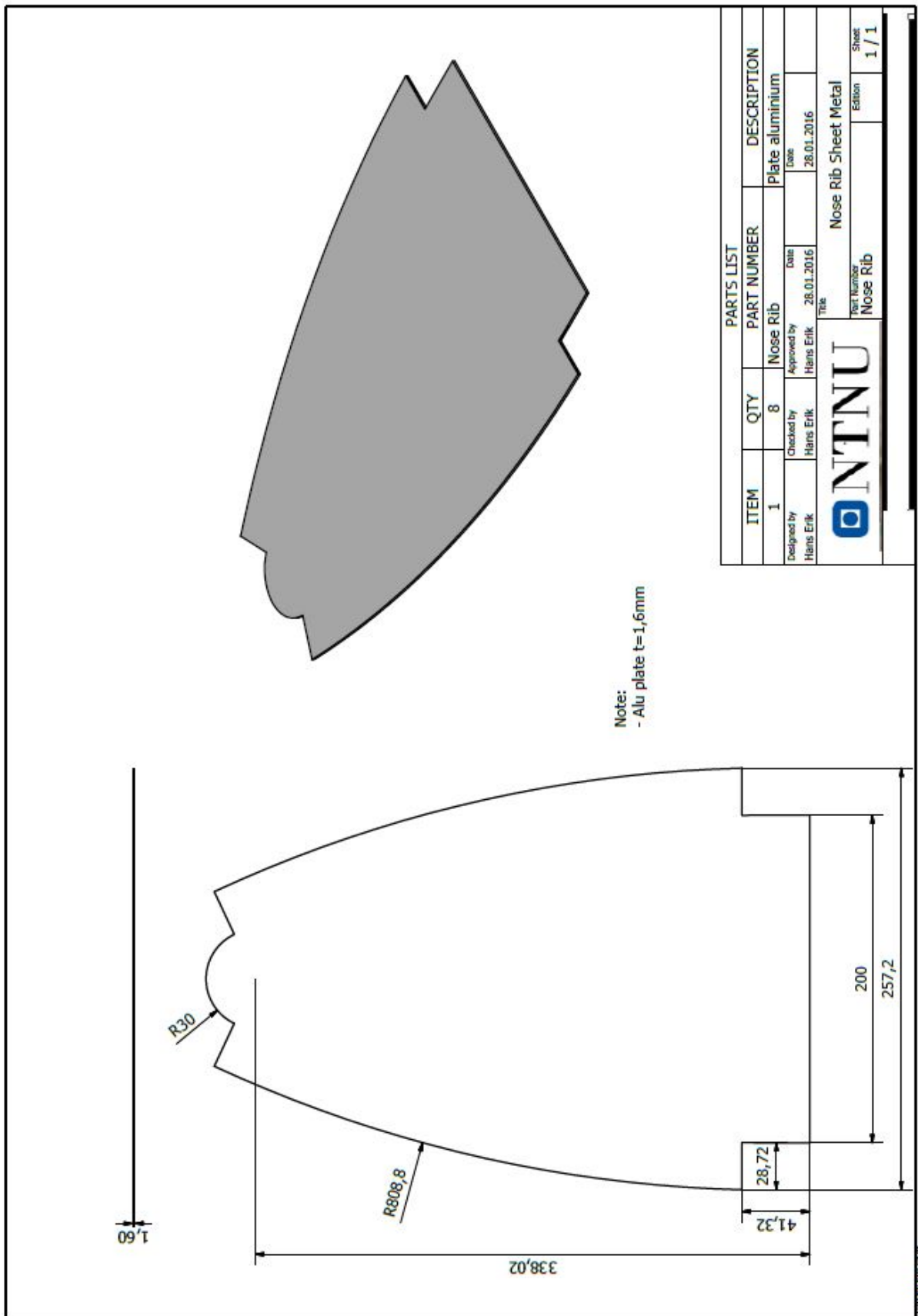


Figure A.6: Nose-rib

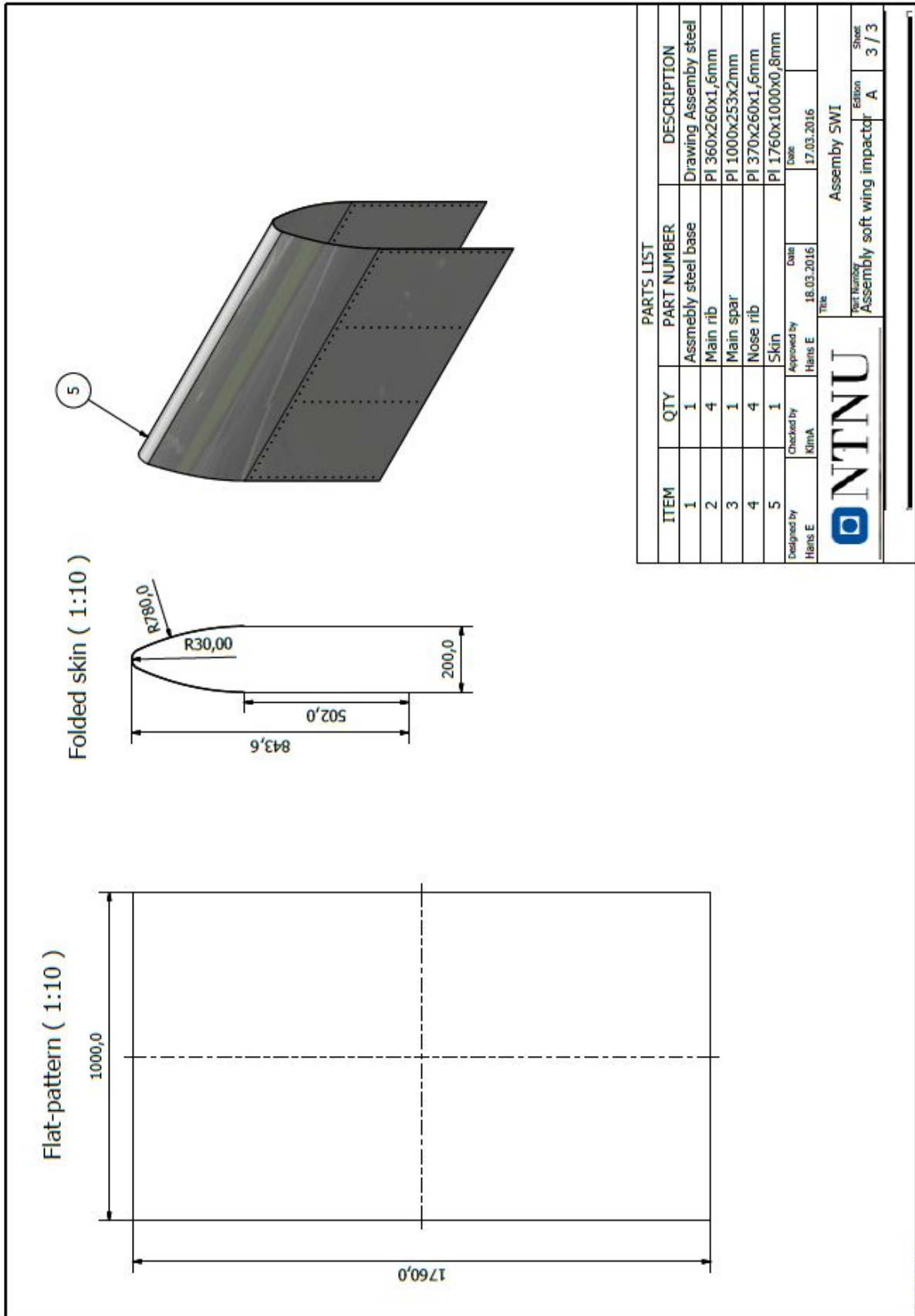


Figure A.7: Skin

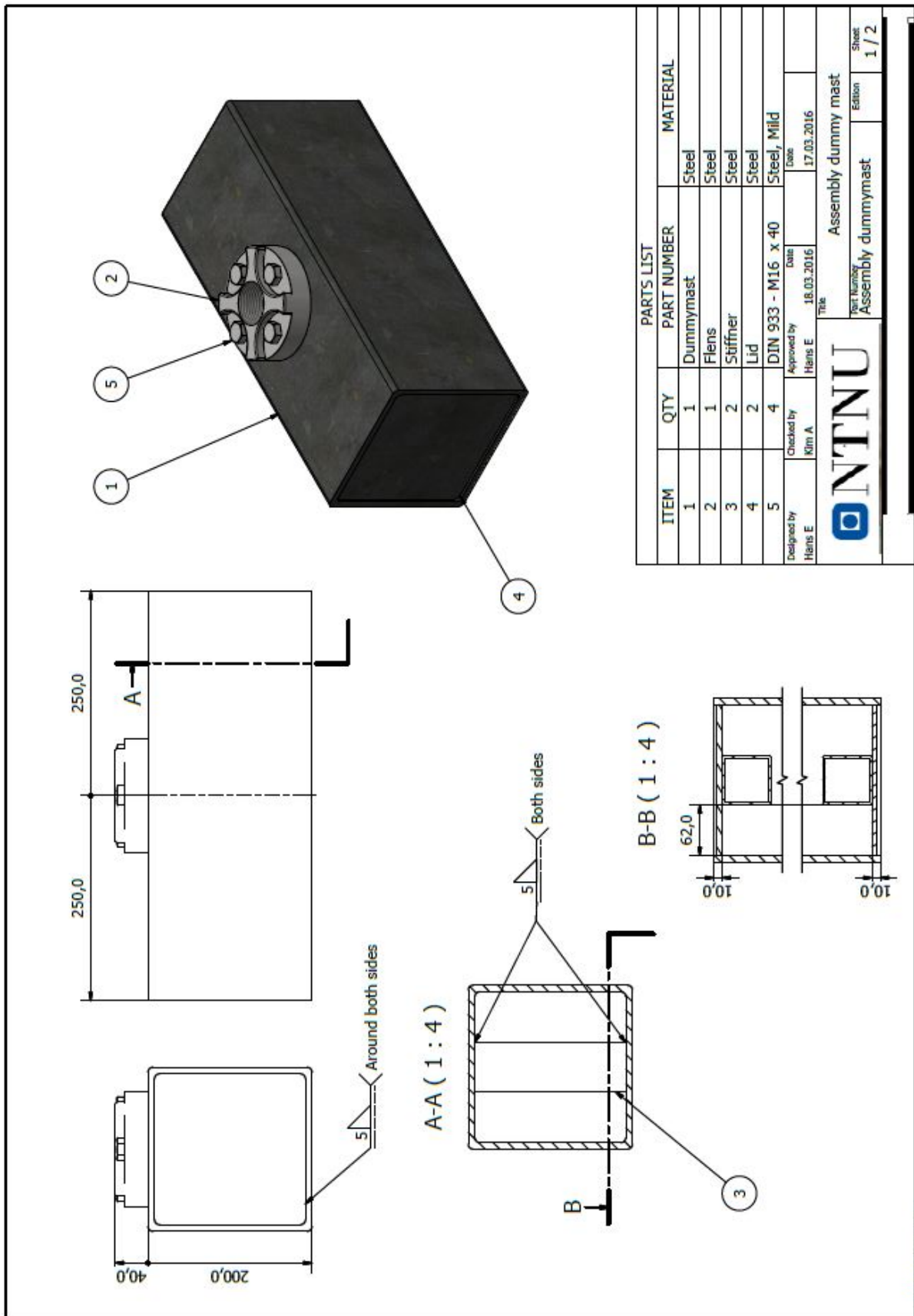


Figure A.8: Mast intruder

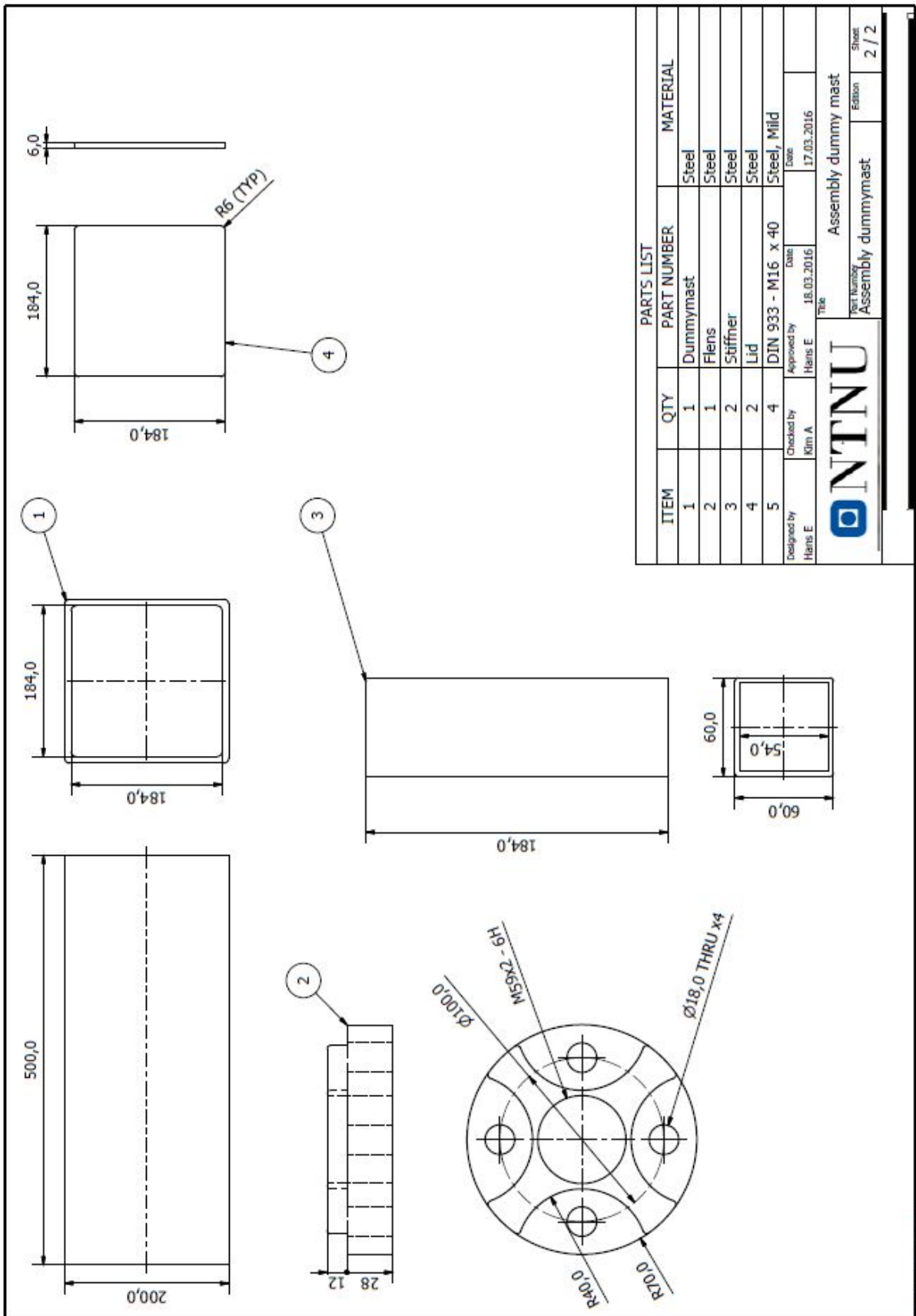


Figure A.9: Mast intruder cut

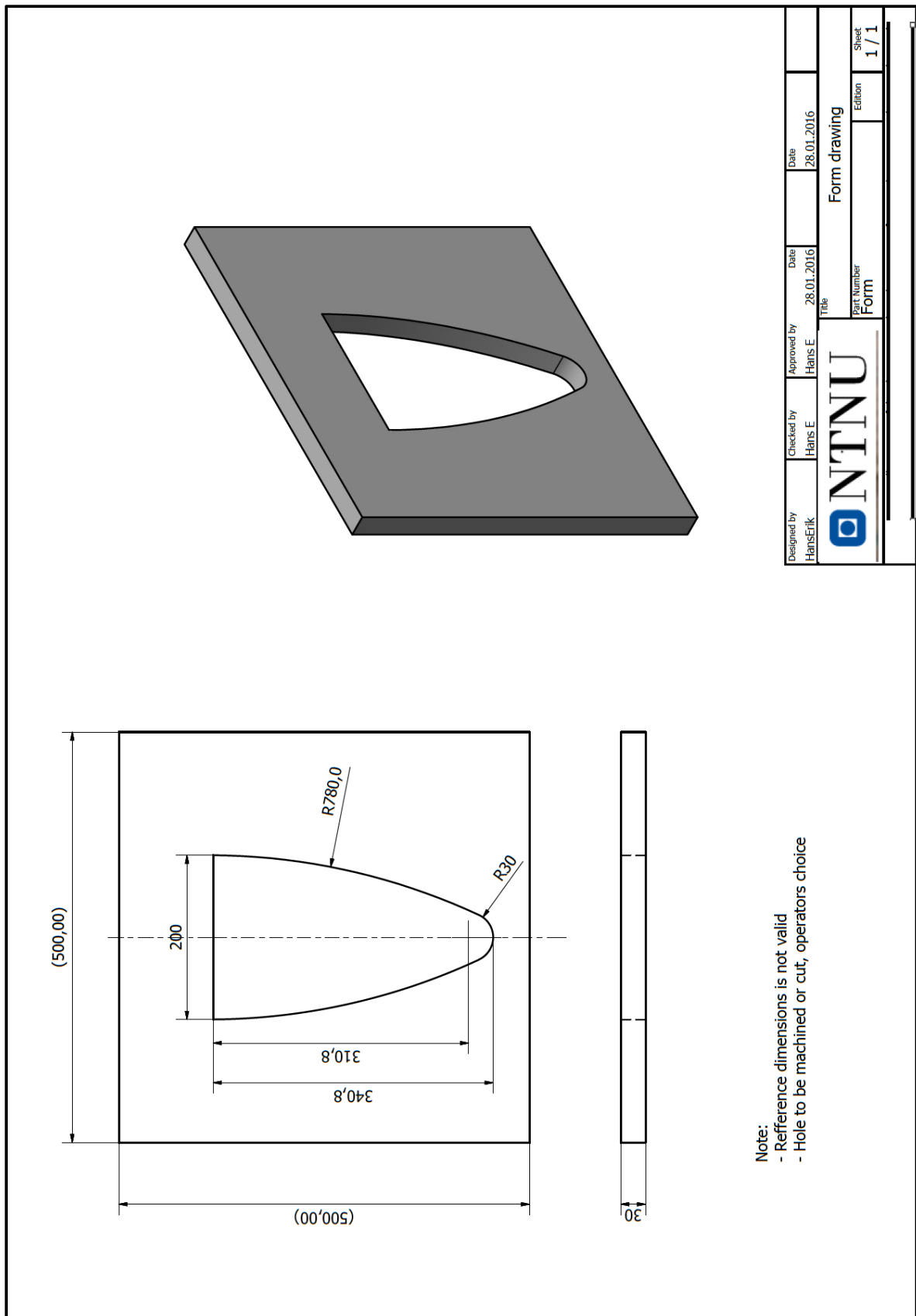


Figure A.10: Form lower part

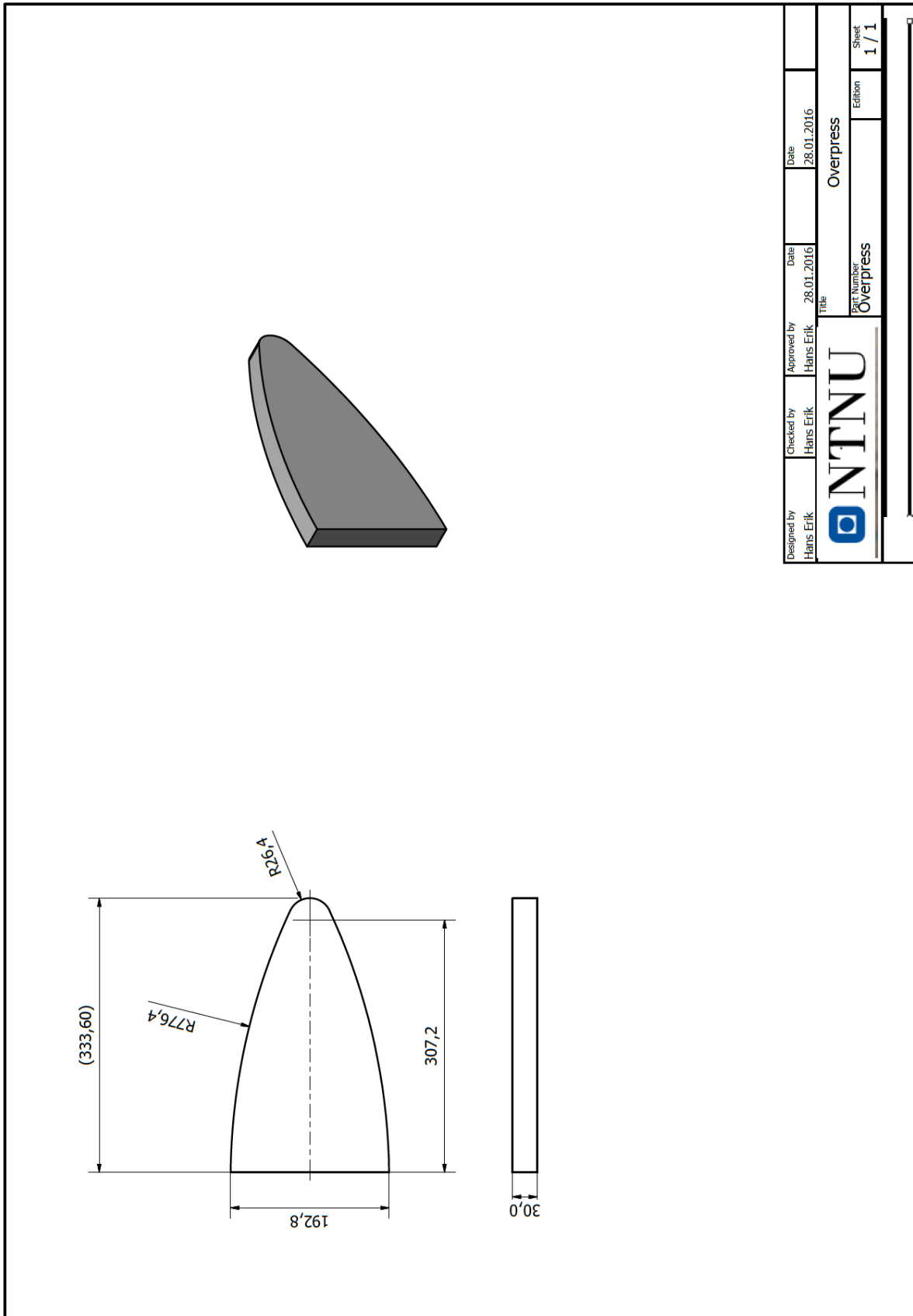


Figure A.11: Form upper part



**Appendix B**

**Paper draft**

# *Soft wing impactor for testing of aviation masts*

Paper draft

Hans Erik Eidem & Kim Andre Krogsæter

*Department of Engineering Design and Materials, NTNU,  
Trondheim, Norway*

## *Abstract*

Due to the imminent danger of colliding into aviation aids located with close proximity along runways or taxiways, ICAO was in the early 80's specifically assigned to develop specifications for frangible lighting structures. As a result, the ICAO Frangible Aids Study Group (FASG) was established in 1981 to subsequently propose design specifications and crash test procedures regarding frangibility of aviation aids and supporting masts. Two specific types of impactors were used for testing and development of aviation lighting structures. These two types were rigid and soft impactors. However, during multiple tests conducted the last decades, the rigid impactor was soon discovered to generate initial peak forces far above the limit of 45kN stated by ICAO FASG. It was also impossible to analyse structural damage since National Aerospace Laboratory (NLR), Netherlands, stated that the pass/fail criteria considering frangibility of an ALS should be based on damage applied to the wing. Damage to the skin was accepted, but damage to supporting wing-structures like the front spar was not.

The Soft-Wing-Impactor (SWI) is based on the proposed design by NLR. In total four soft wing impactors were built and tested by conducting quasi-static compressions tests. These tests were conducted according to the test procedure specified by NLR and Rølvåg. Results were compared to criteria specified by ICAO. Supporting aviation structures could not impose peak forces and energy to an aircraft wing higher than 45kN and 55kJ. These were of main concern considering the validation of a SWI. Test results were also compared to a virtual test carried out by Rølvåg, and physical compression tests carried out by Wiggenraad et.al. These were used as a reference in some of our discussions regarding test results.

Results proved that the SWI's were sensitive to large shear-stress in the transition between the skin and the tip of the nose-ribs. This happened to all SWI's since the test procedure specified to place the intruder in between the two centre nose-ribs.

Test 1 and 2 yielded low peak forces due to rivets with low shear and tensile strength. The force reached 43 and 37kN before the main-spar was detached from the supporting rib-structure. Based on these results, test 3 and 4 were substituted with stronger rivets which yielded sufficient shear and tensile strength based on tests carried out on the rivets. Test 3 and 4 resulted in a peak force of 47 and 55kN. These were therefore sufficient according to the ICAO limit of 45kN. Test 4 was the most reliable and sustainable impactor for use in future tests of aviation masts based on the margin of 10kN.

## I. INTRODUCTION

Each year thousands of flights are committed from both small and large airports worldwide. To provide sufficient safety and avoid misleading aircrafts, various types of signal equipment are located within close proximity of runways and taxiways. According to Federation Aviation Administration (FAA) and International Civil Aviation Organization (ICAO), all international airports worldwide have detailed technical standards developed to ensure safety, and common coding systems implemented to provide global consistency [1][2][3]. Such systems are necessary for providing guidance during landing and take-off in almost any weather condition, to prevent delays, and also to maintain sufficient flow of air and ground traffic. Occasionally, sudden emergencies or incidents occur and emergency landings or aborted take-offs are necessary. Severe collisions with unforeseen objects are rarely controllable, and multiple structures along the runway or taxiways contribute to creating potential risks to both aircraft and passengers. Numerous times such impacts have been recorded. Some more severe than others [4].

For several decades professional organizations worldwide, collectively named ICAO Visual Aids Panel (VAP), have been working on various safety issues regarding aviation lighting structures (ALS) located at airports. In the early 80's, ICAO VAP were specifically assigned to develop specifications for frangible lighting structures. As a result, the ICAO Frangible Aids Study Group (FASG) was established in 1981 to subsequently propose design specifications like requirements, criteria, guidelines and test procedures [5]. Preventing loss of structural integrity of aircrafts during impact and further harm to passengers, was one of the main arguments regarding *frangibility* of an ALS. FASG specified that frangibility of fixed objects located at any area where aircrafts move or approach/leave, must be defined as; "the ability of a structure to break, distort or yield at a certain impact load while absorbing minimal amount of energy and leave minimal damage to the aircraft" [3][6]. Based on their research and work, the Aerodrome Design Manual (ADM) [3] Part 6; Frangibility, was made.

To benchmark and qualify various types of masts and identify damages and dynamics during impacts as a whole, FASG found it necessary to use a reference impactor. Several impactors were designed and tested by various members of ICAO throughout the years, but NLR later came up with an improved version of a SWI made out of aluminium sheets connected to a steel-base in 1988 [5]. This was an 1:1 cut-out of

a wing-section from the Beechcraft Model 80 Queen Air. They used this aircraft as a reference since it was appropriate according to elaborated standards [5][7]. Scandinavian ALS mast manufacturers with help from ICAO members, used it as a standard during various tests from 1991-1997. Canadian ALS mast manufacturers used a slightly different design of a SWI, and also a rigid impactor between 1998-2000.

During the development of frangible requirements, two kinds of impactors have been used for full-scale dynamic testing. Rigid and soft impactors respectively. ICAO still recommend use of rigid impactors contrary to a SWI in their ADM based on arguments established from testing of Canadian ALS's carried out by Zimcik et. Al [8]. They stated that rigid impactors provided conservative and repeatable results, and additionally being rigid in a manner which made it reusable for physical testing. The initial peak force and amount of energy absorbed were within reasonable limits, and the production cost of a single impactor was low. This was pointed out as a conclusion from results of a test campaign which tested aluminium lattice structures.

However, rigid impactors have proven to provide some ambiguous results. Especially during testing of an ALS consisting of a single large fiberglass/polymer tube without integrated couplings. When using a rigid impactor it often tends to slice through the tube while a SWI did not [7][8][9]. From an engineering point of view these results might not always be conservative. Later studies also revealed problems regarding noise and high peak forces during impact both virtual and physical, especially during tests of aluminium lattice structures [7][10]. The rigid impactor did not yield higher kinetic energy values than soft-impactors, and it was not possible to perform further inspections of structural damages. Tower response and failure modes have also proven to be quite different between the two [5][10].

Although ICAO recommend use of a rigid impactor based on many arguments such as inexpensiveness, repeatable, constant contact time regardless of shape and material, short contact duration, etc, the pass/fail criteria considering frangibility of an ALS is based on damage applied to the wing [3]. Damage to the skin is accepted, but damage to supporting structures like the front spar is not. Thus, only soft-impactors allow for damage identification and is therefore the correct choice when testing an ALS. However, there are currently no properly developed standard regarding such impactors. In recent decades, mast manufacturers have been using various designs, but only a few were comparable with respect to the test results, which was mostly due to design inequalities.

## II. DESIGN AND TESTING FOR FRANGIBILITY

### A. Design

According to standards, an aviation lighting structure (ALS) must be strong enough to carry the required amount of equipment on top, as well as being resistant against jet blasts and environmental influences. But on the other hand it is required to fail during sudden impacts with small, commute aircrafts [3]. Equipment located with close proximity along runways and taxiways must be constructed as a frangible structure due to the imminent danger of colliding into it from any approaching

direction. An accidental impact between an aircraft and an ALS can potentially affect the aircraft in three different ways:

- Loss of momentum
- Change of direction
- Suffer from structural damage

ICAO's ADM [3] describes the amount of momentum lost during an impact as a mathematical governed problem solved by using the integral of force over time. This implies the necessity of minimizing and keeping the impact load and duration to a minimum. The affection of friction between mast and impactor during impact enables mast deformation which allows it to entangle the wing. With respect to frangibility criteria this cannot be tolerated. A common solution implies the use of structural and cable segmentation which can be separable to ensure selected break-away points to be disconnected. In case of a one-piece design, frangibility must be ensured by a complete failure of the structure. This involves failure of random members of the structure, and not failure caused by segmentation. By taking these solutions into consideration, impact force and duration will be minimized and can prevent loss of momentum or sudden change of direction.

Regarding consumption of energy, ICAO's ADM [3] explains the structural damage to the aircraft as directly related to the amount of energy absorbed during an impact. With respect to frangibility the amount of energy required can be limited. The energy can be divided into energy for activation of break-away or failure mechanisms, elastic or plastic deformation of obstacles, and acceleration of obstacles up to aircraft velocity. Aircraft velocity, which in this case is not a design variable, and mass to be accelerated, are the main parameters for measuring the amount of kinetic energy required to accelerate the obstacle. The purpose of break-away mechanism is to absorb impact forces through the structural member and by this fail due to overload. A stiff and light structure provides the necessary amount of force transported to break-away points and low amount of energy absorption. Plastic or elastic deformation of the structure depends on the choice of material. High yield-strain alloys imply higher values. The use of light-weight alloys and a frangible structure is preferable for the reason that it decrease the amount of mass to be accelerated. Additionally, the contact area between obstacle and wing affects the amount of energy absorbed. A large contact area prevents obstacles cutting deeply into the wing as a result of force distribution.

Considering the choice of material, frangibility is achieved by using lightweight materials which yield or distort easily [3], either metallic or non-metallic. From a test point of view non-metallic materials are exceptional with respect to frangibility, but considering their elastic modulus and material isotropy, analysing of results are prone to uncertainties due to the material behaviour. Chosen materials for an ALS must be able to withstand all kinds of environmental influences. The ALS needs to be light, brittle and consist of segment or a one-piece structure in order to deflect or fail during a sudden impact to allow safe passage of aircrafts during flight or ground maneuvering.

Allowing the aircraft safe passage, an ALS is required to fail in three different failure modes:

- Fracture
- Windowing
- Bending

One of the main requirements regarding an ALS is that the supporting structure cannot impose peak loads and energy to the aircraft that is higher than:

- 45kN
- 55kJ

Considering the quasi-static compression tests intentionally carried out by the assigned students, these criteria and failure modes will be the requirements to be fulfilled.

### B. Quasi-static testing

The Aerodrome Design Manual (ADM) does not support any proper standard considering testing of aviation masts when using a SWI. However, NLR and Rølvåg have proposed a test procedure regarding a quasi-static compression test of the intended SWI [7][11]. This has been done to cover deformation modes, reaction forces and the consumption of energy related to intrusion of the intruder. The ADM mostly describes regulations targeting aviation masts since a rigid-impactor not have to be tested due to its rigidity. In this case, testing is hence to cover the impact an mast intrusion has on the structural integrity of the SWI, and also cover fracture strain and material hardening.

The quasi-static compression test must be carried out by using a hydraulic rig. An intruder will be pressed through the aluminium parts. It is critical that the SWI is properly mounted to prevent uncertainties in the test results if any movements or tipping has occurred during testing. Rølvåg and NLR emphasized the necessity of using a pair of load cells mounted between the rig foundation and the rigid steel-base of the SWI. The total sum recorded from these cells will be the amount of reaction force created during the compression sequence.

The intended test parameters are:

- 50mm/min (compression speed)
- 500mm (intrusion)
- 45kN (max. peak force)
- 55kJ (max. energy absorption)

The speed is set based on recommendation from previous tests carried out by NLR and Rølvåg. The intrusion length is set based on damage supplied to the main-spar. Any further intrusion is not acceptable since the wing damage is far out of the accepted range considering structural integrity and deformation of the main-spar.

### C. NLR Soft-Wing-Impactor

The latest SWI designed by NLR were based on the commute aircraft Beechcraft Model 80 Queen Air. The SWI was designed as an 1:1 cut-out to replicate the intended wing module. This can be seen in Figure 1. The aerodynamic shape was

however simplified. The reason for choosing this aircraft was due to its mass and take-off speed, which is 3000kg and 140km/h. The intended SWI was for the first time used during a testing campaign carried out by NLR [5].

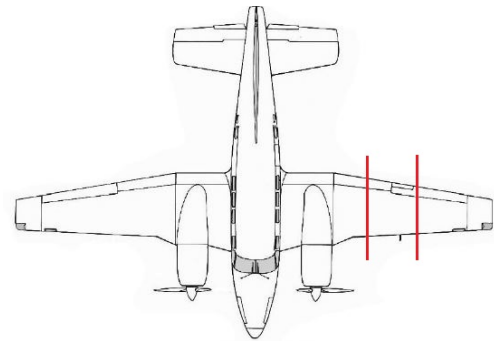


Figure 1 Beechcraft Model 80 Queen Air wing section.

The SWI consists of five unique parts. In Figure 2 one can identify the respective parts;

1. Welded steel base
2. Main-rib; 1,6mm Alu2024T3
3. Main-spar; 2,0mm Alu2024T3
4. Nose-rib; 1,6mm Alu2024T3
5. Skin; 0,8mm Alu2024T3

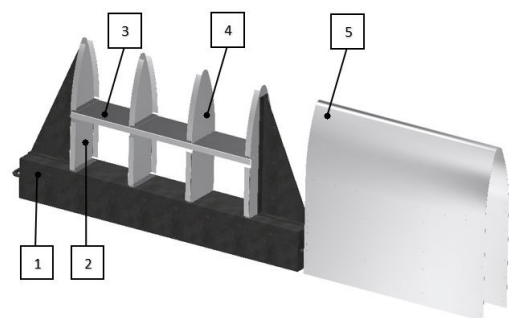


Figure 2 SWI Assembly.

The overall length of the SWI is 1000mm and the overall height is 640mm, which only includes the aluminium section. The widest point on the SWI is across the main-rib section has a width of 200mm. The distance between each of the four main-ribs and nose-ribs are equal, and the main-spar runs across the entire wing section. The SWI is backed by a steel column with a square cross-section of 200x200x8mm. As stated in a compression test carried out by Wiggenraad et. Al [11], steel side-supports are made as an addition to the steel column. This to prevent unrealistic failure mode of the outer support-ribs from collapsing inward during the compression sequence. The individual components are joined together by using rivets, and the outer support ribs are connected to the steel side-supports with bolts.

#### D. "Dummy" intruder mast

The intruder (Figure 3) intended for the SWI compression test is a replica of a Lattix 4220 aviation mast. The reason for using this type of mast is due to the typical aviation mast cross section which must provide realistic reaction forces versus softening intrusion characteristics. A Lattix 4220 mast has a cross-section of 200mm x 200mm, and is built of aluminium. These are delivered in modules with break-away points. The rigid "dummy" mast is constructed of S355JR steel.



Figure 3 Intruder CAD-model

### III. METHODS – MANUFACTURING PROCESS

#### A. Steel-base

The steel-base was built according to the design from NLR and Rølvåg [7]. The steel-base was designed to withstand forces applied to the SWI during the compression test. This way the same steel-base can be used for several tests without any major plastic or elastic deformations. In total two equal steel-bases were built. The intended function of the steel-base was to support the SWI from unrealistic failure modes such as collapsing inward during testing. Figure 4 shows the two manufactured steel bases.



Figure 4 Steel-base

1. Steel beam, 200x200x8mm.
2. Outer steel-supports with welded flat bar flanges.

#### B. Main-rib

The main-ribs were made of 1,6mm thick aluminium 2024-T3 sheet-metal. The sheet-metal was cut by a laser tool and bent in an automatic bending machine. The hole pattern of the bottom section of the main-rib was marked identical to the steel-base and the main-spar. The hole pattern of the main-spar was used

as a measurement for drilling holes at the steel-base since the distance and amount of holes were identical.

#### C. Main-spar

The main-spar was made of a 2mm thick aluminium 2024-T3 sheet-metal. The overall length of the main-spar was equal to the width of SWI, 1000mm respectively. The width of the main-spar was equal to the width of the main-rib and nose-rib, 200mm respectively. It was necessary to be accurate with the hole pattern since the main-spar was mounted between the main-rib and the nose-rib. This transition was crucial with respect to shear forces applied to the rivets. Figure 5 shows the four mounted main-ribs and the horizontal main-spar.

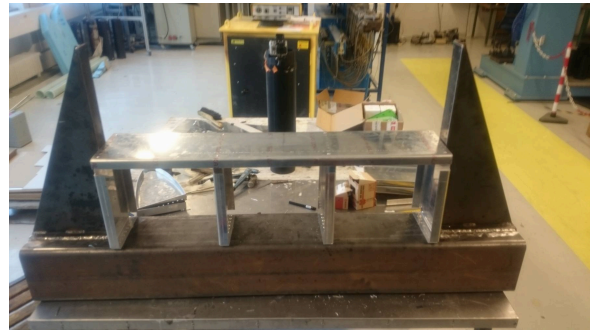


Figure 5 Main-ribs with main-spar

#### D. Nose-rib

The nose-ribs were made of 1,6mm thick aluminium 2024-T3 sheet metal. These supporting ribs were the most complex parts to manufacture. The nose-ribs have flanges that must be bent in order to make a radius (Figure 6). To be able to make this part, a form had to be designed and manufactured.

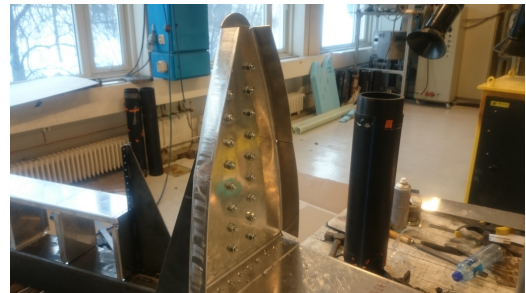


Figure 6 Nose-rib

The sheet metal had to be cut out from a flat-pattern drawing. The flat-pattern model was designed by using the sheet-metal function in NX. Further the plate was pressed through the form by using a hydraulic press (Figure 7). Grease was applied to the plate and form to avoid high shear forces on the aluminium during the stance operation.

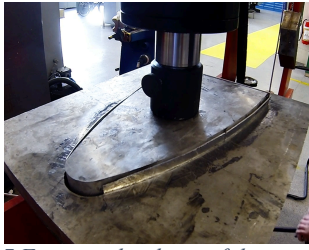


Figure 7 Forming the shape of the nose-rib

#### E. Skin

The skin was made of a 0,8mm thick aluminium 2024-T3 sheet metal. The skin was cut to a width of 1000mm and a length of 1740mm. Since the skin was made out of a thin aluminum plate, it was ductile which made it easy to form. To simplify the assembly of the skin, the form of the leading edge was made in advance by making a tool specifically design to form a radius of 30mm. This was executed by pressing a steel tube down at the middle of the plate. The steel tube had equal radius as the leading edge of the SWI. By doing this the skin fit easily over the nose-rib during the assembly. Figure 8 shows the skin attached at one side of the SWI.

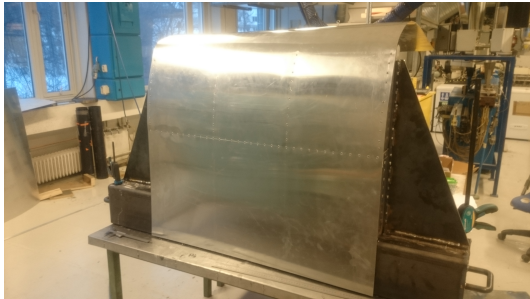


Figure 8 Skin mount

The skin was attached to the rib-structure by using rivets with a center-center distance of 30mm. The center-center distance of the rivets was identical to the one used in the virtual model. In total approximately 300 rivets were used to attach the skin. The holes were drilled with a 0,1mm larger diameter than the rivets, which was the minimum recommended from the supplier, a 3.1mm drill respectively. The rivets were placed in the hole and a pneumatic rivet pistol was used to drive the rivets. To ensure proper connection between the skin and the rib-structure, the rivets were attached simultaneously as the holes were drilled.

#### F. "Dummy" intruder mast

Figure 9 illustrates the manufactured intruder. It was manufactured based on identical measurements with respect to the intruder used in the virtual compression test. In Abaqus the intruder was modelled as a rigid body. Since the intended intrusion mast was modelled as a rigid body to prevent elastic deformation during the compression sequence, the physical mast had to be manufactured identical to the one in Abaqus. To achieve a rigid body for the physical model, stiffeners were

welded inside the beam and lids were welded to each side of the beam.



Figure 9 "Dummy" intruder mast

#### G. SWI-overview

In total four SWI's were built. Identical manufacturing methods were used at each SWI. Impactor number 1 and 2 were identical. Impactor number 3 and 4 have identical designs and materials as 1 and 2, but the rivet quality is improved. The skin rivet diameter is slightly increased on Impactor 4. In this case sealed aluminium rivets were used on impactor 4. Increasing the diameter of the skin rivets to 3,2mm was necessary since 3,2mm was the only standard available from supplier for this type of rivet. Table 1 Rivet overview shows the overview of the rivet strengths used for each impactor.

Table 1 Rivet overview

Part	Impactor 1	Impactor 2	Impactor 3	Impactor 4
Rib rivet diameter (mm)	4	4	4	4
Maximum shear strength* (N)	850	850	1330	1640
Maximum tensile strength* (N)	1200	1200	1910	2220
Skin rivet diameter (mm)	3	3	3	3,2
Maximum shear strength* (N)	800	800	800	1110
Maximum tensile strength* (N)	1000	1000	1000	1400

\*Material data from supplier.

## IV. QUASI-STATIC COMPRESSION TESTS

The Quasi-static compression test was performed in the Construction Laboratory at NTNU. In cooperation with professionals from the laboratory, four tests were carried out.

#### A. Test setup

The hydraulic test rig had to be adjusted especially for the testing of the SWI. The height of the rig was adjusted to an equivalent height as the impactor. A clearance of 5mm was added to the height of the test rig, this to ensure clearance between the SWI and the intrusion mast. shows the rigging of the SWI. It was important to ensure that the SWI was placed in the center in relation to the mast. To ensure this, measurements were taken and controlled before testing.



Figure 10 Rigging of soft wing impactor

### B. Test procedure

The test procedure was made so that all tests were performed identical without any deviations and identical to the virtual test conducted in Abaqus. A test procedure was also necessary for the operators. Based on the procedure they were able to adjust the settings on the test rig equally for each test.

- Mount the intrusion mast to the threaded bolt located at the load cell.
- Install a guide to make sure the intrusion mast will keep its position during the test.
- Place the SWI in center of the intrusion mast.
- Adjust compression settings in Catman (+-2% margin of failure):f
  - 50mm/min
  - 500mm stroke
  - Logging: 10Hz
- Attach strain gauges:
  - Verify the electrical connections
  - Calibrate by adjusting the values equal to zero.
  - Gaugefactor: 2,12
  - Bridgefactor: 1
- Live monitoring to verify force vs. intrusion.
- Start test.
- Record the compression sequence with a camera.
- When finished, receive the final output data.

### C. SWI-Compression tests

The testing was spread over a period of two days. This was necessary due to the reuse of the steel bases. Testing of SWI 1 and 2 took place on the first day, on the second test 3 and 4. After testing of the two first SWI's it was determined to change the rivet quality for the two next builds. The forces obtained in the

two first tests were not sufficient, and it was clear that the rivets used on these did not withstand the applied shear forces created when the intrusion mast entered the main-spar. All four tests were conducted according to the test procedure.

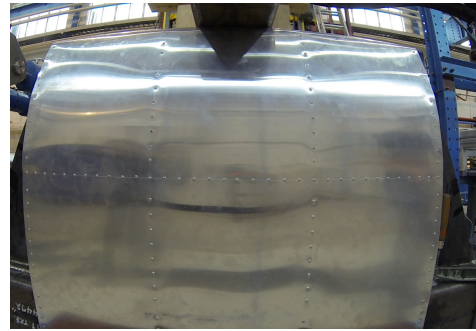


Figure 11 Start of compression test

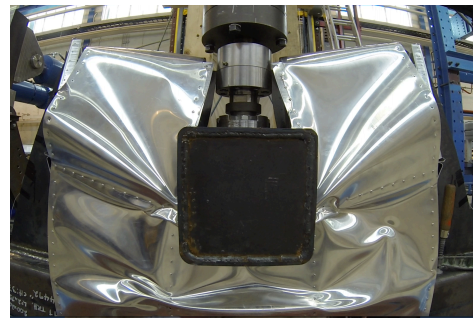


Figure 12 Finished compression test

## V. RESULTS

Test 1 and 2 yielded low peak forces due to rivets with low shear and tensile strength. The force reached 43 and 37kN before the main-spar was detached from the supporting rib-structure. Based on these results, test 3 and 4 were substituted with stronger rivets which yielded sufficient shear and tensile strength based on tests carried out on the rivets. Test 3 and 4 resulted in a peak force of 47 and 55kN. These were therefore sufficient according to the ICAO limit of 45kN. Figure 13 shows the comparisons of all compression tests, including also the virtual compression test.

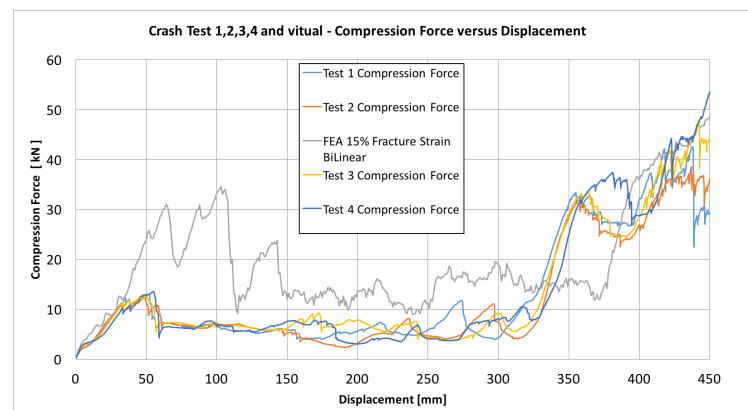


Figure 13 Comparison of the tests

## VI. DISCUSSION

As expected, the force pattern discovered in our test results followed relatively similar patterns as discovered in the test results from the virtual and physical tests carried out by Rølvåg and Wiggenraad et.al. The main differences were the initial peak forces. In the test carried out by Wiggenraad et.al, the main-spar was mounted at a distance of 450mm from the leading edge. The peak force was therefore expected to occur later than in our tests. This corresponded well with our test results. The initial peak force in Wiggenraads test yielded almost three times the peak force compared to our tests. An obvious reason can be that since Wiggenraad et.al. placed the intruder above the nose-rib, larger forces were expected. The design of the outer steel-supports were also slightly different from our steel-base. How this influenced the test results compared to our tests is however yet unknown, but it is believed that the influence is not of major concern. The virtual SWI model designed by Rølvåg was identical to our physical SWI model. Here the main-spar was mounted 340mm from the leading edge. The physical test results however revealed initial peak forces almost 1/3 of the force created in the virtual simulation. The peak force was also maintained at a much longer intrusion distance in the virtual test. Since this is not the optimized Abaqus version, the fracture strain and material hardening are somehow preventing the skin from tearing at an earlier stage which also had an extensive impact on the force distribution. This could be a possible reason for the high initial peak forces which are also maintained longer than in our tests. This can possibly be fixed by tuning the material model in Abaqus based on results disclosed in our tests.

Since the geometry, distance between rivets, material and plate thickness were identical in all four SWI's manufactured in this project, it was expected to achieve approximately similar results. For all four compression tests the initial peak force was reached after a displacement of approximately 50-60mm. At this point the skin began to fail due to high shear forces created in the transition between the skin and the centre nose-ribs. This occurred to all SWI's since the test procedure specified to place the intruder in between the two centre nose-ribs. The skin was torn open and the compression force dropped significantly at an intrusion of 50-70mm. Since the tip of the nose-rib was designed as a sharp edge, the small contact area across the nose created high local shear-stresses. The intruder has a width of 200mm and the distance between the nose-ribs was 350mm. This implies a distance of 75mm on each side. Due to the short distance, the local stress created at the contact area between the nose-rib and the intruder increased rapidly with each millimeter of intrusion. From the tensile test results of the Aluminium 2024-T3, we disclosed a fracture strain of approximately 17.5%. A material elongation of 17.5% before fracture is however not achieved as something is affecting the skin before this limit is reached. Based on the stress concentration across the nose-rib tip, high shear forces are causing the problem in this phase. Unlike the physical testing, the virtual model was not able to recreate the same stress concentration. This could be one of the main reasons of a peak force three times the peak force discovered in our tests. A solution may be to look at different designs of the nose-rib tip so the force acting on the tip is distributed over a larger area. Tuning the material model may also be a solution to improve

this. This will contribute to lowering the stress concentration across each of the nose-ribs.

Furthermore, the compression force was approximately constant from 60 to 310mm. Here the skin suffered from a plastic shear deformation mode. When the stroke was close to 310mm, the skin was stacked towards the main-spar by the intruder and the compression force increased significantly over a short distance of intrusion. Maximum compression force was reached after a displacement of 430mm.

In the aftermath of the two first tests we discovered some problems regarding selection of rivets. The chosen rivets intended for the physical tests were hollow, and after executing test 1 and 2, results revealed that a majority of the rivets were prone to high shear forces. This occurred especially when the intruder entered the main-spar. Rivets mounted through the main-spar and on to the outer supporting ribs were cut off. Graphs (Figure 13) showed significant differences between the virtual and the physical test in test 1 and 2, and the solution was to substitute with stronger rivets. Test 1 and 2 yielded only a peak force of 43 and 37kN which is not within the accepted region with respect to the force limit of 45kN specified by ICAO. Since the SWI is intended for use during tests of aviation masts, the SWI need to sustain larger forces than 45kN. If not, the SWI will be a major concern when analysing results regarding acceptance of aviation masts. In an ideal world, such as in a virtual test, every hole distributes similar amount of force when they are aligned and stretched in one direction. In the physical model, the holes will not be perfectly aligned nor have similar size as manually drilling is an inaccurate process. Unequal distribution of force will cause some rivets to snap before others do. A better solution can be to use CNC-drilling or laser/water-jet cutting. This can however be unnecessarily expensive.

The compression tests disclosed that the skin-rivets had less influence on the test results than rivets used on the structure inside the SWI. This could be seen during tests since the skin tear failure initiated before failure of the rivets. The skin was torn open at an early stage (approximately after 50-60mm), and the maximum applied force at this stage was 1/3 of the force in the virtual test. Test results show that the skin rivets did not have any major impact throughout the compression sequence. In test 4 the skin rivets mounted on the outer supporting ribs towards the leading edge was able to sustain slightly larger forces than in the other tests. This can be seen in the graph where all SWI's were combined. However, this resulted in less than 2-3kN of extra force before also these rivets failed. A validation of various rivets was carried out by executing physical rivet tests in the laboratory. The final results confirmed our choice of new rivets. Rivets used in test 4 were not tested, but based on the applied safety factor and mechanical properties provided from the subcontractor, these yielded the most reliable test results regarding desired shear and force resistance compared to massive rivets. They yielded a peak force of 55kN which is enough to fulfill ICAO's criteria of 45kN.

Another reason for rivet failure can be that, since the outer supporting rib-structure is connected with bolts to the outer steel-supports, the ribs will be slightly pulled inwards. This creates high stress concentrations to the outer rivets mounted at



both ends of the main-spar. This can also be seen in one of the tests from the physical model where two rivets still were attached in the centre of the main-rib at one side. However, in all tests the main-spar was detached from one side during the compression sequence, and nearly all rivets on the opposite side had been cut off. Due to our limited knowledge about rivets specifically designed for the flight industry, we contacted the technical flight department at Notodden. Normally, they use massive rivets that are hammered, but due to regions inside the SWI which are difficult to reach, we decided to use hollow rivets with similar mechanical properties as massive rivets. If one should have made a perfectly correct wing module, massive rivets should have been used. One option can be to use massive rivets only on the rib-structure inside the SWI, but since the hollow rivets used have similar mechanical properties as the massive rivets, the conclusion was to proceed with using hollow rivets.

The structural damage to an aircraft is directly related to the amount of energy accumulated during an impact. The quasi-static compression test showed that the accumulated deformation energy is far below the ICAO limit of 55kJ. During our tests we disclosed a maximum energy accumulation of 8kJ. This even when the force created in the tests (55kN) was exceeding the force limit of 45kN. Based on the low amount of energy accumulated during our tests it was therefore decided to not consider these energy results.

The steel-bases were constructed to withstand supplied compression forces during testing so that elastic and plastic deformations could be ignored. This meant they could be reused for multiple tests. The steel-bases were easy to manufacture and have low material costs. If desired, the steel-bases could be used in a dynamic impact-test. It is however recommended to strengthen the steel side-supports so any moments generated in the impactor due to impacts off its centre line is not affecting the steel-base by plastic deformation or critical deflections which interfere with the results.

## VII. CONCLUSION

The quasi-static compression test results were sensitive to local shear-forces in the transition between the skin and the tip of the nose-ribs. This happened to all four SWI's since the test procedure specified to place the intruder in between the two centre nose-ribs. The reason for high local stress concentrations between the skin and the nose-ribs can be due to the small contact area. Due to these stress concentrations, the tensile tested material elongation of 17.5% is invalid in this phase. This is also the main reason for the mismatch between the virtual and the physical tests in this phase.

Test 1 and 2 yielded low peak force resistance due to rivets with a low shear and tensile strength. The tests resulted in a peak force of 43 and 37kN before the main-spar was detached from the supporting rib-structure. Based on results from test 1 and 2, and results from rivet testing, test 3 and 4 were substituted with stronger rivets which yielded sufficient are sufficient with accordance to shear and tensile strength. Test 3 and 4 resulted in a peak force of 47 and 55kN. Test 3 and 4 is sufficient according to the ICAO limit of 45kN. In future testing of ALS, SWI 4 in

test four will be the most reliable impactor for use. Test results of all four SWI's indicate that the skin rivets have less influence on the overall structure strength, and the main-spar rivets is therefore of main interest regarding the overall strength of the SWI.

The quasi-static compression test results show that the accumulated deformation energy is far below the ICAO limit of 55kJ. During our tests we disclosed a maximum energy accumulation of 8kJ. This low amount of accumulated energy was achieved even when the force created in the tests (55kN) exceeded the force limit. The energy limit stated by ICAO could however be more applicable for testing of heavier aviation masts with integrated cables since these potentially accumulate higher energy values.

Since the optimization of the model (material) in Abaqus has not been considered upon further discussion with Rølvåg. Our tests are crucial when optimizing the virtual model and its material properties. Based on our test results from compression tests and tests carried out on rivets and the aluminium, a closer match between test results from the virtual and our physical tests can be achieved.

The benefits of the work carried out in this thesis will in a long term view contribute to a decrease of critical accidents at airports worldwide, and also an increase of air-traffic safety in general. Standardisation of test procedures regarding ALS's, and comparison of failure modes and results amongst various mast manufactures, are more convenient and feasible due to a qualified, standard SWI.

## VIII. FURTHER WORK

Based on our analysis of test results, some work has to be carried out in order to perfectly optimize the physical and virtual model. This concerns:

- The shape and design of the nose-ribs had influence on the initial peak forces. It is therefor recommended to consider a new design of these. Since the tip of the nose-ribs was designed as a sharp edge, the skin was easily torn up due to high local stress concentration. A new design of the leading edge radius of the nose-ribs may prevent the skin from tearing up at an early stage. If early skin failure is prevented, the initial peak forces may be more similar to the virtual test. It is however sufficient to tune the virtual model based on results from a physical test, and not vice versa.
- A quasi-static compression test does not imply all dynamic forces created in a dynamic test, and inertia and damping forces is therefor not considered. To cover the affection of such forces, a dynamic impact test must be conducted on the SWI's.
- To further optimize the model (material) in Abaqus based on test results from our tests, supervisor Rølvåg will include this in a new master-thesis.

## REFERENCES

- [1] Engineering Office of Airport Safety & Standards, FAA, "150/5340-18F - Standards for Airport Sign Systems." 16-Aug-2010.
- [2] Engineering Office of Airport Safety & Standards, FAA, "150/5340-1L - Standards for Airport Markings." 27-Sep-2013.
- [3] International Civil Aviation Organization, "Aerodrome design manual," Manual, 2006.
- [4] "Pan Am Flight 845," *Wikipedia, the free encyclopedia*. 29-Apr-2016.
- [5] J. F. . Wiggeraad, M. H. van Houten, and C. Rooks, "Development of requirements, criteria and design guidelines for frangibility of structures at airports.," Report, 2003.
- [6] D. G. Zimcik, A. Selmane, and M. H. Farha, "A Study on the Frangibility of Airport Approach Lighting Towers," *ResearchGate*, vol. 45, no. 1, Jan. 1998.
- [7] T. Rølvåg, T. Welo, J. F. . Wiggeraad, and R. V. Houten, "FE simulation of soft wing impactor for aviation mast frangibility testing – sensitivity to model assumptions," *International Journal of Crashworthiness*, DOI: 10.1080/13588265.2016.1168609, May 2016.
- [8] D. G. Zimcik, M. Nejad Ensan, S. Tsang Jenq, and M. Chao Chao, "Finite Element Analysis Simulation of Airport Approach Lighting Towers," Institute of Aeronautics and Astronautics, National Cheng Kung University, DOI: 10.1061/(ASCE)0733-9445(2004)130:5(805), May 2006.
- [9] R. Dinan, D. Duke, and C. Rooks, "Airfield frangibility criteria: Questions and concerns with current standards.," 2014.
- [10] D. Duke, "Impactor studies. Section 1 & 5 - IESALC," Orlando.
- [11] R. H. W. M. Frijns and J. F. . Wiggeraad, "Static compression tests and computer models of wing impactors used for impacts on frangible airport approach lighting towers.," Netherlands Department of Civil Aviation, Netherlands, Nov. 1999.